การเตรียมตัวเร่งปฏิกิริยาคอลลอยดัลโกลด์นาโนคลัสเทอร์ (Au:PVP)

สำหรับการสังเคราะห์เอมีดและปฏิกิริยาออกซิเดชัน

นางสาวพัชรี ปรีดาสุริยะชัย

วิทยานิพนธ์นี้เป็นส่วนหนึ่งของการศึกษาตามหลักสูตรปริญญาวิทยาศาสตรดุษฎีบัณฑิต
สาขาวิชาปิโตรเคมี
คณะวิทยาศาสตร์ จุฬาลงกรณ์มหาวิทยาลัย
ปีการศึกษา 2554
ลิขสิทธิ์ของจุฬาลงกรณ์มหาวิทยาลัย

PREPARATION OF COLLOIDAL GOLD NANOCLUSTER (Au:PVP) AS
CATALYST FOR AMIDE SYNTHESIS AND OXIDATION REACTIONS

Miss Patcharee Preedasuriyachai

A Dissertation Submitted in Partial Fulfillment of the Requirements
for the Degree of Doctor of Philosophy Program in Petrochemistry
Faculty of Science
Chulalongkorn University
Academic Year 2011

Thesis Title Preparation of Colloidal Gold Nanocluster (Au:PVP) as Catalyst for Amide Synthesis and Oxidation Reactions

By Miss Patcharee Preedasuriyachai

Field of Study Petrochemistry

Thesis Advisor Assistant Professor Warinthorn Chavasiri, Ph.D.

Accepted by the Faculty of Science, Chulalongkorn University in Partial Fulfillment of the Requirements for the Doctoral Degree

…………………………………Dean of the Faculty of Science

(Professor Supot Hannongbua, Dr.rer.nat.)

THESIS COMMITTEE

…………………………………Chairman

(Associate Professor Supawan Tantayanon, Ph.D.)

…………………………………Thesis Advisor

(Assistant Professor Warinthorn Chavasiri, Ph.D.)

…………………………………..Examiner

(Associate Professor Wimonrat Trakarnpruk, Ph.D.)

…………………………………Examiner

(Associate Professor Nuanphun Chantarasiri, Ph.D.)

…………………………………External Examiner

(Assistant Professor Tienthong Thongpanchang, Ph.D.)

พัชรี ปรีดาสุริยะชัย   :   การเตรียมตัวเร่งปฏิกิริยาคอลลอยดัลโกลด์นาโนคลัสเทอร์ (Au:PVP) สำหรับการสังเคราะห์เอมีดและปฏิกิริยาออกซิเดชัน. (PREPARATION OF COLLOIDAL GOLD NANOCLUSTER (Au:PVP) AS CATALYST FOR AMIDE SYNTHESIS AND OXIDATION REACTIONS) อ. ที่ปรึกษา วิทยานิพนธ์หลัก: ผศ.ดร. วรินทร ชวศิริ, 125 หน้า.

การวิจัยนี้สามารถเตรียมทองอนุภาคขนาดเล็กซึ่งกระจายตัวบนพอลิเมอร์ที่ชอบน้ำ พอลิ-เอ็นไวนิล 2-ไพโรลิโดน (พีวีพี) โดยอาศัยวิธีการสังเคราะห์แบบควบคุมขนาดอนุภาคของทอง ผ่านการรีดักชันอย่างรวดเร็วของ ทอง(III) ไอออน จากสารละลายน้ำ $HAuCl_4$ กับ $NaBH_4$ ซึ่งมีพีวีพีผสมอยู่ที่ 0 องศาเซลเซียสภายใต้การกวนอย่างรุนแรงในระบบแบทช์ หรือในระบบไมโครฟลูอิดิกรีแอกเตอร์ เพื่อให้ได้ทองอนุภาคขนาดเล็กมีเส้นผ่านศูนย์กลางเฉลี่ยเป็น 1.3 และ 1.1 นาโนเมตรตามลำดับ การที่ไม่พบเซอร์เฟสพลาสมอนแบนด์ ที่ความยาวคลื่น 520 นาโนเมตร ในสเปคตรัมของยูวี/วิซิเบิล แสดงให้เห็นว่าทองอนุภาคขนาดเล็กที่เตรียมได้มีอนุภาคขนาดใหญ่กว่า 2 นาโนเมตรอยู่น้อยมาก ได้ใช้ Au:PVP สำหรับปฏิกิริยาเอ็น-ฟอร์มิลเลชันของเอมีนเป็นครั้งแรก โดยการเกิดปฏิกิริยาผ่านออกซิเดชันของเมทานอล ที่สภาวะรีฟลักซ์ หรือฟอร์มาลีน ที่อุณหภูมิห้อง (27 องศาเซลเซียส) ได้สารผลิตภัณฑ์เอมีดในปริมาณสูง ในการวิจัยส่วนที่สองได้ศึกษาความเลือกจำเพาะของปฏิกิริยาแอลฟาออกซิจิเนชันของไซคลิกเอมีนที่เชื่อมต่อกับวงเบนซีน และปฏิกิริยาดีไฮโดรจิเนชันของเอมีน เพื่อให้ได้สารผลิตภัณฑ์แลกแทม และอิมมีนตามลำดับ ภาวะที่ดีที่สุดสำหรับปฏิกิริยาเอ็น-ฟอร์มิลเลชันของเอมีน, ปฏิกิริยาแอลฟาออกซิจิเนชัน และปฏิกิริยาดีไฮโดรจิเนชันของไซคลิกเอมีนสามารถอธิบายได้ด้วยกลไกการเกิดปฏิกิริยาเหล่านั้น ปฏิกิริยาจะไม่สามารถเกิดได้ถ้าไม่มี Au:PVP หรือเบสในระบบ หรือการใช้ทองที่มีขนาดอนุภาคขนาดใหญ่ นอกจากนี้ปฏิกิริยาจะไม่สามารถเกิดได้ เมื่อทำปฏิกิริยาในระบบที่ไม่มีออกซิเจน

สาขาวิชา_____ปิโตรเคมี_____   ลายมือชื่อนิสิต ....

ปีการศึกษา_____2554_____   ลายมือชื่อ อ. ที่ปรึกษาวิทยานิพนธ์หลัก..............................

4973885023: MAJOR PETROCHEMISTRY

KEYWORDS:GOLD NANOCLUSTERS / N-FORMYLATION / AEROBIC OXIDATION / HOMOGENEOUS / AMINE / AMIDE

PATCHAREE PREEDASURIYACHAI: PREPARATION OF COLLOIDAL GOLD NANOCLUSTER (Au:PVP) AS CATALYST FOR AMIDE SYNTHESIS AND OXIDATION REACTIONS. ADVISOR: ASST. PROF. WARINTHORN CHAVASIRI, Ph.D., 125 pp.

In a typical size-controlled synthesis of colloidal gold nanoclusters, monodispersed ultra-small gold clusters stabilized by hydrophilic polymer, poly(N-vinyl-2-pyrrolidone) (PVP), are prepared in this research by rapid reduction of Au(III) ions of aqueous $HAuCl_4$ with $NaBH_4$ in the presence of PVP at 0 °C under vigorous stir for conventional batch mixing or in a microfluidic reactor to give gold clusters with average diameters of 1.3 and 1.1 nm, respectively. No surface plasmon band was observed at 520 nm in UV/Vis spectrum indicating that there is a negligible population of gold clusters larger than 2 nm. These Au:PVP were first used for N-formylation of amines which were carried out through the oxidation of methanol at reflux temperature or formalin at room temperature (27 °C) with excellent yield of corresponding amides. In the second part, selectivity of α-oxygenation of benzo-fused cyclic amines and dehydrogenation of amines were investigated to furnish corresponding lactams and imines, respectively. The optimized conditions for N-formyaltion of amines and α-oxygenation and also dehydrogenation of cyclic amines were disclosed together with the mechanisms of these reactions. The reaction could not proceed without Au:PVP or base additive or using a large size of gold clusters. In addition, no reaction was observed under anaerobic condition.

Field of Study: ___Petrochemistry___ Student's Signature _____

Academic Year: _____2011_____ Advisor's Signature _____

ACKNOWLEDGEMENTS

CONTENTS

LIST OF TABLES

LIST OF FIGURES

Figure **Pages**

LIST OF SCHEMES

Schemes   **Pages**

LIST OF ABBREVIATIONS

δ	chemical shift (NMR)
J	coupling constant (NMR)
θ	theta
Å	angstrom unit
π^*	pi antibonding orbital
ϕ	diameter
μL	microliter(s)
aq.	aqueous
a.u.	absorbance unit
bs	broad singlet (NMR)
CAS No.	chemical abstracts service number
cm^{-1}	wave number (IR)
ºC	degree Celsius
$CDCl_3$	deuterated chloroform
CDMT	2-chloro-4,6-dimethoxy-1,3,5-trazine
Da	dalton
DBU	diazabicycloundecene
DCC	*N,N'*-dicyclohexylcarbodiimide
DIBALH	diisobutylaluminium hydride
DMSO	dimethyl lsulfoxide
DMF	dimethyl formamide
d	doublet (NMR)
dd	doublets of doublet (NMR)
dt	doublets of triplet (NMR)
EDCI	1-ethyl-3-(3-dimethylaminopropyl)carbodiimide
equiv.	equivalent
EtOAc	ethyl acetate
EtOH	ethanol

eV	electronvolt
$FeCl_3$	iron(III) chloride
g	gram(s)
h	hour(s)
HCHO	formaldehyde
HCOOH	formic acid
HCOOMe	methyl formate
HCO_2NH_4	ammonium formate
Hz	hertz
K	kelvin
K_2CO_3	potassium carbonate
KOAc	potassium acetate
m	multiplet (NMR)
mL	milliliter(s)
mM	millimolar
mmol	millimole
m.p.	melting point
Me	methyl group
MeOH	methanol
MHz	megahertz
NaF	sodium fluoride
min	minute
NaOMe	sodium methoxide
nm	nanometer(s)
NMR	nuclear magnetic resonance
PAA	poly(acrylic acid)
PEO-PPO	poly(ethylene oxide)-poly(propylene oxide) block copolymer
pH	potential of hydrogen ion
Ph	phenyl group
PoPD	poly(o-phenylenediamine)
PS	polystyrene
PTLC	precipitation thin-layer chromatography

q	quartet (NMR)
rpm	revolution per minute
s	singlet (NMR)
t	triplet (NMR)
t-BuO$_2$H	t-butyl hydroperoxide
t-BuOH	t-butanol
THPC	tetrakis(hydroxymethyl)phosphonium chloride
TLC	thin layer chromatography
TOF	turnover frequency
Ts	tosyl group

CHAPTER I

INTRODUCTION

1.1   Gold nanocluster as a catalyst

Gold complexes having Au(I) or Au(III) states are well–established as the best choice for different kinds of organic reaction in both heterogeneous and homogeneous processes involving oxidation, reduction, carbon-carbon bond formation, carbon-heteroatom formation, nucleophilic addition and so on [1-4]. In contrast, metallic gold or Au(0) is one of gold species that is very popular for being chemically inert and also known as the most stable metals and resistant to oxidation, because of the highest ionization energy. There is remarkably different chemical character between metallic gold and gold complexes (Figure 1.1).
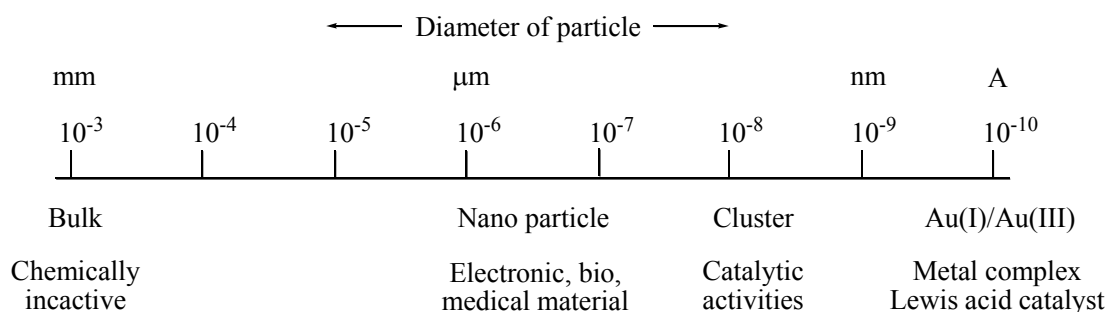
Figure 1.1 Size dependence for the character of gold.

Interestingly, the discovery by Haruta and co-workers in 1987, Au nanoparticles were highly active catalysis for CO and H_2 oxidation, NO reduction, water-gas shift reaction, CO_2 hydrogenation, and catalytic combustion of methanol [5,6]. The size dependence of cluster was observed and the TOF was drastically increased with a decrease in the diameter around 3-4 nm of gold clusters at 273 K. The oxidation by gold nanoparticles has become a hot topic in chemistry. In particular, an aerobic oxidation using molecular oxygen as an oxidant has attracted as the development for environmentally friendly catalysis processes. Many reports involving aerobic oxidation of small sized gold clusters have been presented. Rossi

and co-workers was firstly demonstrated the aerobic oxidation of small sized gold clusters without supporter as a catalyst for the oxidation of glucose. However, the gold clusters with supporter avoid particle aggregation in solution and preserved the activity for longer [7]. This observation is in good agreement with bare gold clusters in the gas phase which can catalyze the oxidation of CO by O_2 [8]. Among the investigation on CO oxidation, the adsorption of molecular oxygen on gold clusters was described (Figure 1.2) [9]. Electron will transfer from metal oxide supporter to activate Au cluster and follow by electron transfer from Au cluster to oxygen molecule. The superoxo-like species was generated by partial electron transfer from 5d orbital of gold clusters to the antibonding π^* orbital of O_2 [10]. The electron transfer from gold nanocluster to molecular oxygen was observed using $Au_nO_2^-$ photoelectron spectroscopy [11]. In addition, the adsorption of water on Au cluster is expected to assist the electron donation and increase the activity (Figure 1.3) [12].
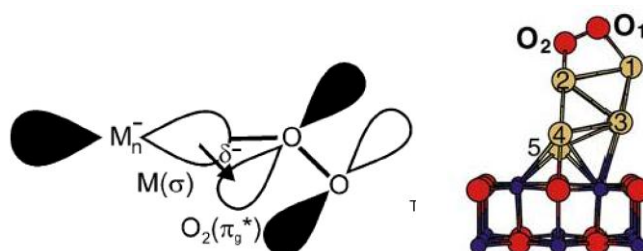
Figure 1.2 Adsorption of molecular oxygen on the gold clusters surface [9]
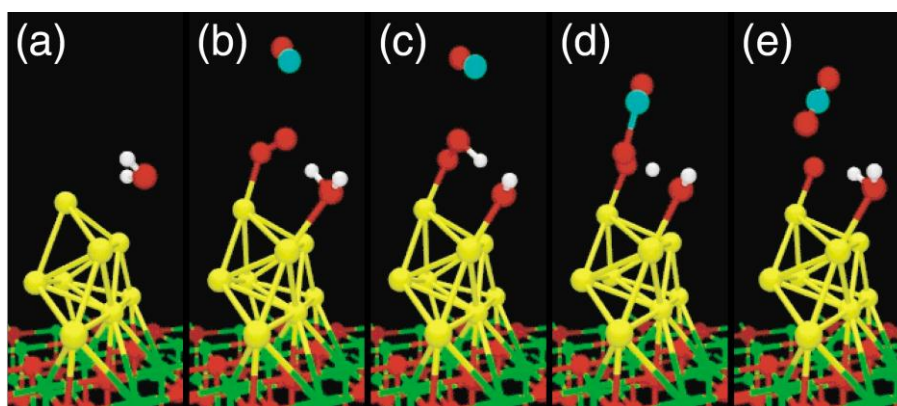
Figure 1.3 Adsorption of water on gold clusters surface enhancing the activity of gold in CO oxidation [12].

The primary role of the supporter is to avoid the aggregation of nanoclusters. The preparation of gold nanoclusters was succeeded by using many kinds of materials. The second role is the act of support in the reaction mechanism to boost the ability of gold catalyst. The strategies to stabilize gold nanoclusters against the aggregation are shown in Figure 1.4.
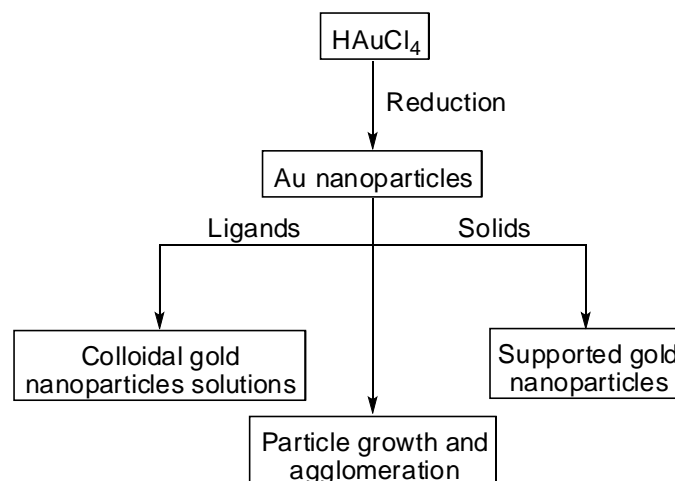
Figure 1.4 Strategies to stabilize gold nanoclusters against agglomeration.

Many kinds of heterogeneous gold catalysts have been developed. The most widely reported supports were inorganic solids such as charcoal [13], silica [14], alumina [15], and metal oxides [15-16]. There were highly active and stable in the oxidation reaction such as CO, alcohols, cyclohexane, styrene, propene and *etc*. (Scheme 1.1) [17,18]. The controlling of particle size and the structures of their interfaces with solid supports is difficult. Therefore, it is difficult to clearify in the principle for the fabrication of active gold catalysts. To make the ideal system with small gold clusters less than 1 nm for activation of molecular oxygen, the colloidal gold clusters has been developed.

Oxidation of cyclohexene
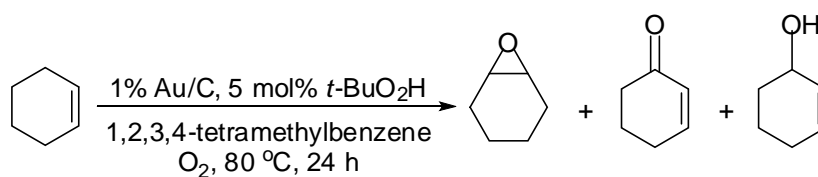
Oxidation of propene
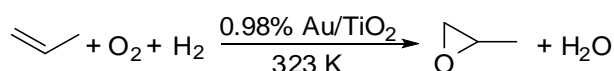
Oxidation of alcohols
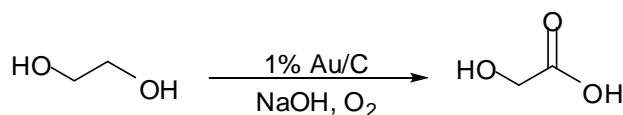
Scheme 1.1 Oxidation by heterogeneous Au nanocluster catalysts.

Colloidal gold clusters represent as a bridge between homogeneous and heterogeneous catalysis called "*quasi*-homogeneous" which are dispersed in a medium with multiple but weak coordination to organic stabilizers. Thus, the cluster surface can expose to have catalytic activity. In addition, the cluster size can be controlled to give more fine clusters than that of heterogeneous catalysts which the effect of the size of clusters is important for activity of reaction. Furthermore, the homogeneous catalytic system is expected to have higher catalytic activity than heterogeneous system.

1.2 Preparation and characterization of colloidal nanogold

1.2.1 Overview [17,19-20]
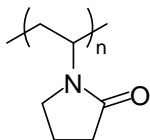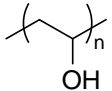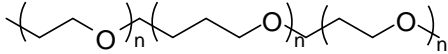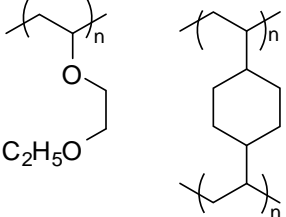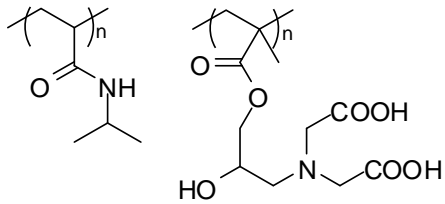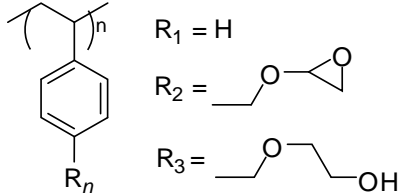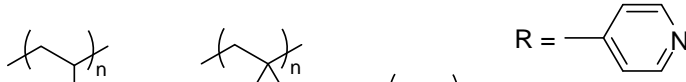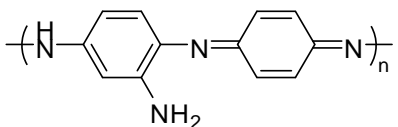
The general material for preparing of colloidal gold nanoclusters is tetrachloroauric acid ($HAuCl_4$) obtained from the mixture of nitric acid and hydrochloric acid (*aqua regia*) with gold metal. The formation of gold nanoclusters on polymer was done by the reduction of gold ions (Au^{3+}).

The main role of stabilizer was to reduce the mobility of the metal nanoparticles to inhibit the aggregation or cohesion of Au(0) at a very early stage, then the nanometer-sized of gold clusters was obtained. The average size of clusters could be controlled by the nature of polymer and concentration between polymer and gold ion in the solution. The amount of reducing agent was also one of factors for the size distribution of clusters. In addition, the temperature at the reduction process was very important. The high temperature could induce the aggregation of gold nanoclusters to bigger size and destroy the catalytic activity, because of the weak coordination between gold clusters and polymer.

The polymer on the gold cluster could act as the protecting layer against the cohesion of nanoclusters, so that the gold clusters could be treated as normal chemical compounds. They could keep in the powder form by freeze-dry method and then redispersed in liquid media. The polymer was an ideal for catalytic applications, because the multiple and weak coordination between gold clusters and polymer could expose gold surface to substrates, and then permitted catalytic conversion. In contrast with the stabilization of gold clusters by organic ligands such as alkylthiol, arylthiol or phosphines, the strong adsorption of thiol on the gold cluster surface could deactivate the catalytic activity of gold nanoclusters [19].

Some stabilizing polymers that are used in the preparation of colloidal gold nanoclusters are listed in Table 1.1.

Table 1.1 Structure of stabilizing polymers [20]

Description	Structure
PVP	
PVA	
PEO-PPO	
THPC	
star EOEOVE	
PNIPAM	
PS	
PAA-1 PAA-2 PAA-3	
PoPD	

The polymers in this list usually contained oxygen, nitrogen, or sulfur moieties for introducing the coordination of gold clusters. Poly(*N*-vinyl-2-pyrrolidone) (PVP) had the oxygen moiety to interact with the metal clusters, so PVP was used as the stabilizing material for many transition metals such as platinum, palladium or rhodium including gold [20-22]. The weak point of *quasi*-homogeneous catalyst was the ultra filtration on a membrane filter is required for the recovery process after use in the reaction. Thus, polyacrylamide (PAA) microgels [23] with no dispersible in water were used and it could be simply recovered by filtration in the same as for heterogeneous catalyst. To use *quasi*-homogeneous ability, the star(EOEOVE) (EOEOVE = 2-(2-ethoxy)ethoxyethyl vinyl ether) [24] or poly(*N*-isopropyl-acrylamide) (PNIPAM) [25] which can disperse in water at low temperature (< 40 °C) and easily precipitated at above 40 °C. Both of them could easily separate by their lower critical solution temperature (LCST) type phase-separation behavior.

Herein, the gold nanocluster stabilized by hydrophilic polymer, PVP, was selected as *quasi*-homogeneous catalysis in this study, because of the simple preparation and stability both in water solution or powder form and also no deactivation of gold clusters from stabilization of PVP.

1.2.2 PVP-stabilized gold clusters

The typical method for size-controlled colloidal nanogold, monodisperse ultra-small gold clusters stabilized by PVP (Au:PVP) involved the rapid reduction of Au(III) ions (HAuCl$_4$) with a strong reducing agent (NaBH$_4$) in the presence of PVP dispersing in water at O°C. The brownish solution was immediately obtained after mixed AuCl$_4^-$ and BH$_4^-$ (Scheme 1.2). The batch mixing process [26] and microfluidic reactor [27] were developed to get the smaller size of gold clusters (Figure 1.5). The size of Au:PVP clusters prepared by microfluidic reactor was smaller than that from batch process, because of the more homogeneous mixing solution by overlaying laminated substreams (70 micrometers thick) between AuCl$_4^-$ and NaBH$_4$ than vigorous stirred solution in batch process. The larger size of gold clusters was prepared by reduction of additional AuCl$_4^-$ with a weak reducing agent (Na$_2$SO$_3$). The reduction of Au(III) occurred only on the surfaces of the cluster seed. The growing of

small clusters was depended on the amount of addition of $AuCl_4^-$ ions. Thus, a series of monodisperse Au:PVP clusters with average diameters in the range of 1.1-9.5 nanometers were prepared by gradually increasing the concentration ratio of $AuCl_4^-$ to Au(0) [28].

$$HAuCl_4 + PVP\ (K = 30) \xrightarrow[\text{H}_2\text{O, 273 K}]{\text{NaBH}_4} Au:PVP\text{-}1$$

$$Au:PVP\text{-}1 + HAuCl_4 \xrightarrow[\text{H}_2\text{O, 273 K}]{\text{Na}_2\text{SO}_3} Au:PVP\text{-}n$$

n = 1,2,3,4,5,6,7
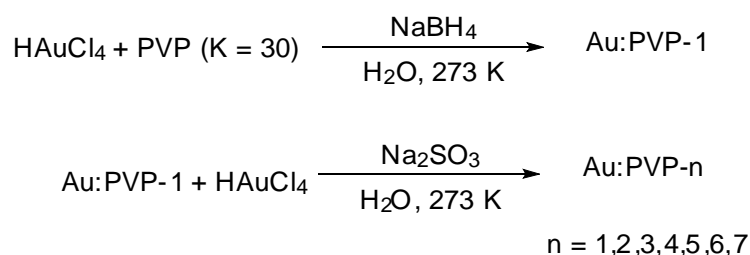
Scheme 1.2 Preparation of Au:PVP.
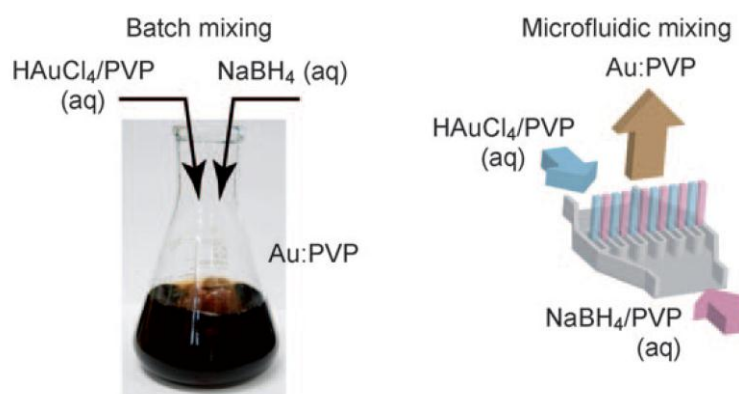
Figure 1.5 Method for preparing Au:PVP in batch process and microfluidic reactor [20].

The Au:PVP clusters have been characterized by transmission electron microscopy (TEM), powder X-ray diffraction (XRD), X-ray absorption near edge structure (Au L_3-edge XANES), extended X-ray absorption fine structure (EXAFS) analysis, X-ray photoelectron spectroscopy (XPS) and matrix-assisted laser desorption ionization (MALDI) mass spectrometry (Figure 1.6). The XRD measurement afforded a broad (111) corresponding to face-centered cubic (fcc) structure of gold nanoclusters. The XPS analysis showed core-level peaks of C(1s), N(1s), O(1s), and Au(4f). The Au(4f$_{7/2}$) binding energy of 83.5 eV agree well with those of typical Au(0) nanoparticles. Au:PVP did not contain ion species such as

$AuCl_4^-$ or $AuCl_2^-$, because the signal of Cl was not observed. The intensity of 11.93 keV in the Au L_3-edge XANES was smaller than the bulk gold, thereby the gold clusters in Au:PVP was anionic character than bulk gold due to electron was transferred from 5d orbital through the interaction with PVP.
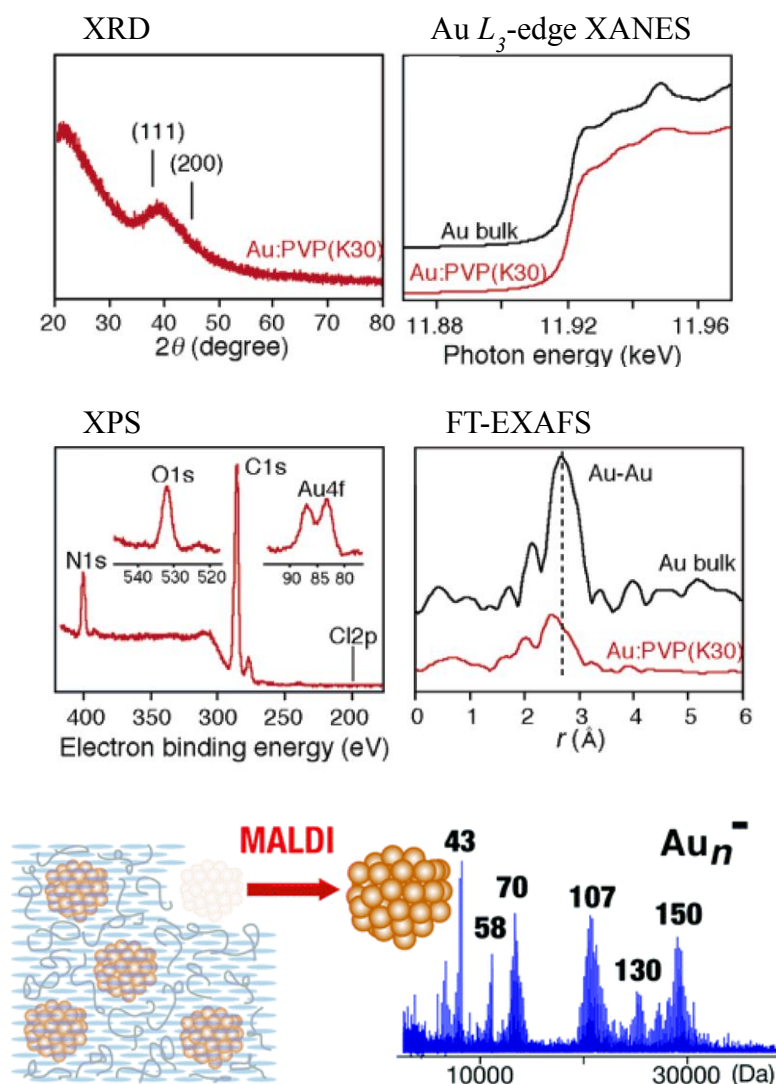
Figure 1.6 Characterization data of Au:PVP [26-27,29].

XRD and EXAFS measurements supported the production of smaller gold clusters by microfluidic mixing. Negative-ion MALDI mass spectra of Au:PVP was taken at the lowest possible laser fluence to suppress fragmentation of the clusters (Figure 1.6). A series of magic numbers for the gold cluster size have been discovered as 35, 43, 58, 70, 107, 130, and 150 [29].
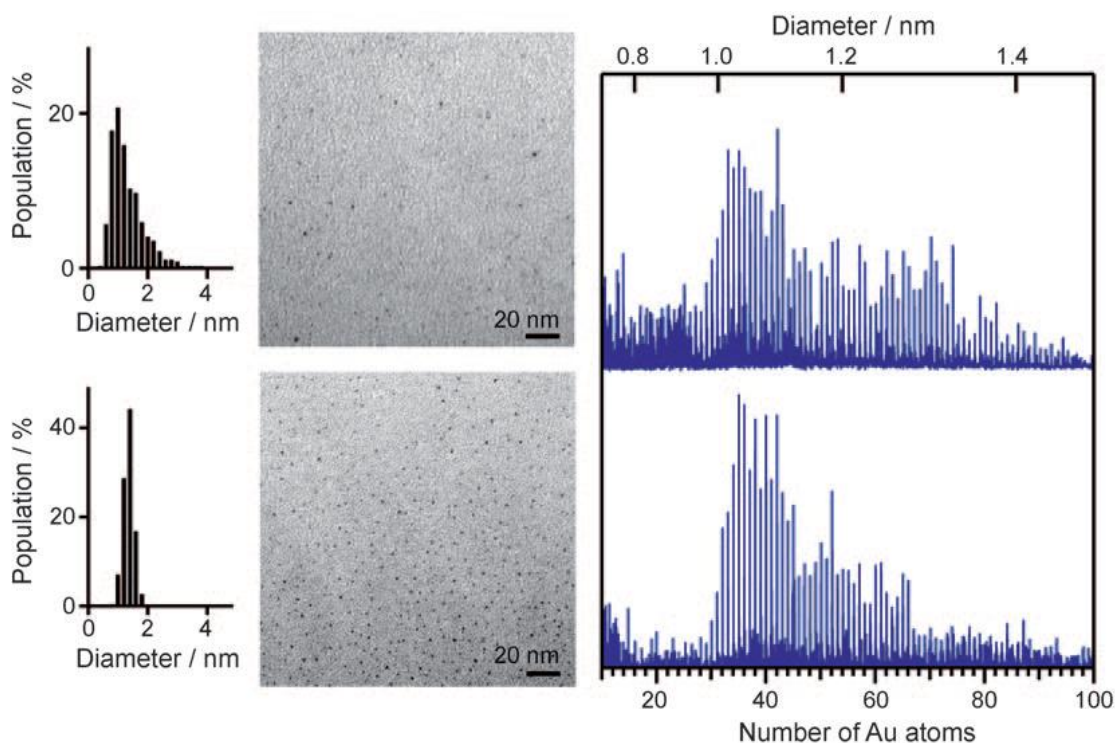
Figure 1.7 TEM images and core-size distributions of Au:PVP prepared by batch mixing (top) and microfluidic mixing (bottom) [27].

Size distributions of Au nanoclusters were displayed in Figure 1.7. These data indicated that the narrow and smaller sizes of clusters were obtained from microfluidic mixing method [27].

The UV/Vis absorption spectrum of Au:PVP was presented in Figure 1.8 [28]. 1.3 nm of Au:PVP showed no surface plasmon band, because there was no metallic character on small size of gold clusters. On the other word, there was a negligible population of gold clusters larger than two nanometers. In addition, the surface Plasmon bands of ~520 nanometer were caused by metallic character of gold nanocluster that appeared in the UV/Vis absorption spectrum in Figure 1.8 of bigger size of Au:PVP clusters. Likewise, TEM images are shown in Figure 1.9. Gold clusters size exhibited in the images with average diameters.
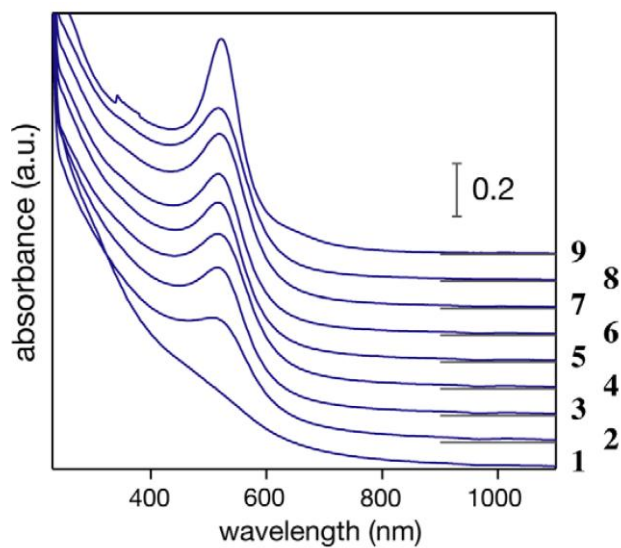
Figure 1.8 UV/Vis absorption spectra of Au:PVP [28].
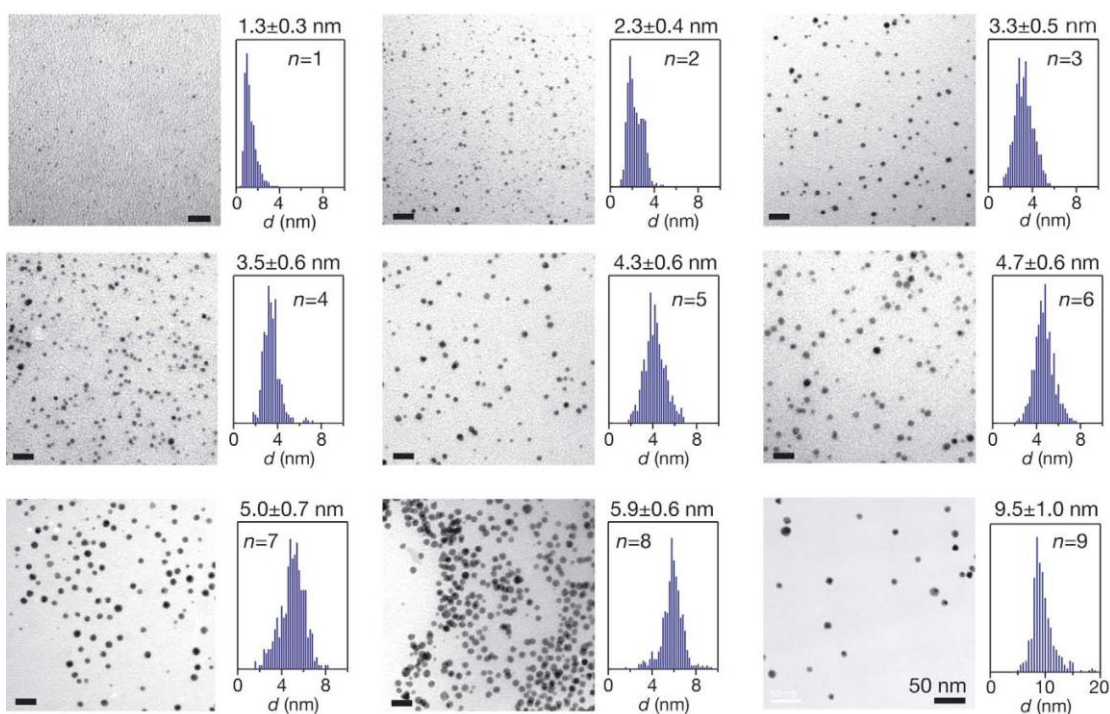
Figure 1.9 TEM images of Au:PVP and size distribution [28].

The electron release from PVP to gold cluster was observed by Fourier transform infrared spectroscopy (FT-IR) using adsorbed CO as a probe (Figure 1.10) [30]. The different amounts of PVP in Au:PVP cluster ([PVP]/[Au] = 40-250) was detected in CH_2Cl_2 by FT-IR. The free CO dissolved in the solvent were monitored

and showed the population of adsorbed CO. The results showed that the adsorbed CO gradually decreased with the increase of the PVP concentration. It regarded that PVP was bound more strongly gold cluster than CO. The wavenumber of C-O bond was red-shift from 2107 to 2098 cm^{-1} when PVP concentration increased. This result implied that additional PVP could donate more electronic charge to the gold cluster. Thus, the electron rich gold clusters donated the electron to oxygen molecule to be active molecular oxygen on cluster surface (Figure 1.10).
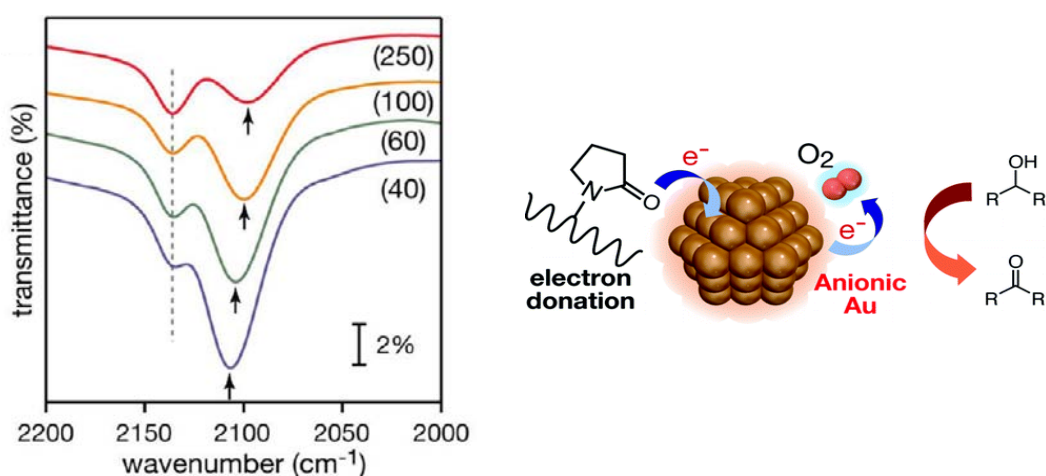
Figure 1.10 FTIR spectra of ^{12}CO adsorbed on Au:PVP with various PVP concentrations and the electron donating from PVP to gold clusters to active molecular oxygen [30].

1.3   Application of PVP-stabilized gold clusters as an oxidation catalyst

1.3.1   Oxidation of alcohol in water [28,30,31]

As shown above, Au:PVP could promote the aerobic oxidation and played the important role as an oxidation catalyst by adsorbing molecular oxygen to be superoxo form as an oxidant. Tsukuda, Sakurai and Tsunoyama firstly developed the 1.3 nm of Au:PVP and used it in the oxidation of alcohol in water. Various types of alcohol including primary and secondary alcohols could be easily oxidized giving the corresponding carboxylic acids and ketones, respectively (Schemes 1.3 and 1.4).

Benzylic

X = H 85%

Me 93%

NO$_2$ 94%

Alipatic

$$C_5H_{11}CH_2OH \xrightarrow[\text{H}_2\text{O, 67 }^{\circ}\text{C, 24 h}]{\substack{\text{2 atom\% Au:PVP} \\ \text{300 mol\% K}_2\text{CO}_3}} C_5H_{11}COOH$$

> 99%
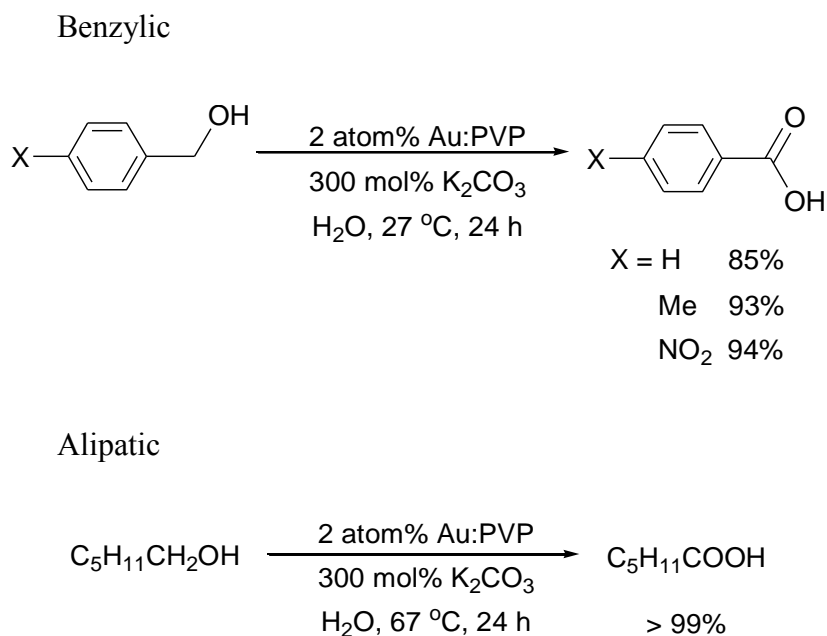
Scheme 1.3 Aerobic oxidations of primary alcohols catalyzed by Au:PVP [28,31].

Benzylic

98%

> 99%

Aliphatic

98%
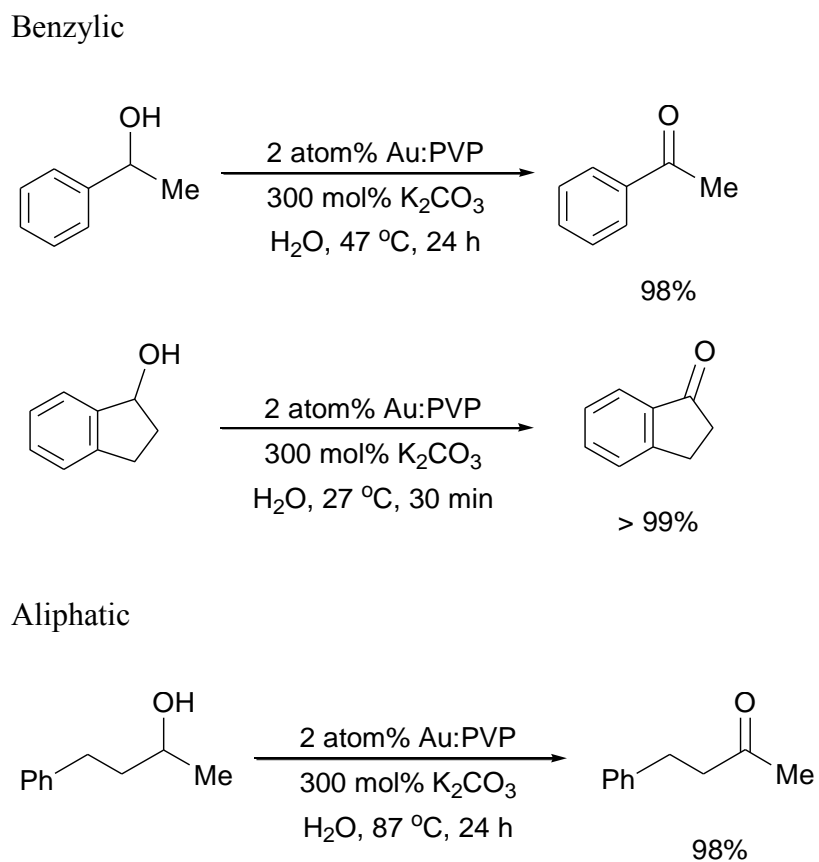
Scheme 1.4 Aerobic oxidations of secondary alcohols catalyzed by Au:PVP [30,31].

The reactions did not proceed under the reaction without base or oxygen because these molecular oxygens act as an oxidant for aerobic oxidation. In contrast with Pd nanocluster case, the aerobic oxidation can proceed in the absence of base because of different mechanism. The oxidation of Pd(0) nanoclusters proceeds *via* oxidative addition on Pd surface to afford the alkoxide and hydride. Then, β-hydrogen elimination from adsorbed alkoxide to form Pd-hydride and the corresponding aldehyde were rate-determing step. Finally, molecular oxygen removed the hydride species from the Pd surface (Figure 1.11) [32].
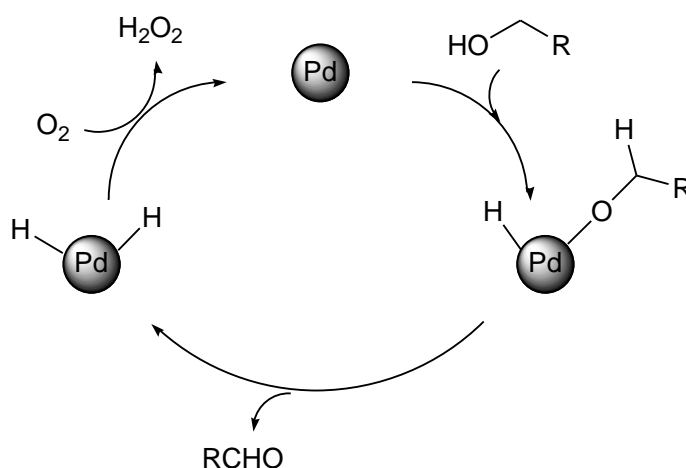
Figure 1.11 Proposed mechanism of Pd nanoclusters catalyst in aerobic oxidation of alcohol.

In contrast, the oxidative addition on Au:PVP was not favored. On the basis of Au cluster in gas phase, molecular oxygen was activated by adsorption on negative Au surface to form peroxo-like species [11]. Thus, the smaller gold clusters in Au:PVP were negatively charged, they should activate oxygen molecule by donation of electronic charge from clusters. The proposed mechanism of Au:PVP in aerobic oxidation of alcohol are shown in Figure 1.12. Sakurai and co-workers proposed that the excess electronic charges on gold surface were transferred to molecular oxygen to form superoxo or peroxo species. Then, these active species abstracted hydrogen from alcohol to become the corresponding aldehyde. Furthermore, 5-10% silver doped in Au:PVP could increase the activity in the oxidation of alcohol due to the increasing electron donation to the gold moiety [33].
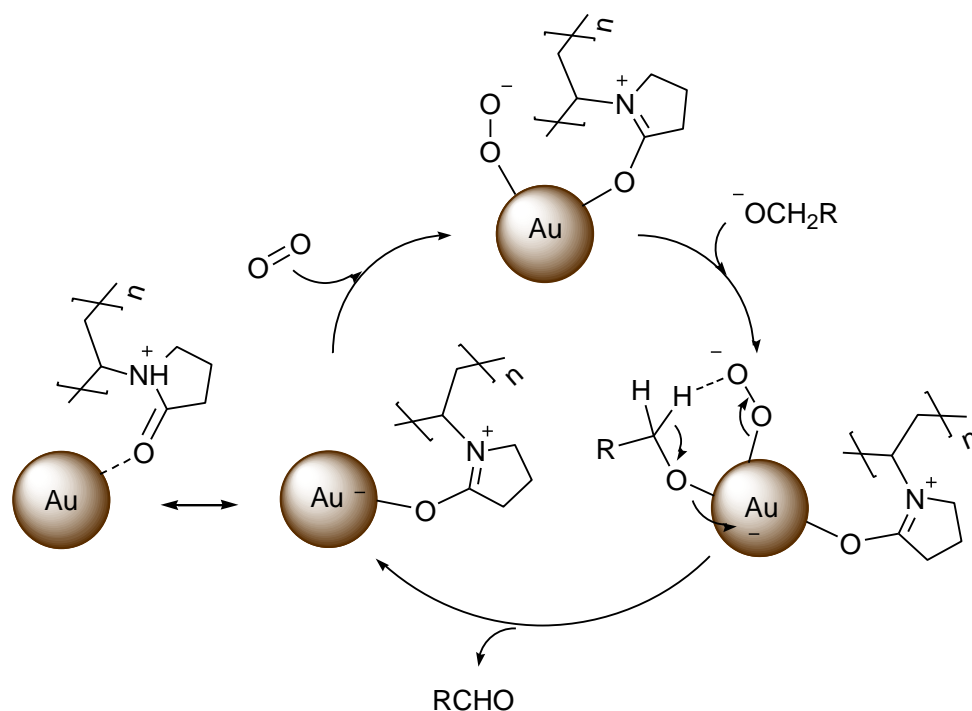
Figure 1.12 Proposed mechanism of Au:PVP in aerobic oxidation of alcohol.

Another mechanism has recently been proposed by Kobayashi and Chechik [34]. They detected a Au-H intermediate in the oxidation of alcohol on Au:PS catalyst by using spin-trapping techniques in ESR spectroscopy (Figure 1.13). They proposed that hydrogen or hydride was transferred to gold clusters followed by H-abstraction by oxygen molecule to form HOO$\cdot$ radical. The different mechanisms were associated with various charge states of clusters involving different supporters. Au:PPh$_3$ clusters and Au/CeO$_2$ catalysts were also observed Au-H adduct, in both of which gold was positively charged [35]. This difference should depend on the functional groups present on the polymers and cluster size to show the different catalytic performance.
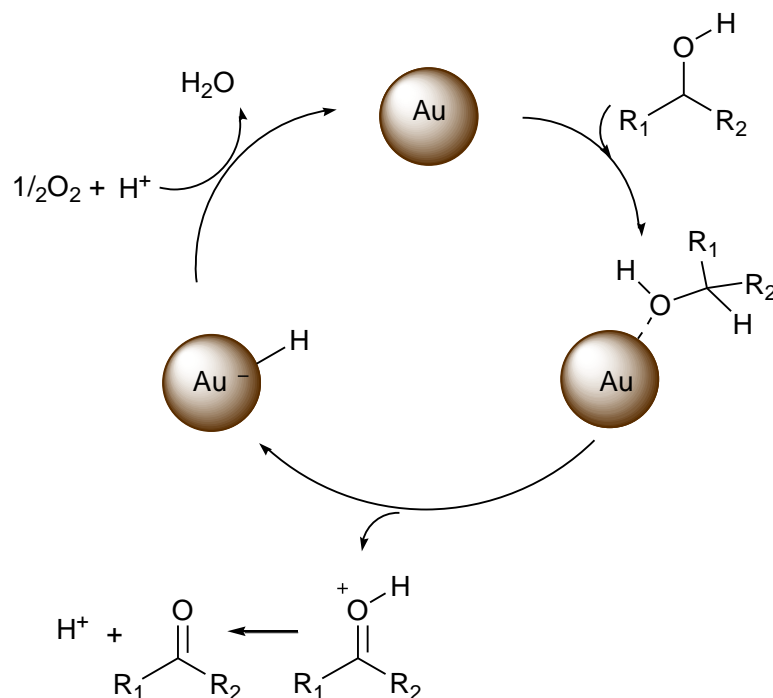
Figure 1.13 Proposed mechanism of Au:PS in aerobic oxidation of alcohol.

1.3.2 Oxygenation of benzylic ketones [36]

Au:PVP could promote the autoxidation type reaction and α-hydroxylation reaction of benzylic ketones. The selectivity of product was controlled by changing the solvent and base (Scheme 1.5). The formation of α-peroxide intermediate from bond cleavage proceeded spontaneously in aqueous media to give the autoxidation products. In contrast, the α-hydroxylation product was obtained in the presence of dimethyl sulfoxide (DMSO) as a solvent.
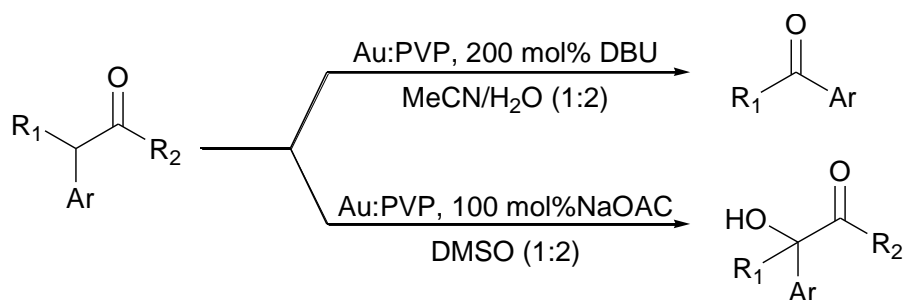
Scheme 1.5 Oxygenation of benzylic ketones catalyzed by Au:PVP.

The possible mechanism was shown in Figure 1.14. Au clusters would activate molecular oxygen to form superoxo-like species and the enolate of ketone substrates was adsorbed onto the Au cluster surface. Autoxidation took place predominantly in water/acetonitrile medium to give the corresponding peroxide intermediate. Peroxide was transformed to the corresponding aryl ketones with cleavage of carbon-carbon bond and α-hydroxylation product was obtained by reduction of peroxide with cleavage of oxygen-oxygen bond in DMSO. The carbon-carbon bond cleavage from peroxide intermediate could proceed without water, but the peroxide intermediate was produced at the beginning. In addition, DMSO worked as a reductant in *α*-hydroxylation pathway.
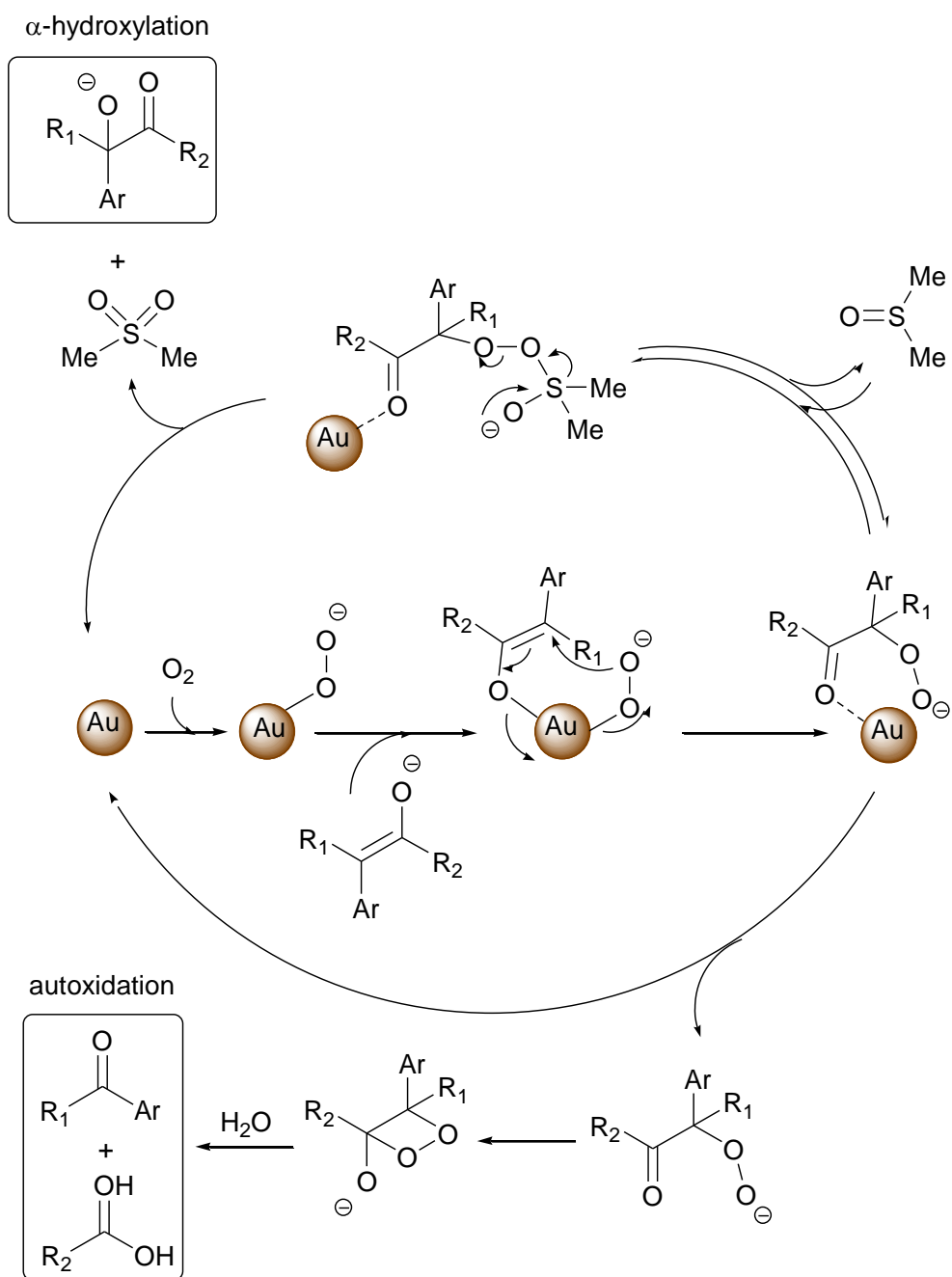
Figure 1.14 Proposed mechanism of Au:PVP in oxygenation of benzyl ketone.

1.3.3 Oxidation of organoboron compounds.

Au:PVP could promote the homocoupling reaction of arylboronic acids [26]. The aerobic oxidation of phenyl boronic acid in aqueous K_2CO_3 could proceed under aerobic conditions to give biphenyl and phenol (Scheme 1.6) [36].
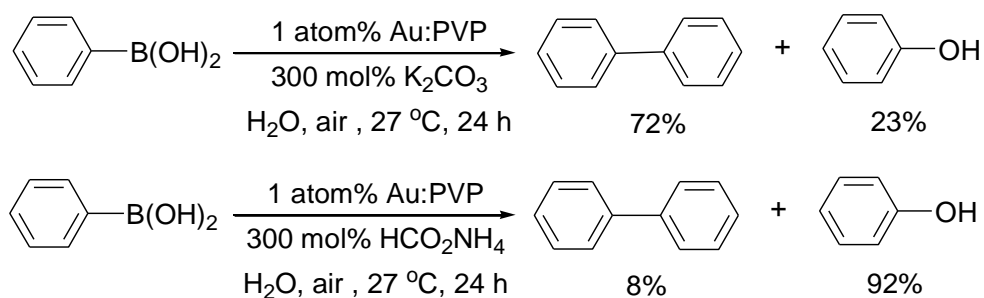
Scheme 1.6 Homocoupling and oxygenation of phenylboronic acid.

The homocoupling of phenylboronic acid was catalyzed by Au:PVP giving biphenyl, but the latter product may not produce by a direct gold catalyzed process. The oxidation of phenylboronic acid with H_2O_2 co-product in the coupling reaction may be possible. In addition phenol could be selective generated in ammonium formate as reductant.

To yield only biphenyl by gold nanoclusters catalyzed carbon-carbon formation reaction, the potassium aryltrifluoroborate ($ArBF_3K$) was used [37]. Biphenyl was formed selectively and quantitatively in the Au:PVP-catalyzed aerobic oxidation of $PhBF_3K$ under weakly basic to neutral conditions (pH 9.18-6.86, Scheme 1.7).
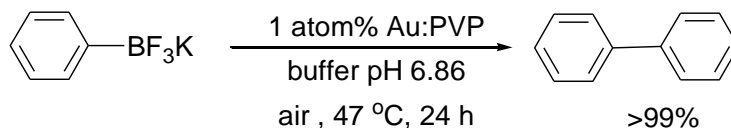
Scheme 1.7 Selective homocoupling from potassium phenyltrifluoroborate.

1.4 Application of PVP-stabilized gold clusters as a formal Lewis acidic catalyst

1.4.1 Intramolecular addition of alcohols to alkenes

Gold cluster surface could adsorb molecular oxygen, so that an electron-deficient site of cluster surface after the adsorption of oxygen could behave as a formal Lewis acid. Intramolecular hydroalkoxylation of alkenes was promoted by Lewis acid catalysts. To study the Lewis acid ability of gold clusters, Sakurai and co-workers investigated this reaction with Au:PVP as catalyst [38]. The hydro-alkoxylation did not occur under inert atmosphere or the bigger size (9.5 nm) of Au:PVP clusters, but 10 atom% of 1.3 nm of Au:PVP in the presence of DBU and H_2O/DMF at 50°C under aerobic conditions, tetrahydrofuran derivative was obtained in 87% yield from alkenyl alcohol (Scheme 1.8). This observation indicated that molecular oxygen was essential and ion species of gold was not active species for this reaction.

catalyst	conditions	yield
Au:PVP (1.3 nm)	under air	87%
Au:PVP (1.3 nm)	degassed condition	0%
Au:PVP (9.5 nm)	under air	0%
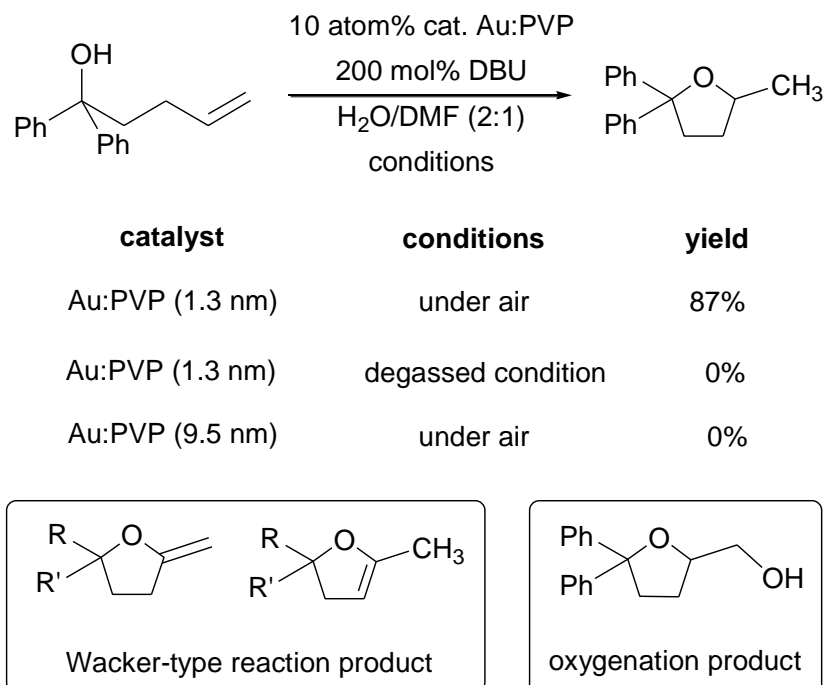
Scheme 1.8 Intramolecular hydroalkoxylation catalyzed by Au:PVP.

Normally, under aerobic oxidation conditions, γ-hydroxyalkenes underwent Wacker-type oxidation or oxygenation. In contrast, Au:PVP catalyst could proceed the reaction without Wacker-type reaction products or the oxygenation product. It was thought that molecular oxygen generated a reaction center of Lewis acid character on the cluster surface. The proposed mechanism was presented in Figure 1.15. The reaction proceed *via* the nucleophilec adsorption of alkoxide onto cationic site of gold cluster surface followed by cyclization, giving alkyl-Au intermediate. The oxygenation, β-elimination and protonation did not occur. The hydrogen was introduced from formyl group of DMF to give the product with regeneration of gold catalyst.
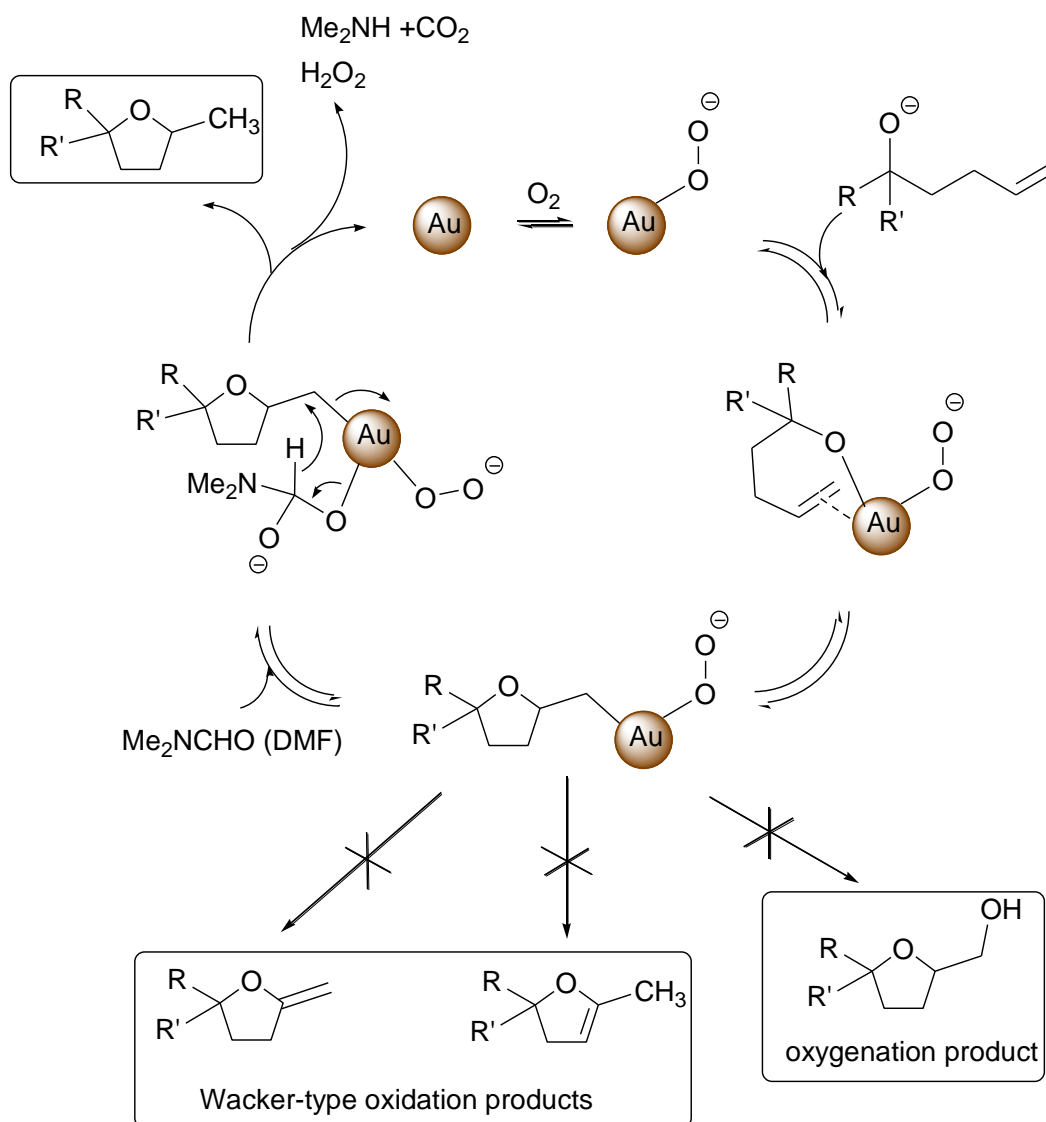
Figure 1.15 Proposed mechanism of intramolecular hydroalkoxylation catalyzed by Au:PVP.

1.4.2 Intramolecular addition of toluenesulfonamide

By analogy to the similar reactions of γ-hydroxyalkenes, it would be expected that the reaction of γ-(toluenesulfonylamino)alkenes should proceed in the presence of Au:PVP as a catalyst under aerobic conditions. The intramolecular addition of amine to carbon-carbon multiple bond proceed under similar hydroalkoxylation condition, 5 atom% of Au:PVP with 300 mol% of Cs_2CO_3 at 50°C in ethanol as solvent under aerobic condition (Scheme 1.9) [39]. The excellent yields of cycloaddition were

obtained, except for *p*-toluenesulfonyl protected alkenyl amide without *β*-substituted group. Only 41% yield was obtained because of lacking a germinal effect.
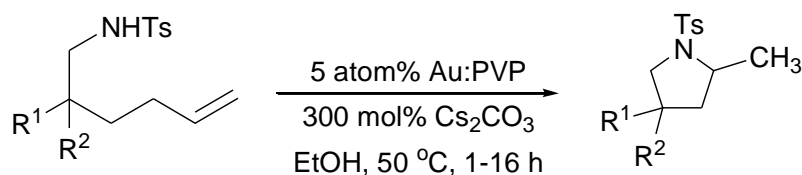
R1	R²	yield
Ph	Ph	>99%
Me	Ph	93%
H	Me	89%
Ph	Ph	81%
Me	Ph	41%

Scheme 1.9 Intramolecular addition of toluenesulfonamide.

Interestingly, aerobic oxidation of benzylic alcohol occurred predominantly to afford corresponding ketone (Scheme 1.10), because the aerobic oxidation of benzylic alcohol proceeded rapidly even at room temperature. On the other hand, benzylic oxidation could not proceed in the case of toluenesulfonamide. Cyclization took place to provide tricyclic product.
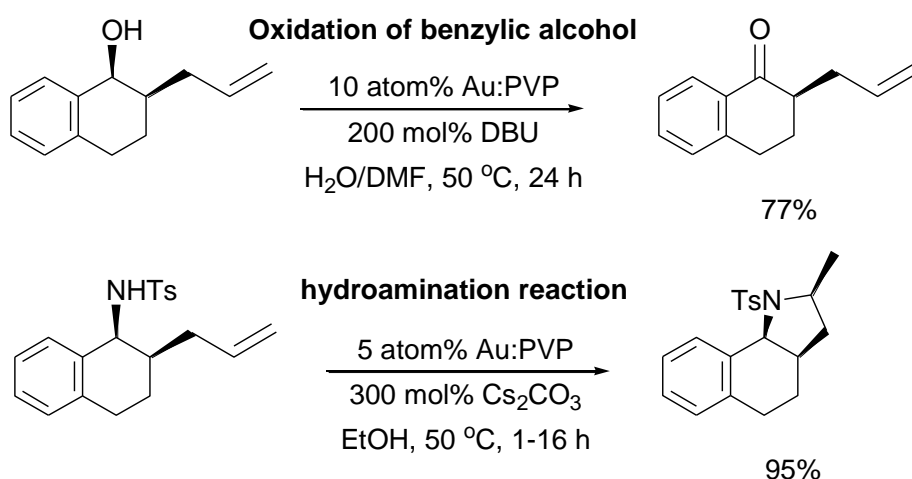
Scheme 1.10 Comparison between the oxidation of benzylic alcohol and intramolecular addition of toluenesulfonamide.

The proposed mechanism is shown in Figure 1.16. The formation of superoxo-like species by adsorption of molecular oxygen on gold cluster surface was the initiated step. The toluenesulfonamide anion generated in basic conditions promoted the intramolecular addition to π-activation of olefin, which activated by adsorption on electron-deficient site of gold surface. Toluenesulfonamide anion attacked olefin from the opposite side of adsorbed to afford alkyl-Au intermediate. Ethanol should be adsorbed on the cluster surface as ethoxide and then hydrogen of ethyl group was abstracted to yield the corresponding cyclized product.
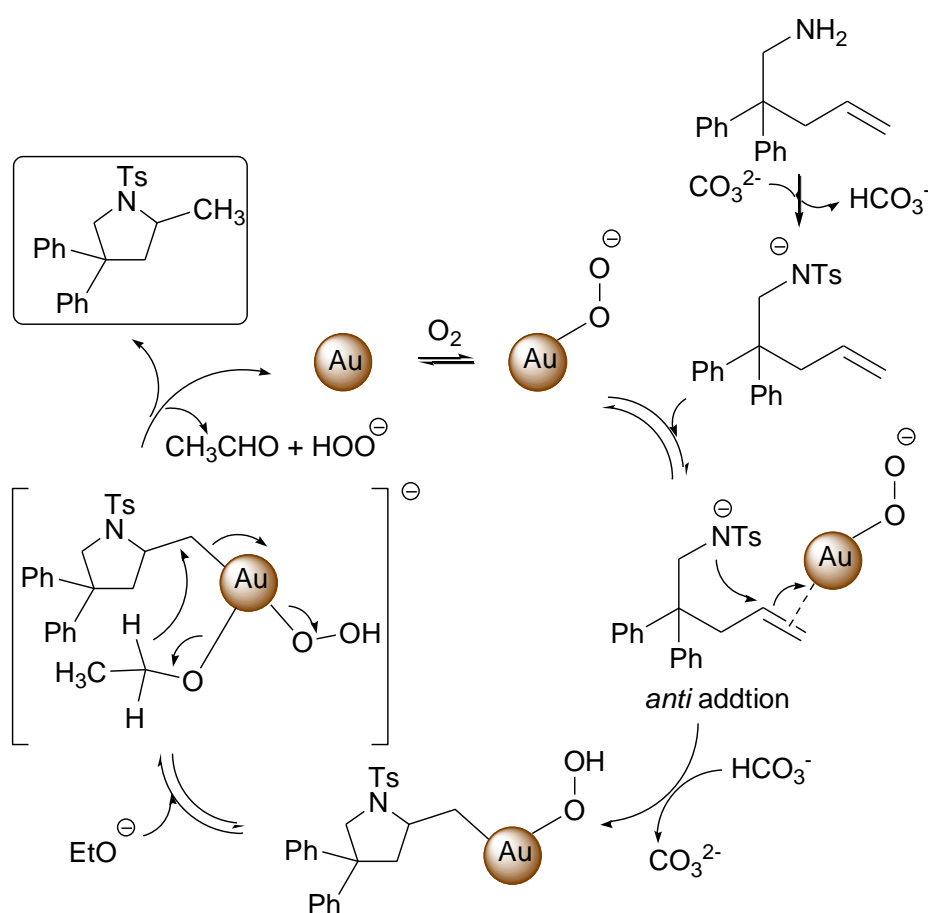
Figure 1.16 Proposed mechanism of intramolecular addition of toluenesulfonamide catalyzed by Au:PVP.

1.4.3 Intramolecular addition of primary amines

Catalysts for cyclization of primary amines are normally not stable to moisture and air. Au:PVP could be utilized in cyclization of primary amines under neutral or slightly acidic conditions with formic acid derivatives as reductants. In addition, the reaction was dependent on the acidity of solvent (Scheme 1.11) [40].
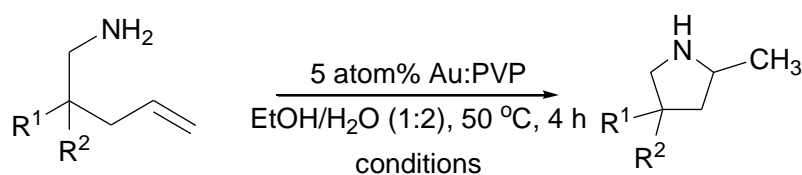
conditions	yield
1000 mol% HCO_2NH_4	83%
400 mol% HCO_2H, pH = 6.86 buffer	80%
1000 mol% HCO_2H, 500 mol% NH_4OH pH = 4.01 buffer	94%

Scheme 1.11 Intramolecular hydroamination of primary amines.
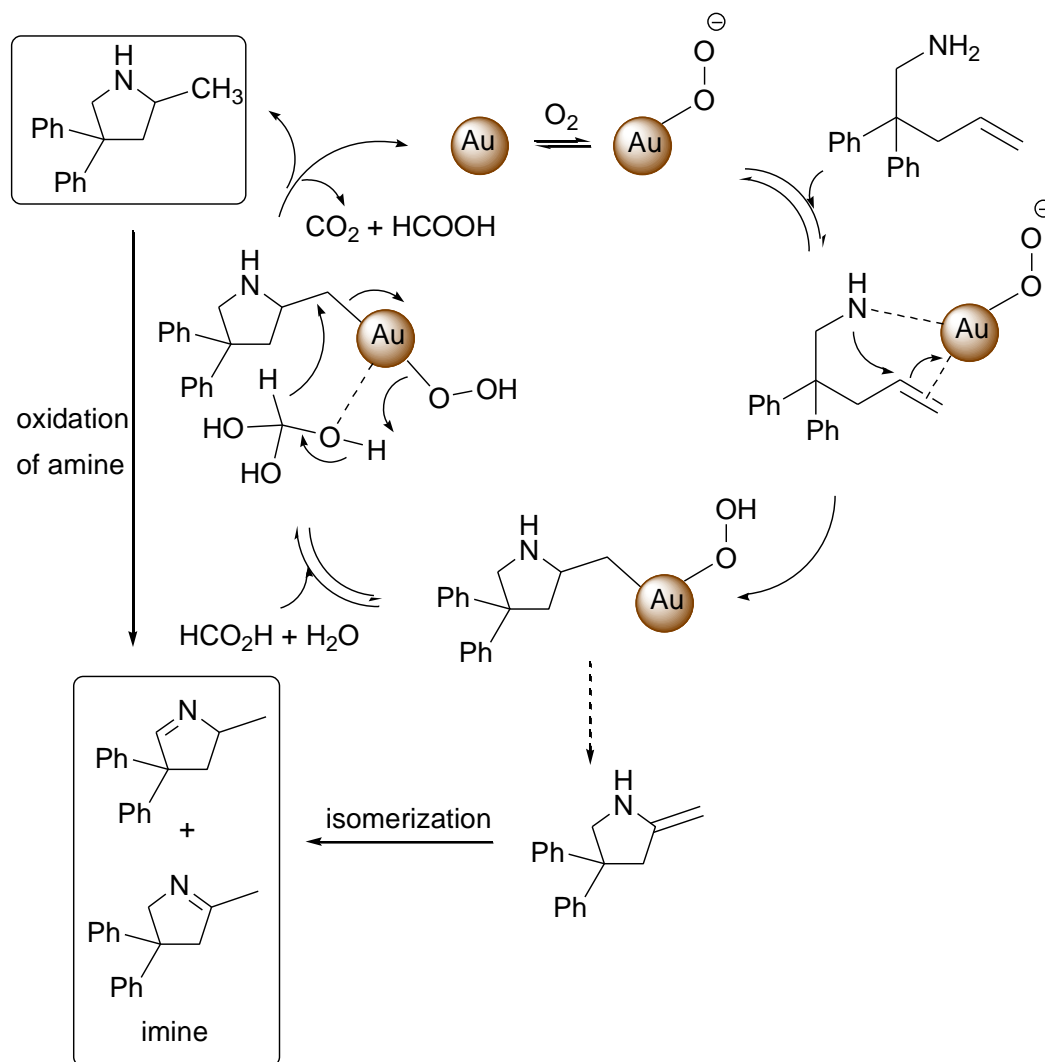
Figure 1.17 Proposed mechanism of intramolecular hydroamination of primary amines.

In this reaction, basic condition was not necessary because primary amines possessed high nucleophilicity and could adsorb on surface of gold cluster even under neutral or slightly acidic conditions. The formal Lewis acid character of gold clusters might be more efficient under neutral or slightly acidic conditions. In Figure 1.17, the reaction began with N-H bond insertion to olefin followed by the formation of alkyl-Au intermediate. Selective hydrogenation from formic acid may occur instead of adsorption of ethanol on gold cluster surface under neutral or slightly acidic conditions. Hydrogen of formyl group was abstracted to form cyclic amine. In addition, the formation of two imines may occur through secondary oxidation of

amine product as a major pathway or through isomerization followed by β-hydrogen elimination form the alkyl-Au intermediate as a minor pathway.

1.5   Objective of this research

Since Au:PVP has been widely explored, the quasi-homogeneous catalyst of gold clusters in catalysis application should be fascinated. Thus, air and moisture stable catalyst Au:PVP will be prepared for exploring 2 reactions. Firstly, the *N*-formylation of amine with MeOH oxidation or formalin condition was optimized and mechanism pathways were described endorsing with many of evidences. Secondly, the selectivity between α-oxygenation and dehydrogenation of amines was scrutinized.

CHAPTER II

EXPERIMENTAL

2.1   Instrument and equipments

^{1}H NMR spectra were measured on a JEOL JMN LAMBDA 400 spectrometer at 23°C at 400 MHz. $CDCl_3$ was used as a solvent and the residual solvent peaks were used as an internal standard (^{1}H NMR: 7.26 ppm).

GC/MS data was collected on a Shimadzu GCMS QP-2010 gas chromatograph interfaced with mass spectroscopy.

GC data was collected on a Shimadzu GCMS QP-2010 gas chromatograph. Hexadecane was used as an internal standard.

UV/Vis spectroscopic data was recorded by HITACHI, U-2010 from 200-1100 nm at room temperature (27°C).

TEM images were recorded with transmission electron microscopes operated at 300 kV (Hitachi H-9500, JEOL JEM-3100FEF).

2.2   Chemicals

Silica gel column chromatography was performed on Kanto 60N, Wako Wakosil C-300, or Yamazen Hi-Flash column using a Yamazen YFLC purification system. TLC analysis was performed using Merck silica gel 60 F_{254} and preparative TLC was conducted using Wako Wakogel B-5F. GPC was performed with Japan Analytical Industry LC-908W, LC-9201 using chloroform as a solvent. Other reagents and solvents were commercially purchased from TCI and Wako chemicals and further purified according to the standard methods, if necessary.

2.3   Syntheses

2.3.1   Preparation of gold nanoclusters stabilized by poly(*N*-vinyl-2-pyrroli-done): Au:PVP nanoclusters [26,28]

To the aqueous solution of HAuCl$_4$ (1 mM, 50 mL) was added 555 mg (0.0139 mmol) of poly(*N*-vinyl-2-pyrrolidone) (PVP). The mixture was further stirred for 30 minutes under a bath of 0°C. Then, the aqueous solution of NaBH$_4$ (0.1 M, 5 mL) was rapidly added into the mixture under vigorous stirring. The color of the reaction mixture immediately turned from pale yellow to dark brown, indicating the formation of small Au nanoclusters (NCs). The hydrosol of the Au:PVP NCs was dialyzed three times by centrifugal ultrafiltration (MWCO = 10 kDa) using 10 mL of H$_2$O. Finally, the Au:PVP clusters were concentrated by ultrafiltration and diluted with miliQ H$_2$O to the total volume that made the concentrations of Au atoms and PVP monomers be 0.5 and 50 mM, respectively. The solution of Au:PVP was then concentrated and freeze-dried and could be kept for longer time without any aggregation of nanoclusters.

2.3.2   Characterization of Au:PVP nanoclusters [26,28]

The precise characterizations were reported in previous reports. The UV/Vis and TEM were used to monitor the reproducibility of the preparative method.

2.3.2.1 Optical spectroscopy

UV/Vis absorption spectra of hydrosols of the Au:PVP NCs were recorded by a UV/Vis spectrophotometer. All measurements were performed at room temperature. An example of UV/Vis absorption spectrum of Au:PVP is recorded as shown in Figure 2.1.
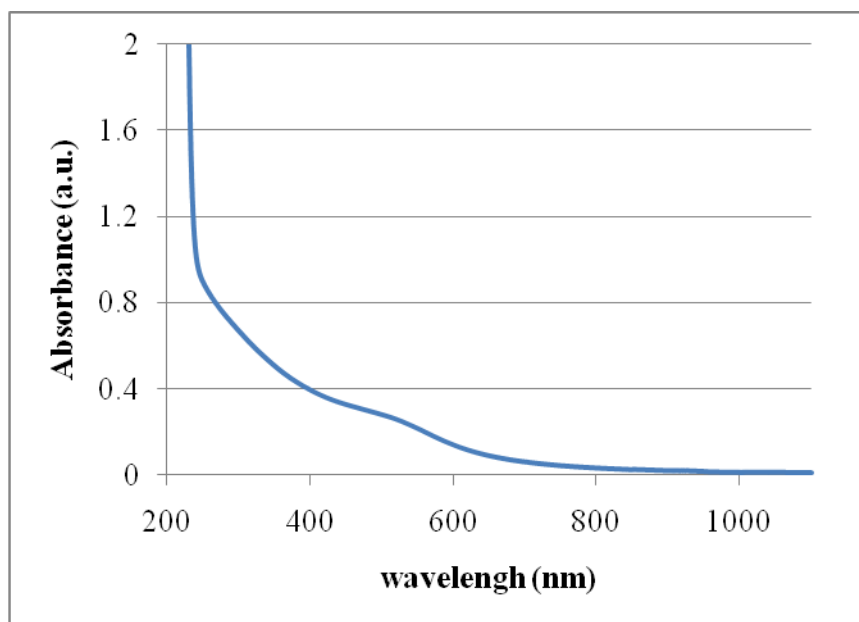
Figure 2.1 UV/Vis absorption spectrum of Au:PVP

The spectrum shows no surface plasmon band at 520 nanometers. This indicated that no metallic character in the Au:PVP clusters.

2.3.2.2 Transmission electron microscopy (TEM)

TEM images were recorded with electron microscopes operated at 300 kV. Typical magnification of the images was 100,000. The diameters of more than 500 particles are measured and plotted as the histograms in Figure 2.2. The average diameters of Au:PVP (K-30) are determined to be 1.3±0.3 nanometers.
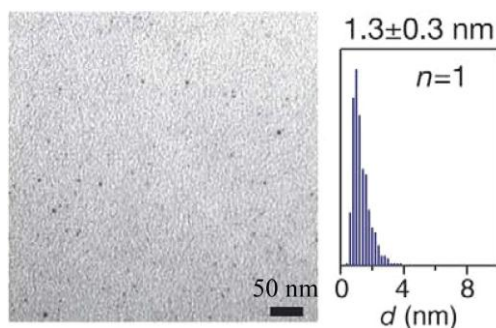
Figure 2.2 TEM image and the size distribution of Au:PVP.

2.3.3 Typical procedure of *N*-formylation

2.3.3.1 *N*-Formylation under MeOH oxidation conditions.

A mixture of amine (0.1 mmol) in MeOH (5 mL) with LiOH (0.2 mmol, 200 mol%) and 1 mM of aq Au:PVP (10 mL) hours in a glass tube (ϕ = 30 mm) was stirred vigorously (1300 rpm) at 80°C (bath temperature) for 4-24. The mixture was extracted with EtOAc (4×15 mL). The organic layers were washed with brine and dried over anhydrous Na_2SO_4 and purified by PTLC.

2.3.3.2 *N*-Formylation under formalin oxidation conditions

A mixture of amine (0.1 mmol), 1 mM of aq Au:PVP (1-10 atom%) with NaOH (0.1 mmol, 100 mol%) or $NaHCO_3$ (0.05 mmol, 50 mol%) and EtOH (5 mL) was prepared. 37% of formalin solution (0.15 mmol, 6.2 µL, 150 mol%) was directly added to the reaction mixture (50 mol% × 3 within 30 min) and stirred vigorously (1300 rpm) at room temperature (27°C). The extraction and purification method were carried out the same as that mentioned in 2.3.3.1. In the case of piperidine (**1l**), the yield of *N*-formylation was calculated using GC with hexadecane as an internal standard. The calculation method is shown in Appendix section.

The products were identified by ^{1}H NMR spectral data or GC comparing with those of the authentic samples.

2a
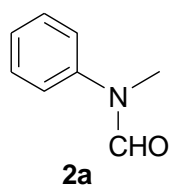
N-Methyl-formanilide (2a): CAS No. [93-61-8], ^{1}H NMR: δ 3.32 (s, 3H), 7.16-7.19 (m, 2H), 7.26-7.30 (m, 1H), 7.40-7.44 (m, 2H), 8.48 (s, 1H). Experimental data was reported in ref. 41.

3a
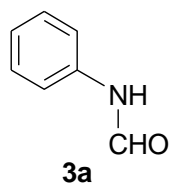
Formanilide (3a): CAS No. [103-70-8], ^{1}H NMR: δ 8.98 (d, *J* = 11.5, 1H,), 8.39 (bs, 1H), 7.57 (m, 1H), 7.60-7.57 (m, 2H), 7.42-7.31 (m, 4H), 7.26-7.05 (m, 4H). Experimental data was reported in ref. 42.

2b
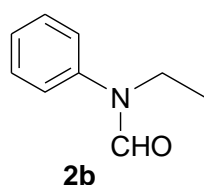
N-Ethylformanilide (*2b*): CAS No. [5461-49-4], ^{1}H NMR: δ 8.36 (s, 1H), 7.38-7.46 (m, 2H), 7.27-7.33 (m, 1H), 7.13-7.21 (m, 2H), 3.87 (q, *J* = 7.2 Hz, 2H), 1.16 (t, *J* = 7.2 Hz, 3H). Experimental data was reported in ref. 43.

2d
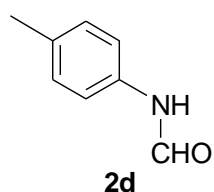
p-Methylformanilide (2d): CAS No. [3085-54-9], ^{1}H NMR: δ 8.61 (d, *J* = 11.6 Hz, 1H), 7.83 (bs, 1H), 7.42 (d, *J* = 10.8 Hz, 1H), 7.15 (t, *J* = 8.8 Hz, 2H), 6.98 (d, *J* = 8.4 Hz, 1H), 2.33 (s, 3H). Experimental data was reported in ref. 44.

2e
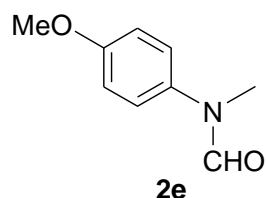
N-(4-Methoxyphenyl)formamide (2e): CAS No. [5470-34-8], ^{1}H NMR: δ 8.33 (s, 1H), 7.07-7.12 (m, 2H), 6.89-6.95 (m, 2H), 3.81 (s, 3H), 3.26 (s, 3H). Experimental data was reported in ref. 42.

2h
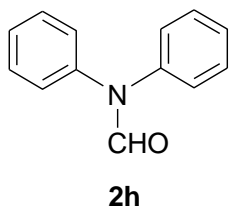
N,N-Diphenylformamide (2h): CAS No. [607-00-1], ^{1}H NMR: δ 8.67 (s, 1H), 7.44-7.36 (m, 4H), 7.35-7.26 (m, 4H), 7.21-7.14 (m, 2H). Experimental data was reported in ref. 45.

2i
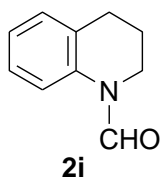
1-Formyl-1,2,3,4-tetrahydroquinoline (2i): CAS No. [2739-16-4], ^{1}H NMR: δ 8.79 (s, 1H), 7.04-7.24 (m, 4H), 3.81 (t, *J* = 6.1 Hz, 2H), 2.82 (t, *J* = 6.5, 2 H), 1.96 (tt, *J* = 6.3, 6.2 Hz, 2H). Experimental data was reported in ref. 46.

2j
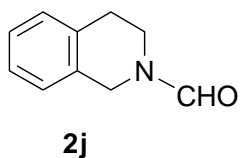
2-Formyl-1,2,3,4-tetrahydroisoquinoline (2j): CAS No. [1699-52-1], ^{1}H NMR: δ 8.26 (s, 1H×0.4), 8.20 (s, 1H×0.6), 7.07-7.25 (m, 4H), 4.69 (s, 2H×0.6), 4.55 (s, 2H×0.4), 3.79 (t, *J* = 6.2 Hz, 2H×0.4), 3.65 (t, *J* = 5.9 Hz, 2H×0.6), 2.98-2.84 (m, 2H). Experimental data was reported in ref. 47.

2k
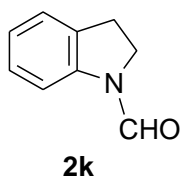
1-Formylindoline (2k): CAS No. [2861-59-8], ^{1}H NMR: δ 8.93 (s, 1H), 7.22-7.26 (m, 1H), 7.14-7.19 (m, 2H), 7.02-7.07 (m, 1H), 4.06 (t, *J* = 8.0 Hz, 2H), 3.15 (t, *J* = 8.0 Hz, 2H). Experimental data was reported in ref. 48.

2l
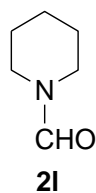
N-Formylpiperidine (2l): This product was identified by GC and comparing with authentic sample. CAS No. [2591-86-8]. Experimental data was reported in ref 42.

2m
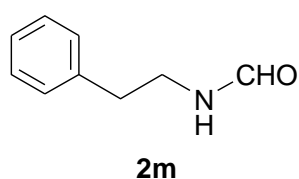
N-(2-Phenylethyl)formamide (2m): CAS No. [23069-99-0], ^{1}H NMR: δ 8.14 (s, 1H), 7.14-7.40 (m, 5H), 5.56 (bs, 1H), 3.59 (dt, 6.8, 6.4 Hz, 2H), 2.85 (t, J = 6.8 Hz, 2H). Experimental data was reported in ref. 49.

2n
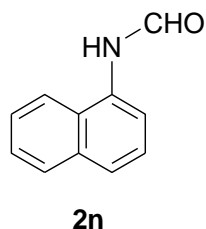
N-Formyl-1-naphthylamine (2n): CAS No. [6330-51-4], ^{1}H NMR: δ 8.62 (d, J = 11.2 Hz, 1H), 8.12 (bs, 1H), 7.70-8.06 (m, 3H), 7.42-7.65 (m, 3H), 7.33 (d, J = 3.6 Hz, 1H). Experimental data was reported in ref. 50.

3b
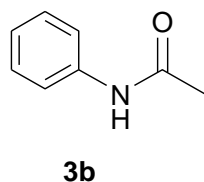
Acetanilide (3b): CAS No. [103-84-4], ^{1}H NMR: δ 7.49 (d, J = 7.8 Hz, 2H), 7.32 (t, J = 7.9 Hz, 2H), 7.08-7.15 (m, 1H), 2.18 (s, 3H). Experimental data was reported in ref. 51.

2.3.4   Procedure of mechanism study for *N*-formylation of amines

2.3.4.1 Variation of formyl source in *N*-formylation of amines

A mixture of *N*-methylaniline (**1a**) (0.05 mmol, 5.4 μL), 1 mM of aq Au:PVP (10 atom%) 5 mL with LiOH (0.1 mmol, 200 mol%) and EtOH (2.5 mL) was prepared. One of the formyl reagents, HCHO, HCOOMe or HCOOH (0.05 mmol, 100 mol%) was directly added to the reaction mixture and stirred vigorously (1300 rpm) at 50°C under air for 1 hour. 0.1 mL of the reaction mixture was taken and diluted with brine and extracted with EtOAc 0.5 mL three times. The organic layer was collected and transferred to a vial and then added 50 μL of 6 mM hexadecane solution as an internal standard. %Yield of product was calculated by GC.

2.3.4.2 Isotope labeling experiment for *N*-formylation of 1a

A mixture of *N*-methylaniline (**1a**) (0.01 mmol, 1.1 μL), 0.5 mM of aq Au:PVP (10 atom%) 2 mL with LiOH (0.02 mmol, 200 mol%) and 99% of $^{13}CH_3OH$ (1 mL) was stirred vigorously (1300 rpm) at 80°C (bath temperature) for 4-24 hours in a glass tube (ϕ = 30 mm). The reaction mixture (0.2 mL) was taken and diluted with brine and extracted with EtOAc 0.5×3 mL. The organic layer was collected and then added 50 μL of 6 mM hexadecane solution as an internal standard. %Yield of products was calculated by GC. The calculation of %yield and %^{13}C products are described in Appendix section.

2.3.5   Synthesis of starting materials for oxygenation of amines

2.3.5.1 Bromination of 1,2,3,4-tetrahydroquinoline to 6-bromo-1,2,3,4-tetra-hydroquinoline (1q)

1,2,3,4-Tetrahydroquinoline (100 mg, 0.75 mmol) was dissolved in *N,N*-dimethylformamide (DMF) (1 mL) and cooled to 0°C. *N*-Bromosuccinimide (NBS) (134 mg, 0.75 mmol) was added dropwise under ice cooling (0°C) over 30 minutes and the mixture was stirred for 1-1.30 hours. The mixture was diluted with H_2O, extracted with EtOAc or Et_2O and washed with sodium bisulfite, water, brine, dried over anhydrous $MgSO_4$. The organic layer was concentrated and purified by flash

column chromatograph (gradient 5%-30% EtOAc in hexane) afforded 6-bromo-1,2,3,4-tetrahydroquinoline (137 mg).

1q
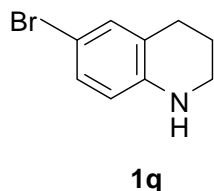
6-Bromo-1,2,3,4-tetrahydroquinoline (1q): CAS No. [22190-35-8], ^{1}H NMR: δ 6.98-7.07 (m, 2H), 6.34 (d, *J* = 8.5 Hz, 1H), 3.83 (bs, 1H), 3.28 (t, *J* = 6.6 Hz, 2H), 2.72 (t, *J* = 6.6 Hz, 2H), 1.81-2.00 (m, 2H). Experimental data was reported in ref. 52.

2.3.5.2 Synthesis of 6-methoxy-1,2,3,4-tetrahydroquinoline (1p)

1q   **1p**
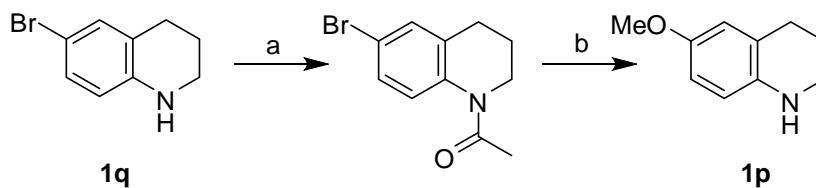
a) Acetylation of 6-bromo-1,2,3,4-tetrahydroquinoline (1q)

6-Bromo-1,2,3,4-tetrahydroquinoline (636 mg, 3.0 mmol) was dissolved in acetic anhydride (30 mL) and KOAc (3.0 g, 30.6 mmol) was added. The solution was heated at 80°C for 5 hours. The work-up procedure was performed by adding water (30 mL), then the mixture was extracted with CH_2Cl_2 (3×30 mL). The combined organic phases were washed with water (2×30 mL), dried over anhydrous Na_2SO_4, and concentrated *in vacuo*. The crude products were purified by flash column chromatograph. 96% of 1-acetyl-6-bromo-1,2,3,4-tetrahydroquinoline was obtained.
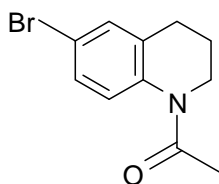
1-Acetyl-6-bromo-1,2,3,4-tetrahydroquinoline: CAS No. [22190-40-5], ^{1}H NMR: δ 7.28-7.32 (m, 2H), 7.26 (s, 1H), 3.76 (t, *J* = 6.6 Hz, 2H), 2.71 (t, *J* = 6.6 Hz, 2H), 2.22 (s, 3H), 1.90-2.00 (m, 2H). Experimental data was reported in ref. 53.

b) Methoxylation and deacetylation of 1-(6-bromo-3,4-dihydroquinolin-1(2*H*)-yl)ethanone

NaOMe solution was prepared from Na metal (303.6 mg, 13.2 mmol) with dried MeOH under inert atmosphere. 1-(6-Bromo-3,4-dihydroquinolin-1(2H)-yl)ethanone was dissolved in the solution of NaOMe in 4 mL of MeOH which was flushed by N_2. Methyl formate (117.1 mg, 1.95 mmol) was added to the mixture and then CuBr (93.2 mg, 0.65 mmol) was added. The reaction was refluxed for 1.5 hours at 70°C. MeOH was removed from the reaction by *vacuo*. 20% aq HCl was added to the reaction solution with gentle heating. The mixture was neutralized and extracted with Et_2O 3 times. The combined organic phases were washed with water (2×30 mL), dried over anhydrous Na_2SO_4, and concentrated *in vacuo*. The crude products were purified by flash column chromatograph. 67% of 1-(6-bromo-3,4-dihydroquinolin-1(2*H*)-yl)ethanone was obtained.
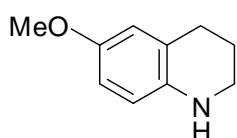
1p

6-methoxy-1,2,3,4-tetrahydroquinoline (1p): CAS No. [120-15-0], ^{1}H NMR: δ 6.60 (dd, *J* = 2.9, 8.5 Hz, 1H), 6.56 (d, *J* = 2.9 Hz, 1H), 6.45 (d, *J* = 8.5 Hz, 1H), 3.73 (s, 3H), 3.25 (t, *J* = 5.4 Hz, 2H), 2.75 (t, *J* = 6.6 Hz, 2H), 1.88-1.97 (m, 2H). Experimental data was reported in ref. 54.

2.3.5.3 Synthesis of 2,3,4,5-tetrahydro-1*H*-benzo[*b*]azepine (1r) and 1,2,3,4,5,6-hexahydrobenzo[*b*]azocine (1s) [55]

n = 0,1
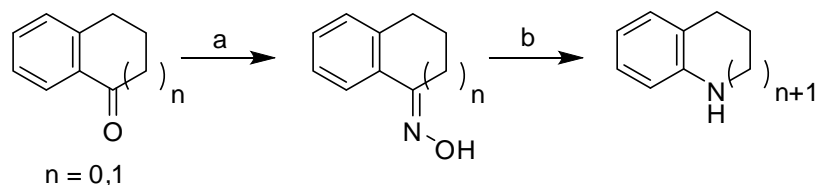
a) General procedure for oxime formation

To a solution of ketone compound (6 mmol) in pyridine (10 mL) was added hydroxylamine hydrochloride (762 mg, 10.96 mmol) at room temperature. After the mixture was stirred for 1.5 hours, pyridine was removed under reduced pressure. The residue was diluted with water, extracted with EtOAc and the combined organic extracts were washed with brine, dried over anhydrous $MgSO_4$, and evaporated under reduced pressure to give the crude material. Purification by silica gel column (100% hexane to 20% EtOAc in hexane) afforded corresponding oxime.
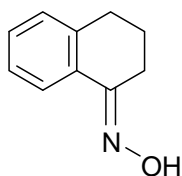
3,4-Dihydronaphthalen-1(2H)-one oxime: CAS No. [3349-64-2], ^{1}H NMR: δ 8.63 (bs, 1H), 7.90 (dd, *J* = 7.8, 1.1 Hz, 1H), 7.24-7.29 (m, 2H), 7.18 (dd, *J* = 7.6, 0.8 Hz, 1H), 2.82 (dt, *J* = 6.6, 2.4 Hz, 2H), 2.79 (t, *J* = 6.1 Hz, 2H), 1.81-1.95 (m, 2H). Experimental data was reported in ref. 56.
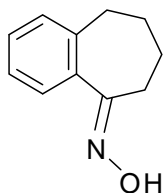
(E)-6,7,8,9-Tetrahydrobenzo[7]annulen-5-one oxime: CAS No. [17910-25-7], ^{1}H NMR: δ 7.52 (bs, 1H), 7.38 (dd, *J* = 7.4, 1.2 Hz, 2H), 7.17-7.35 (m, 2H), 7.13 (dd, *J* = 7.4, 1.2 Hz, 2H), 2.68-2.84 (m, 2H), 1.71-1.85 (m, 2H), 1.60-1.71 (m, 2H). Experimental data was reported in ref. 57.

b) Reductive ring-expansion reaction of carbocyclic ketoximes fused to a benzene ring

To a stirred solution of ketoximes from procedure **a** (2.815 mmol) in CH$_2$Cl$_2$ (28 mL) was added DIBAL-H (16.5 mL, 16.85 mmol, 1.02 M in *n*-hexane) over 10 min at 0-5°C (internal temperature) under an argon atmosphere. Stirring was continued for 5 min at 0 °C and for 2-2.5 hours at room temperature. NaF powder (3.38 g, 80.5 mmol) and water (2.2 mL) were added at 0 °C, and the resulting mixture was stirred for 30 min at the same temperature. Then, the reaction mixture was filtered through a celite pad. The filter cake was washed with EtOAc, and the combined organic solutions were evaporated to give the crude product. Purification by preparative TLC yielded the corresponding product (**1r** or **1s**) in 72-77%.

1r
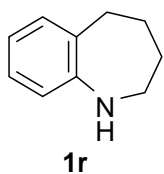
2,3,4,5-Tetrahydro-1H-benzo[b]azepine (1r): CAS No. [1701-57-1], ^{1}H NMR: δ 7.10 (d, *J* = 7.3 Hz, 1H), 7.03 (dt, *J* = 7.5, 1.5 Hz, 1H), 6.82 (t, *J* = 7.3 Hz, 1H), 6.73 (d, *J* = 7.8 Hz, 1H), 3.77 (bs, 1H), 3.04 (t, *J* = 5.4 Hz, 2H), 2.77 (t, *J* = 5.4 Hz, 2H), 1.74-1.88 (m, 2H), 1.60-1.70 (m, 2H). Experimental data was reported in ref. 58.
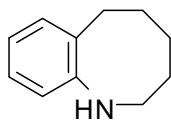
1s

1,2,3,4,5,6-Hexahydro-1-benzazocine (1s): CAS No. [7124-93-8], ^{1}H NMR: δ 7.12 (dt, *J* = 7.5,1.6 Hz, 1H, 7.06 (dd, *J* = 7.5, 1.6 Hz, 1H), 6.93 (dt, *J* = 7.5, 1.6 Hz, 1H), 6.89 (dd, *J* = 7.5, 1.6 Hz, 1H), 3.14-3.26 (m, 2H), 2.81-2.89 (m, 2H), 1.61-1.83 (m, 2H), 1.45-1.54 (m, 4H). Experimental data was reported in ref. 58.

2.3.5.4 Synthesis of 2-methyl-1,2,3,4-tetrahydroisoquinoline (1u)

To a solution of 1,2,3,4-tetrahydroisoquinoline (**1j**) (439.2 mg, 3.3 mmol) in 98% formic acid (6.6 mL) was added 37% HCHO solution (4.3 mL). The mixture was stirred and refluxed under nitrogen atmosphere for 4 hours. Then, formic acid was removed under reduced pressure. The residue was neutralized by diluted NaOH and saturated Na_2CO_3 and extracted with Et_2O. The combined organic solutions were evaporated to give the crude product and purified by column chromatograph. 2-Methyl-1,2,3,4-tetrahydroisoquinoline (**1u**) was obtained in 97% yield.
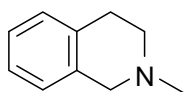
1u

2-Methyl-1,2,3,4-tetrahydroisoquinoline (1u): CAS No. [1612-65-3], ^{1}H NMR: δ 7.09-7.40 (m, 4H), 4.83 (s, 2H), 4.08 (t, *J* = 6.6 Hz, 2H), 3.60 (s, 3H), 3.21-3.33 (m, 2H). Experimental data was reported in ref. 59.

2.3.6 Typical procedure of oxygenation of benzo-fused heterocyclic amines

2.3.6.1 α-Oxygenation of 1,2,3,4-tetrahydroquinoline (1i)

A test tube (ϕ = 30 mm) was placed with **1i** (13.3 mg, 0.10 mmol), NaOH (8 mg, 0.20 mmol), and EtOH (5 mL). The aqueous solution of Au:PVP (1 mM, 10 mL = 10 atom%) was added, and the reaction mixture was stirred vigorously (1300 rpm)

at 27 °C for 24 hours. The reaction mixture was extracted with EtOAc or Et$_2$O (3×10 mL), and then washed the organic layers with brine, dried over anhydrous Na$_2$SO$_4$, and concentrated *in vacuo*. The crude products were separated by PTLC. The products were identified by ^{1}H NMR spectral data comparing with those of the authentic samples.
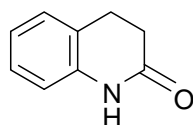
3i

3,4-Dihydroquinolin-1(2H)-one (3i): CAS No. [553-03-7], ^{1}H NMR: δ 8.50 (bs, 1H), 7.26-7.18 (m, 2H), 6.99 (t, *J* = 7.6 Hz, 1H), 6.79 (d, *J* = 7.6 Hz, 1H)), 2.98 (t, *J* = 7.6 Hz, 2H), 2.65 (dd, *J* = 7.6, 6.0 Hz, 2H). Experimental data was reported in ref. 60.

2.3.6.2 *α*-Oxygenation of 1,2,3,4-tetrahydroisoquinoline (1j)

A test tube (ϕ = 30 mm) was placed with **1j** (13.3 mg, 0.10 mmol), NaOH (8 mg, 0.20 mmol), and H$_2$O (5 mL). The aqueous solution of Au:PVP (1 mM, 10 mL = 10 atom%) was added, and the reaction mixture was stirred vigorously (1300 rpm) at 90°C for 24 hours. The reaction mixture was extracted with EtOAc or Et$_2$O (3×10 mL), and then washed the organic layers with brine, dried over anhydrous Na$_2$SO$_4$, and concentrated *in vacuo*. The crude products were separated by PTLC. The products were identified by ^{1}H-NMR spectral data comparing with those of authentic samples.

3j

3,4-Dihydroisoquinolin-2(1H)-one (3j): CAS No. [1196-38-9], ^{1}H NMR: δ 8.02 (dd, *J* = 7.6, 1.2 Hz, 1H), 7.96 (bs, 1H), 7.39 (dt, *J* = 7.6, 1.6 Hz, 1H), 7.29 (dt, *J* = 7.6, 0.8 Hz, 1H), 7.16 (d, *J* = 7.2 Hz, 1H), 3.52 (dt, *J* = 6.6, 3.0 Hz, 2H), 2.92 (t, *J* = 6.6 Hz). Experimental data was reported in ref. 61.

2.3.6.3 *α*-Oxygenation of 6-methoxy-1,2,3,4-tetrahydroquinoline (1p)

A test tube (ϕ = 30 mm) was placed with **1p** (13.3 mg, 0.10 mmol), NaOH (8 mg, 0.20 mmol), and *t*-BuOH (5 mL). The aqueous solution of Au:PVP (1 mM, 10 mL = 10 atom%) was added, and the reaction mixture was stirred vigorously (1300 rpm) at 90°C for 24 hours. The reaction mixture was extracted with EtOAc or Et$_2$O (3×10 mL), and then washed the organic layers with brine, dried over anhydrous Na$_2$SO$_4$, and concentrated *in vacuo*. The crude products were separated by PTLC.
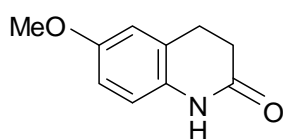
3p

6-Methoxy-3,4-dihydroquinolin-2(1H)-one (3p): CAS No. [54197-64-7], ^{1}H NMR: δ 8.02 (bs, 1H), 6.66-6.76 (m, 3H), 3.93 (s, 3H), 2.91 (t, *J* = 7.2 Hz, 2H), 2.61 (t, *J* = 7.6 Hz, 2H). Experimental data was reported in ref. 62.
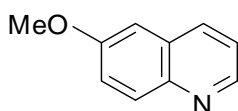
4p

6-Methoxyquinoline (4p): CAS No. [5263-87-6], ^{1}H NMR: δ 8.77 (dd, *J* = 4.2, 1.6 Hz, 1H), 8.04 (dd, *J* = 8.7 Hz, 2H), 7.32-7.42 (m, 2H), 7.08 (d, *J* = 2.8 Hz, 1H), 3.94 (s, 3H). Experimental data was reported in ref. 63.

2.3.6.4 *α*-Oxygenation of 1-(6-bromo-3,4-dihydroquinolin-1(2*H*)-yl)ethanone (1q)

A test tube (ϕ = 30 mm) was placed with **1q** (13.3 mg, 0.10 mmol), NaOH (8 mg, 0.20 mmol), and EtOH (5 mL). The aqueous solution of Au:PVP (1 mM, 10 mL = 10 atom%) was added, and the reaction mixture was stirred vigorously (1300 rpm) at 27 °C for 24 hours. The reaction mixture was extracted with EtOAc or Et$_2$O (3×10 mL), and then washed the organic layers with brine, dried over anhydrous Na$_2$SO$_4$, and concentrated *in vacuo*. The crude products were separated by PTLC. The products

were identified by ^{1}H NMR spectral data and comparing with those of authentic samples.

3q
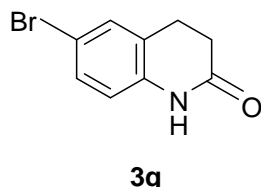
6-Bromo-3,4-dihydroquinolin-2(1H)-one (3q): CAS No. [3279-90-1], ^{1}H NMR: δ 9.21 (bs, 1H), 7.26 (s, 1H), 7.21-7.25 (m, 1H), 6.70 (d, J = 8.8 Hz, 1H), 2.93 (t, J = 8.1, Hz, 2H), 2.60 (t, J = 8.1 Hz, 2H). Experimental data was reported in ref. 64.

4q
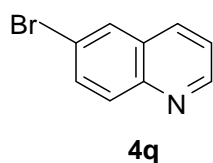
6-Bromoquinoline (4q): CAS No. [5332-25-2], ^{1}H NMR: δ 8.93 (bs, 1H), 8.09 (d, J = 8.0 Hz, 1H), 7.99 (d, J = 8.8 Hz, 2H), 7.79 (dd, J = 8.8, 2.0 Hz, 1H), 7.44 (m, 1H). Experimental data was reported in ref. 52.

2.3.6.5 α-Oxygenation of 2,3,4,5-tetrahydro-1*H*-benzo[*b*]azepine (1r)

A test tube (φ = 30 mm) was placed with **1r** (13.3 mg, 0.10 mmol), NaOH (8 mg, 0.20 mmol), and H_2O (5 mL). The aqueous solution of Au:PVP (1 mM, 10 mL = 10 atom%) was added, and the reaction mixture was stirred vigorously (1300 rpm) at 90 °C for 24 hours. The reaction mixture was extracted with EtOAc or Et_2O (3×10 mL), and then washed the organic layers with brine, dried over anhydrous Na_2SO_4, and concentrated *in vacuo*. The crude products were separated by PTLC. The products were identified by ^{1}H NMR spectral data.

3r
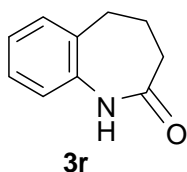
4,5-Dihydro-1H-benzo[b]azepin-2(3H)-one *(3r)*: CAS No. [4424-80-0], ^{1}H NMR: δ 7.83 (bs, 1H), 7.19-7.25 (m, 2H), 7.13 (dt, *J* = 7.6, 1.2 Hz, 1H), 6.96 (d, *J* = 8 Hz, 1H), 2.80 (t, *J* = 7.2 Hz, 2H), 2.36 (t, *J* = 7.2 Hz, 2H), 2.16-2.29 (m, 2H). Experimental data was reported in ref. 65.

2.3.6.6 *α*-Oxygenation of indoline (1s)

A test tube (ϕ = 30 mm) was placed with **1s** (13.3 mg, 0.10 mmol), NaOH (8 mg, 0.20 mmol), and EtOH (5 mL). The aqueous solution of Au:PVP (1 mM, 10 mL = 10 atom%) was added, and the reaction mixture was stirred vigorously (1300 rpm) at 27 °C for 24 hours. The reaction mixture was extracted with EtOAc or Et$_2$O (3×10 mL), and then washed the organic layers with brine, dried over anhydrous Na$_2$SO$_4$, and concentrated *in vacuo*. The crude products were separated by PTLC. The product **3s** was obtained only 5% yield.

3s
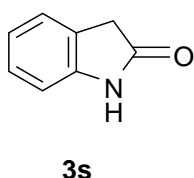
Oxindole (3s): CAS No. [59-48-3], ^{1}H NMR: δ 9.10 (bs, 1H), 7.22 (d, *J* = 8.0 Hz, 1H), 7.17 (d, *J* = 6.7 Hz, 1H), 7.02 (dd, *J* = 8.0, 7.4 Hz, 2H), 6.87 (dd, *J* = 7.4, 6.7 Hz, 1H), 3.56 (s, 2H). Experimental data was reported in ref. 66.

2.3.6.7 *α*-Oxygenation of 2-methyl-1,2,3,4-tetrahydroisoquinoline (1t)

A test tube (ϕ = 30 mm) was placed with **1t** (13.3 mg, 0.10 mmol), NaHCO$_3$ (8 mg, 0.10 mmol), and *t*-BuOH (5 mL). The aqueous solution of Au:PVP (1 mM, 10 mL = 10 atom%) was added, and the reaction mixture was stirred vigorously (1300 rpm) at 27 °C for 24 hours. The reaction mixture was extracted with EtOAc or Et$_2$O

(3×10 mL), then washed the organic layers with brine, dried over anhydrous Na$_2$SO$_4$, and concentrated *in vacuo*. The crude products were separated by PTLC.

3t
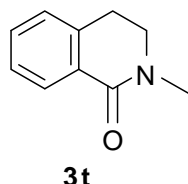
3,4-Dihydro-2-methyl-1(2H)-isoquinoline (3t): CAS No. [6772-65-2], ^{1}H NMR: δ 8.07 (d, *J* = 6.8 Hz, 1H), 7.39 (td, *J* = 7.4, 1.8 Hz, 1H), 7.32 (t, *J* = 7.4 Hz, 1H), 7.16 (dd, *J* = 7.6 Hz, 1H), 3.55 (t, *J* = 6.8 Hz, 2H), 3.15 (s, 3H), 2.99 (t, *J* = 6.8 Hz, 2H). Experimental data was reported in ref. 67.

2.3.7 Typical procedure of dehydrogenation of benzo-fused heterocyclic amines

2.3.7.1 Dehydrogenation of 1,2,3,4-tetrahydroisoquinoline (1j)

A test tube (φ = 30 mm) was placed with **1j** (13.3 mg, 0.10 mmol), NaOH (8 mg, 0.20 mmol), and DMF (15 mL). Dried Au:PVP (10 atom%) was added, and the reaction mixture was stirred vigorously (1300 rpm) at 90 °C for 6 hours. The reaction mixture was extracted with EtOAc or Et$_2$O (3×10 mL), and then washed the organic layers with brine, dried over anhydrous Na$_2$SO$_4$, and concentrated *in vacuo*. The crude products were separated by PTLC.

4j
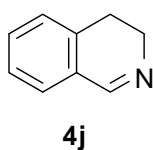
3,4-dihydroisoquinoline (4j): CAS No. [3230-65-7], ^{1}H NMR: δ 8.12 (d, *J* = 7.6 Hz, 1H), 7.50 (t, *J* = 7.6 HZ, 1H), 3.57 (dt, *J* = 7.6 Hz, 1H), 7.27 (d, *J* = 7.6 Hz, 1H), 6.88-7.09 (m, 1H), 3.63 (dt, *J* = 6.6, 2.8 Hz, 2H), 3.05 (t, *J* = 6.6 Hz, 2H). Experimental data was reported in ref. 68.
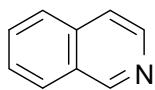
5j

Isoquinoline (5j): CAS No. [119-65-3], ^{1}H NMR: (400 MHz, ref. 7.26 ppm for CHCl$_3$ in CDCl$_3$) δ 9.16 (s, 1H), 8.44 (d, *J* = 5.7 Hz, 1H), 7.79 (d, *J* = 7.66 (d, 8.1 Hz, 1H), 7.55 (dt, *J* = 5.6, 1.1 Hz, 1H), 7.53 (d, *J* = 6 Hz, 1H), 7.45 (dt, *J* = 8.1, 1.1 Hz, 1H) Experimental data was reported in ref. 69.

2.3.7.2 Aromatization of indoline (1s)

A test tube (ϕ = 30 mm) was placed with **1s** (13.3 mg, 0.10 mmol), NaOH (8 mg, 0.20 mmol), and *t*-BuOH (5 mL). The aqueous solution of Au:PVP (1 mM, 10 mL = 10 atom%) was added. The reaction mixture was stirred vigorously (1300 rpm) at 27 °C for 24 hours. The reaction mixture was extracted with EtOAc or Et$_2$O (3×10 mL), and then washed the organic layers with brine, dried over anhydrous Na$_2$SO$_4$, and concentrated *in vacuo*. The crude products were separated by PTLC.
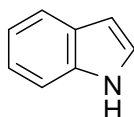
4s

Indole (4s): CAS No. [120-72-9], ^{1}H NMR: δ 8.18 (bs, 1H), 7.73 (d, *J* = 8.0 Hz, 1H), 7.46 (d, *J* = 8.0 Hz, 1H), 7.24-7.33 (m, 2H), 7.16-7.23 (m, 1H), 6.59-6.67 (m, 1H). Experimental data was reported in ref. 70.

CHAPTER III

N-FORMYLATION OF AMINES UNDER AEROBIC METHANOL OXIDATION OR FORMALIN CONDITION

3.1   Introduction and Literature reviews

3.1.1   *N*-Formylatoin of amines

Formylation is a very potential process in synthetic organic chemistry. These important amide groups in natural product, polymer, and pharmaceutical fields could be introduced by the reactions of carboxylic acids or their derivatives with amines (Scheme 3.1) [71-73]. It must be noted that this reaction required careful exclusion of moisture. Other methods have been addresses including Staudinger reactions, aminocarbonylation of halides with CO and amines, mercury-catalyzed rearrangements of ketoxime, and transition metal catalyzed carbonylation of alkenes and alkynes with amines. However, these processes not only contain complex procedures but also produce toxic chemical wastes.
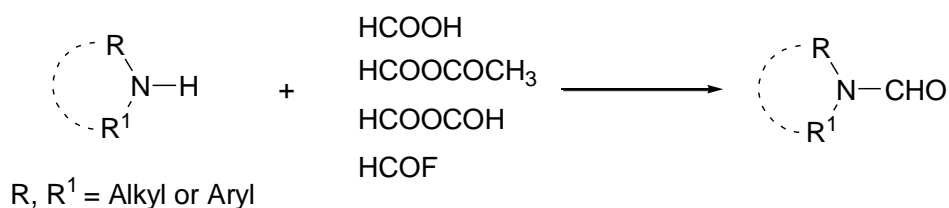
Scheme 3.1 *N*-formylation of amines.

From literatures, various approaches are available for *N*-formylation using different reagents such as chloral, formic acid with DCC or EDCL, ammonium formate, CDMT, and some solid-supported reagents [74]. However, the disadvantages of these methodologies are expensive and toxic formylating agents or toxic organic solvents are used. Besides, the side products were formed or applicable only for

aromatic amines. Some examples of the formylation were reported using $ZnCl_2$, $FeCl_3$, $AlCl_3$, and $NiCl_2$ [75].

Direct synthesis of amides by reacting alcohols or aldehydes with amines has recently attracted growing interest, because of the more environmentally benign and the wide availability of the starting materials.

3.1.2 *N*-Formylation of amines *via* the MeOH oxidation

Up to now, only few examples have been reported on *N*-formylation of amine using MeOH. This method leads to the development of environmentally benign processes. Besides, starting materials are inexpensive and the produced intermediates are important in organic synthesis.

In 2009, Reddy and coworkers described *N*-formylation reaction by catalytic oxidation of MeOH in the presence of primary or secondary amines and H_2O_2 using a liquid phase reaction system over basic copper hydroxyl salts ($Cu_2(OH)_3Cl$). The catalyst was prepared by precipitation method using aq NH_3 and NaOH as precipitating agents. The oxidation of MeOH by H_2O_2 was proceeded in the presence of $Cu_2(OH)_3Cl$ catalyst to afford CO_2 and H_2, followed by condensation of CO_2 with amines to afford desired product (Figure 3.1) [76].
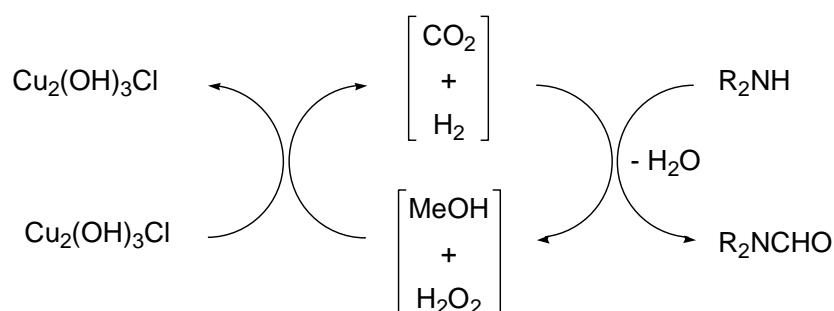
Figure 3.1 Schematic pathway to produce active components for the *N*-formylation of primary or secondary amines with $Cu_2(OH)_3Cl$ and H_2O_2.

N-formylation of amines using gold nanoparticles catalyst was firstly published in 2009 by Ishida and Haruta. Gold nanoparticles supported on NiO

catalyzed the one pot *N*-formylation of amines with MeOH and molecular oxygen at 100°C in 5 hours leading to formamide with 90% selectivity. This process generated methyl formate *in situ* from the MeOH oxidation, followed by reaction with amines to give corresponding formylation product (Figure 3.2) [77].
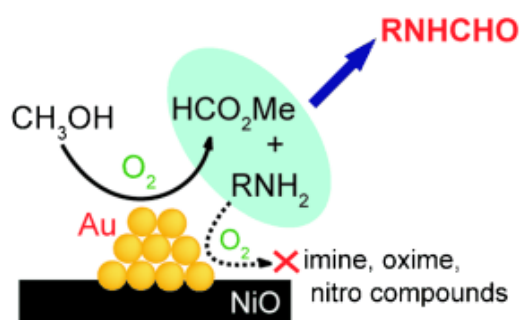
Figure 3.2 *N*-Formylation of amines *via* the aerobic oxidation of methanol over supported gold nanoparticles [77].

3.1.3 *N*-Formylation of amines *via* the condensation with formaldehyde

A year later, Madix and co-workers demonstrated the highly selective oxygen-assisted formylation of dimethylamine with formylation of dimethylamine with HCHO driven by metallic silver surfaces as a catalyst [78]. Direct acylation of dimethylamine with HCHO to *N,N*-dimethylformamide proceeded with 100% selectivity at lower oxygen concentrations on silver surfaces; this reaction proceeded *via* nucleophilic attack of adsorbed dimethylamide on HCHO with subsequent β-H elimination from the adsorbed hemiaminal. The catalytic cycle for this reaction using metallic silver surfaces was shown in Figure 3.3.
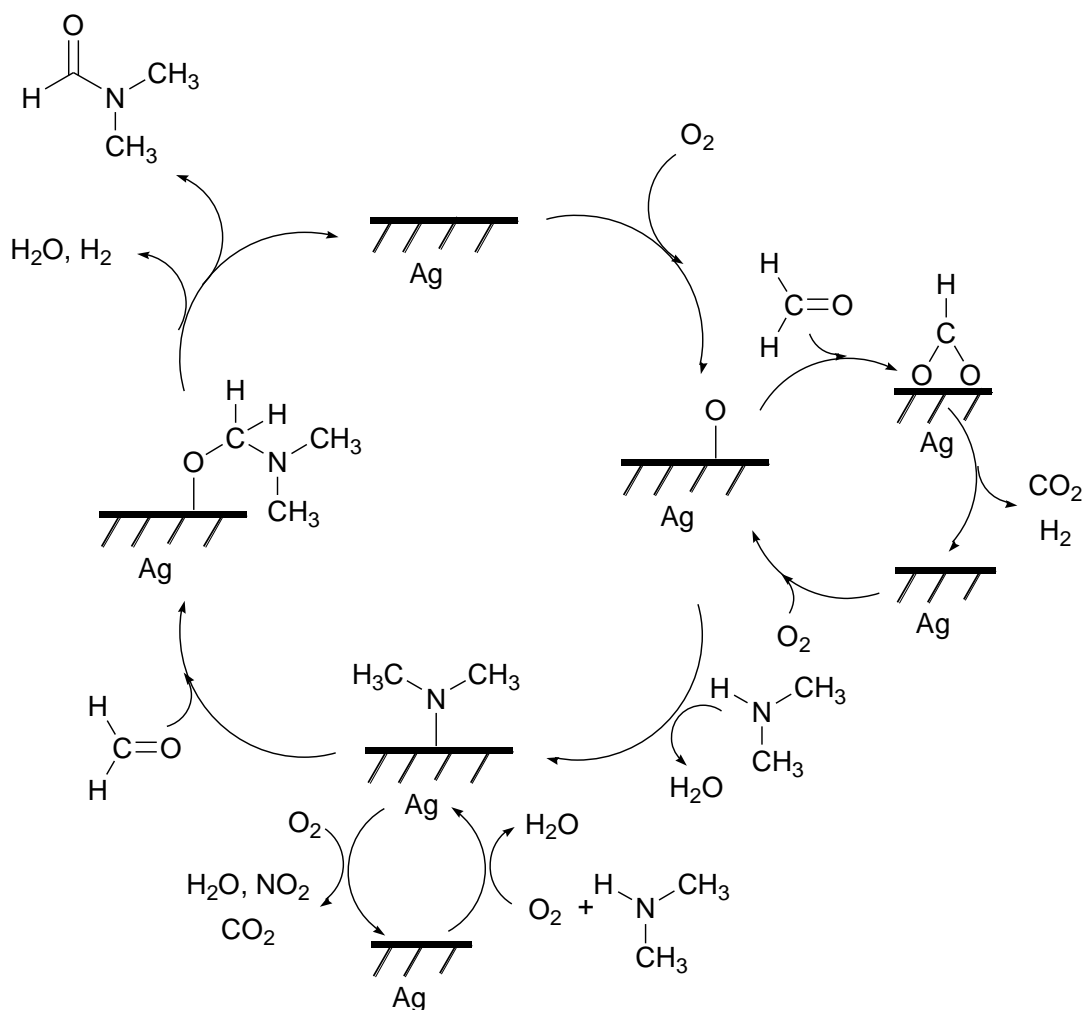
Figure 3.3 The catalytic cycle for silver-mediated acylation of dimethylamine with formaldehyde.

Friend and co-workers investigated the cross-coupling between dimethylamine and HCHO approaching up to 100% selectivity at low coverage of adsorbed oxygen atom on metallic gold to form *N,N*-dimethylformamide through a pathway with a low activation energy (Figure 3.4) [79]. The coupling reaction occurs through the attack of nucleophilic $(CH_3)_2N$ anion on the carbonyl carbon of the aldehyde. Nuclephilic intermediate is formed by the reaction of its conjugate acids and adsorbed oxygen atom.
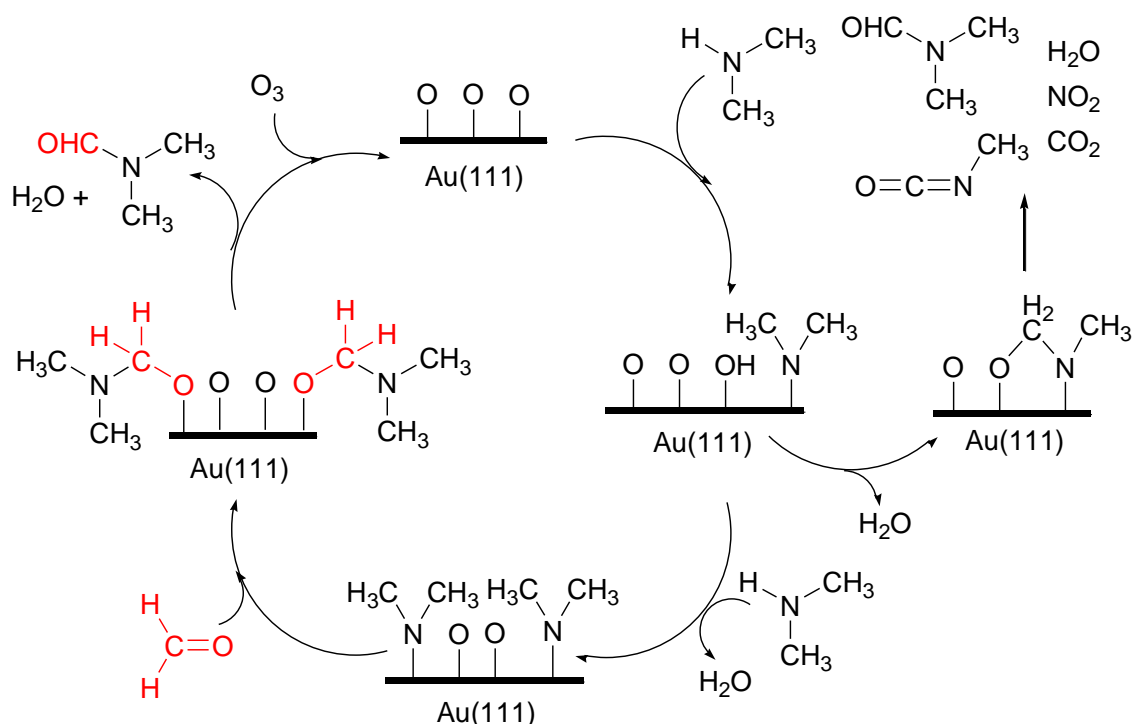
Figure 3.4 The catalytic cycle for gold-mediated acylation of dimethylamine with formaldehyde.

However, the development of practical procedures for *N*-formylation by aerobic oxidation for a wide scope of amines are still needed. Stemmed from the work addressed by Sakurai and co-workers concerning gold nanoclusters stabilized by PVP which could act as an excellent *quasi*-homogenous catalyst for the aerobic oxidation of benzylic alcohols in 2004 (Scheme 3.5, described in Chapter I), the investigation of *N*-formylation by the MeOH oxidation was first investigated.
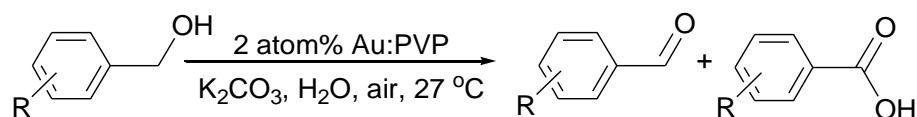
Scheme 3.2 Oxidation of benzylic alcohol catalyzed by Au:PVP.

The *N*-formylation of amines may proceed in the corresponding conditions, MeOH could be oxidized to formyl source *in situ*, followed by the condensation with amines to form *N*-formylation products (Figure 3.5).
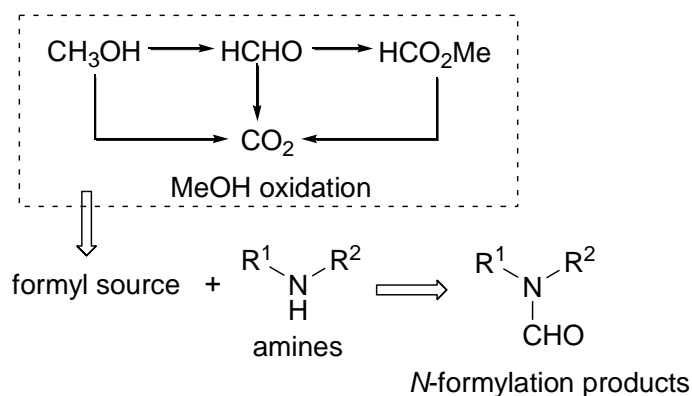
Figure 3.5 *N*-formylation of amines by MeOH oxidation concept.

3.2   Objective of this work

To investigate the highly selective direct *N*-formylation using MeOH or HCHO as a formyl source in the presence of Au:PVP under aerobic conditions. Furthermore, the mechanism of *N*-formylation of amines under aerobic MeOH oxidation conditions was scrutinized in details.

3.3   Results and discussion

3.3.1   Optimization study for aerobic MeOH oxidation condition

3.3.1.1 Screening conditions with and without additive

According to Sakurai's works in 2004 on the oxidation of benzyl alcohol, the aerobic oxidation condition was performed for *N*-formylation reaction under MeOH oxidation. *N*-formylation of *N*-methylaniline **1a** was screened and used as a model reaction. The screening results are listed in Table 3.1.

Table 3.1 The reactions of **1a** under aerobic MeOH oxidation conditions

Entry	Conditions		% Recovery of 1a	% Yield[a]		
	Au:PVP (atom%)	DBU (mol%)		2a	3a	4a
1	10	-	no reaction			
2	-	200	no reaction			
3	10	200	41	54	4	1
4	PVP (10 mol%)	200	no reaction			

[a] GC yields using hexadecane as an internal standard.

The reaction did not occur with either no DBU (entry 1) or Au:PVP (entry 2). 54% of *N*-formylated product **2a** was obtained when 10 atom% of Au:PVP was used in the presence of 200 mol% of DBU (entry 3). In addition, no reaction was observed in the case of using PVP without gold nanoclusters (entry 4).

3.3.1.2 Variation of bases

The variation of bases was explored and **2a** was obtained in moderate to excellent yield (61-94%) as shown in Table 3.2.

Table 3.2 The variation of bases in *N*-formylation of **1a** under aerobic MeOH
oxidation conditions
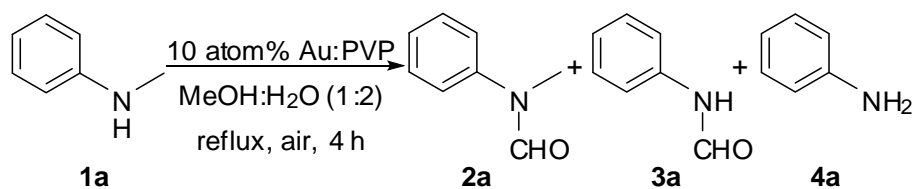
Entry	Base (mol%)	% Recovery of 1a	% Yield[a]		
			2a	**3a**	**4a**
1	DBU (200)	41	54	4	1
2	$Bu_4N^+OH^-$ (200)	8	85	4	3
3	NH_3 (300)	66	31	1	3
4	CsOAc (300)	92	4	-	3
5	$KHCO_3$ (300)	28	61	3	7
6	K_2CO_3 (300)	10	83	4	3
7	KOH (300)	1	95	4	-
8	NaOH (300)	2	94	4	1
9	LiOH (300)	-	94	5	-

[a] GC yields using hexadecane as an internal standard.

As shown in Table 3.2, the basic conditions were found to be important for the oxidation of MeOH to generate the key intermediate for *N*-formylation. The reaction could not complete when organic bases such as DBU and $Bu_4N^+OH^-$ were used, only 54 and 85% of **2a** were observed (entries 1 and 2). These results indicated that when the stronger base was used, the higher conversion of *N*-formylation was obtained. Then, 300 mol% of inorganic bases were tried (entries 3-9) in the reaction at reflux MeOH-H_2O. 31% of **2a** was observed when NH_3 was used (entry 3) and only 4% of **2a** was obtained in the case of CsOAc (entry 4). It must be noted that the color of the reaction mixture was changed from dark brown to red in both cases because during the reaction aggregated nano-sized gold was formed by OAc^- and NH_3 during the reaction. In addition, the color of the reaction mixture was changed immediately when

formic acid or carboxylic acid was directly added into the solution. The basicity was also important. *N*-formylated product **2a** was formed in 61, 83 and 95% when using KHCO$_3$, K$_2$CO$_3$ and KOH, respectively (entries 5-7). These results indicated that the stronger bases enhanced the rate of reaction. Thus, when hydroxide bases (entries 7-9) were used, 94-95% of **2a** was obtained under each condition with 98-100% conversion. In addition, it was noticed that the stronger the bases used, the less amount of by product **3a** and **4a** were formed and hydroxide gave the best results (entries 7-9). For convenience, the powder LiOH was selected for all further reactions explored.

3.3.1.3 Effect of Temperature

The effect of temperature on the reaction was examined and the results are presented in Table 3.3.

Table 3.3 The effect of temperature in *N*-formylation of **1a** under aerobic MeOH oxidation conditions
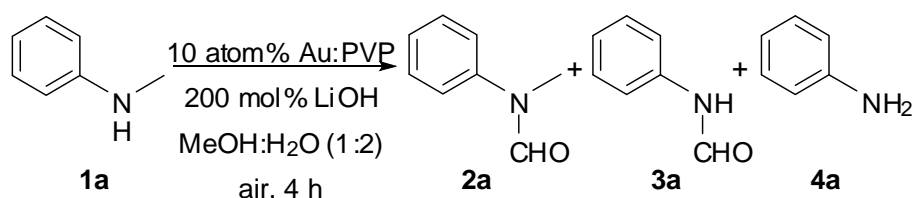
Entry	Temperature (°C)	% Recovery of 1a	% Yield[a]		
			2a	**3a**	**4a**
1	27	no reaction			
2	50	16	80	2	2
3	80	-	94	5	-

[a] GC yields using hexadecane as an internal standard.

No reaction was observed at 27 °C (entry 1) which was the same as that observed earlier in the case of the oxidation of benzyl alcohol. The reaction could proceed at 50 °C giving the products **2a**, **3a**, and aniline (**4a**) in 80, 2 and 2% yield, respectively with the recovered **1a** in 16% yield (entry 2). Under reflux condition

(entry 1), the reaction proceeded smoothly in the presence of 10 atom% of Au:PVP, affording *N*-formyl-*N*-methylaniline (**2a**) in 94% yield along with the formation of *N*-formylaniline (**3a**) in 5% yield, which is produced *via* oxidative demethylation followed by *N*-formylation. The generation of by-products **3a** and **4a** would be discussed later.

3.3.1.4 Effect of catalyst and base loading

The amount of Au:PVP and base (LiOH) are also important. Next investigation involved the study on the effect of the amount of catalyst and base loading. The results are shown in Table 3.4.

Table 3.4 The effect of amount of Au:PVP and LiOH in *N*-formylation of **1a** under aerobic MeOH oxidation conditions

Entry	Conditions		% Recovery of 1a	% Yield[a]		
	Au:PVP (atom%)	LiOH (mol%)		2a	3a	4a
1	5	200	9(2)	81(89)	6(8)	4(2)
2	10	300	-	94	5	-
3	10	200	-	94	5	-
4	10	150	-	93	6	1
5	10	100	4(-)	88(92)	5(7)	2(1)

[a] GC yields using hexadecane as an internal standard.
(-) yield of product at 8 hours.

When catalyst loading was reduced to 5 atom%, **2a** was obtained after 4 and 8 hours in 81 and 89% yield, respectively along with 10% of total yield of by-products **3a** and **4a** (entry 1). By varying the amount of base up to 300 mol%, the same result was obtained as that observed using 200 mol% (entries 2-3). While lower the amount

of base, the reaction rate was obviously slower. When the reaction was carried out by using 150 mol% LiOH, 93% of **2a** was observed with 7% of total by-products **3a** and **4a** (entry 4). The slightly decrease of **2a** along with the increase of **3a** and **4a** was observed. It might be because of the slower rate of the condensation of amine **1a** and HCHO than *N*-demethylation of **1a**. When the oxidation of MeOH was slow, the rate of the condensation of amine and HCHO would decrease and the formation of imine intermediate *via* oxidative dehydrogenation was increased. The higher yield of by-products was observed when only 100 mol% of LiOH was present in *N*-formylation of **1a**. *N*-formylated product **2a** was afforded in 88% yield with the recovered **1a** in 4%. If the reaction was prolonged for 8 hours, *N*-formylation product **2a** was obtained in 92% with by-products **3a** and **4a** in 7 and 1% yield, respectively (entry 5).

3.3.1.5 Effect of solvent ratio

It might be interesting to investigate the reaction media whether water would affect on the reaction rate. The results are shown in Figure 3.6. It was found that the amount of water played a crucial role in this reaction. When the reactions were carried out in MeOH/H_2O of 25/75, 50/50 and 75/25 ratio at 50°C for 4 hours, the reaction rate drastically decreased and the yield of **2a** was declined while **1a** was recovered. In addition, less than 2% of **2a** was obtained in 100% MeOH (Figure 3.6). This could be explained that *N*-formylation of amine **1a** could not proceed under condition without water, because the poor solubility of base in MeOH even if the oxidation of MeOH was carried out at 50°C. The condensation of amine and HCHO was slow under weak base condition, so the excess amount of HCHO in solution would aggregate Au:PVP nanoclusters and destroyed their activities.
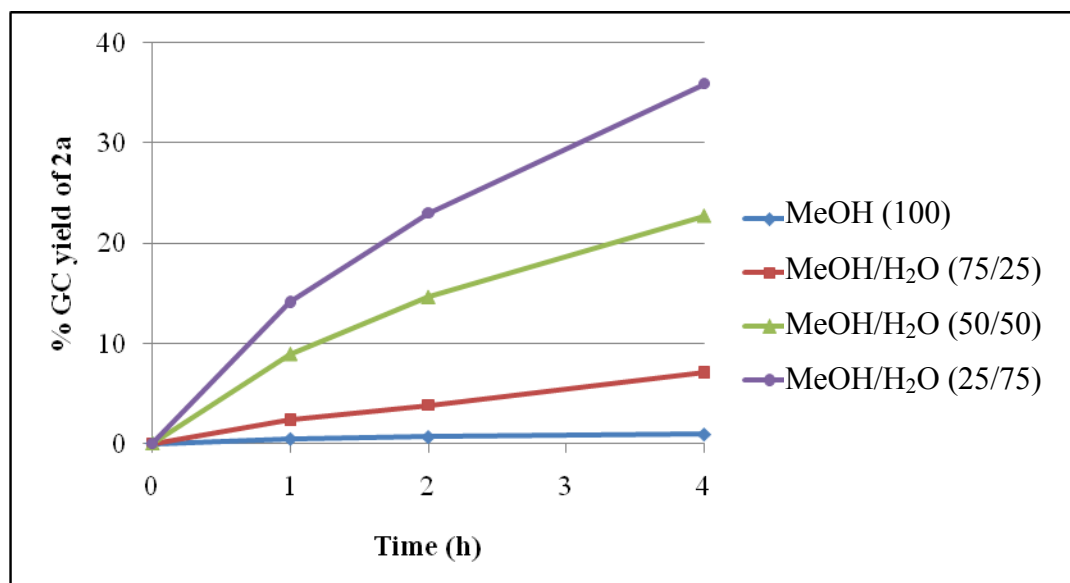
Figure 3.6 The effect of solvent ratio on *N*-formylation of **1a** under aerobic MeOH oxidation conditions.

3.3.1.6 Effect of concentration of reaction mixture

Previous literatures revealed that the concentration of the reaction using Au:PVP as a catalyst could affect on the rate of oxidation. With the high concentration of free ion in the solution of Au:PVP could cause the aggregation of Au:PVP clusters to the bigger ones, and then the activity of Au:PVP would be destroyed. The variation of the concentration of reaction mixture was investigated and results are shown in Table 3.5.

Table 3.5 The variation of total volume of reaction mixture
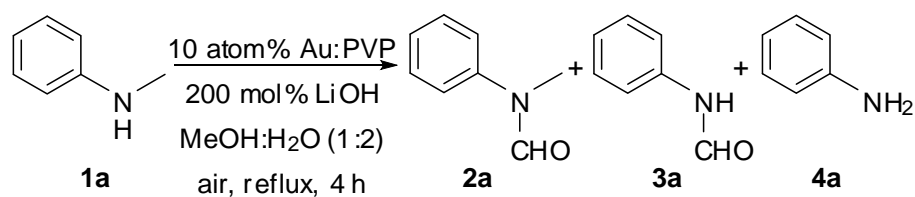
Entry	Total volume (mL)	Time (h)	% Recovery of 1a	% Yield[a]		
				2a	3a	4a
1	15	1	7	89	4	2
		4	-	94	5	-
2	7.5	1	8	90	3	2
		4	1	94	5	-
3[b]	1.5	1	40	45	-	2
		4	3	82	2	2

[a] GC yields using hexadecane as an internal standard.
[b] color change from dark brown to red.

The result showed that the reaction rates were not different under the conditions studied in entries 1 and 2. 89 and 90% of **2a** were obtained after 1 hour and 94% after 4 hours under both conditions. In contrast, the aggregation of Au:PVP was observed in the latter condition observed by the color change of solution mixture from dark brown to red. The lower yield of **2a** was observed in 45% after 1 h with 40% recovery of **1a** and 82% yield at 4 h.

3.3.2 Mechanism study for *N*-formylation of amines under aerobic MeOH oxidation condition

3.3.2.1 Formyl source for *N*-formylation of amines under MeOH oxidation condition

The main formyl source for *N*-formylation of amines was generated from aerobic oxidation of MeOH. Many kinds of product from the oxidation of MeOH using gold nanoclusters was reported such as HCHO, formic acid (HCOOH), methyl

formate (HCOOMe), or CO_2. To clarify the possible intermediate in the formylation reaction, different types of formyl sources were used instead of MeOH and the results are shown in Table 3.6.

Table 3.6 The variation of formyl sources

Entry	Formyl reagent (mol%)	% Recovery of 1a	% Yield[a]		
			2a	3a	4a
1	-	no reaction			
2	HCHO	21	81	-	1
3	HCOOMe	no reaction			
4	HCOOH	no reaction			

[a] GC yields using hexadecane as an internal standard.

All reactions were carried out under EtOH:H_2O (1:2) instead of MeOH:H_2O (1:2) at 50°C to avoid the oxidation of EtOH producing acetaldehyde. Formyl reagents were directly added to the solution mixture using 100 mol% for all reactions. In the case of without formyl sources, no reaction was observed (entry 1). When HCHO solution was added, 81% yield of **2a** was obtained with 21% recovery of **1a** (entry 2). The yield of **2a** from directly adding HCHO in entry 2 was obtained nearly equal to that from optimized conditions at 50°C with 80% of **2a** and 16% recovery of **1a** were observed (entry 2, Table 3.3). In contrast, neither addition of HCOOMe nor HCOOH, no reactions were observed (entries 3 and 4). These results indicated that a possible pathway for *N*-formylation should involved the hemiaminal formation by the condensation of amine and HCHO intermediate which generated from the oxidation of MeOH at reflux temperature rather than the condensation with HCOOH or HCOOMe from over oxidation of MeOH (Scheme 3.3).
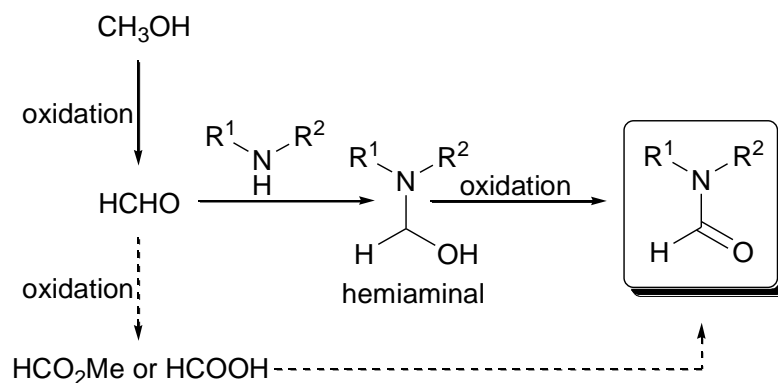
Scheme 3.3 Possible formyl source diagram for *N*-formylation of amine and MeOH.

These results were different from a report on the reaction on heterogeneous Au/NiO published by Ishida and Haruta [77]. They reported that Au/NiO catalyzed the oxidation of MeOH affording HCO_2Me under conditions (0.5 MPa O_2, 100 °C, 5 h) as the formyl source which it might react with benzylamine to give *N*-formyl product. In addition, the hemiaminal intermediate was proposed to stem from the reaction of dimethylamine and HCHO on the surface of Au or Ag catalyst [78-79].

3.3.2.2 Kinetic study of *N*-formylation of amines under aerobic MeOH oxidation condition

As the results above, the optimization condition of *N*-formylation of amines under aerobic MeOH oxidation condition is 10 atom% of Au:PVP with 200 mol% of LiOH at reflux MeOH-H_2O (1:2) under air for 4 hours. The kinetic study for *N*-formylation of amines was carried out with this optimization condition and %yield of each product was investigated by GC using hexadecane as an internal standard.
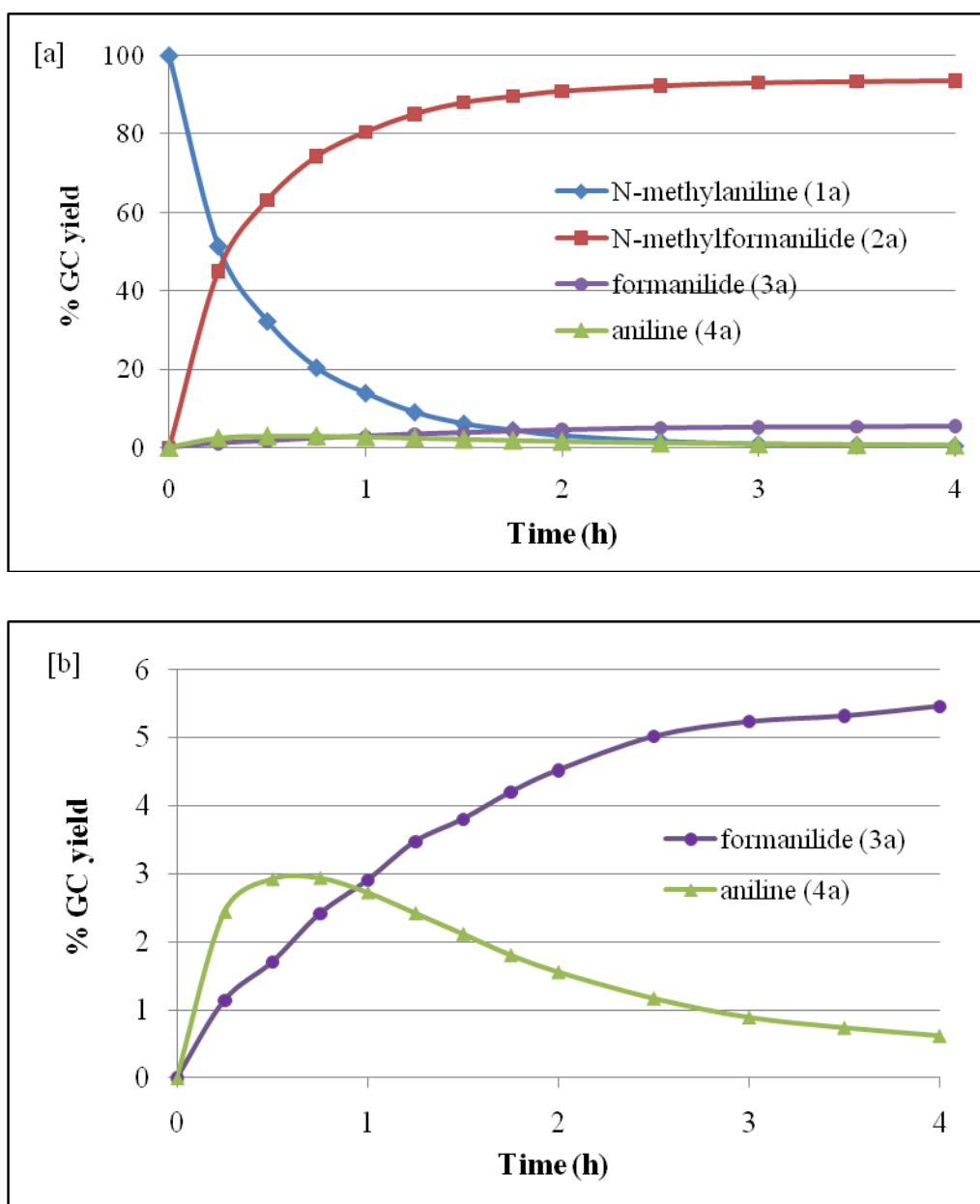
Figure 3.7 [a] The kinetic study of *N*-formylation of *N*-methylaniline (**1a**) and [b] the expanded profiles of aniline (**4a**) and formanilide (**3a**).

The formation of by-products **3a** and **4a** was observed from *N*-formylation of **1a**. Thus, a kinetic study of *N*-formylation of **1a** was investigated and the result was shown in Figure 3.7. The *N*-formylation was started with the fast rate and almost of products which could be obtained was *N*-formylation product **2a** with other minor products **3a** and **4a** in less amount than 6% (Figure 3.7[a]). As expected, aniline (**4a**) was observed during the reaction, with the amount of **4a** being increased until 1 hour

less than 3%, then gradually decreased. In the case of the formation of **3a**, the *N*-formylation was observed from the beginning and increasing during the reaction proceeded (Figure 3.7[b]).

In addition, *N*-formylation of **4a** could proceed under aerobic oxidation of MeOH at reflux MeOH-H_2O with 10 atom% of Au:PVP in the presence of 200 mol% of LiOH furnishing $HCONH_2$ (**3a**) in 50% yield (Scheme 3.4).
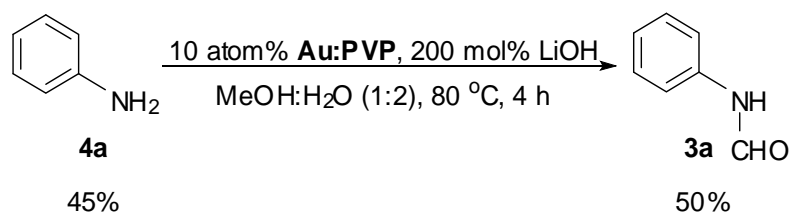
Scheme 3.4 *N*-formylation of aniline (**4a**) under aerobic MeOH oxidation condition.

Even though the reaction rate of *N*-formylation of **4a** was slower than that of **1a**, by-product **3a** could obtain from *N*-formylation of **4a** *via* *N*-demethylation of **1a** and followed by the *N*-formylation of **4a**.

3.3.2.3 Proposed mechanism for *N*-formylation of amines under aerobic MeOH oxidation catalyzed by Au:PVP

MeOH oxidation under reflux temperature (80 °C) gave aldehyde species (Figure 3.8). The main route of *N*-formylation of amines under aerobic MeOH oxidation condition was the condensation of amines with HCHO leading to hemiaminal (**a**) followed by the aerobic oxidation to afford amide product **A** (*path A*). However, because of the slow rate of MeOH oxidation, the condensation of amine with HCHO intermediate was retarded. Therefore, formamide **3a** and aniline **4a** were observed as by-products under this condition. Another pathway was proposed that an oxidative dehydrogenation of amines in *path B* generated imines at reflux temperature. Then, the hydration of imines under basic aqueous solution would transform through imines and hemiaminal (**b**). The reaction could proceed into two pathways from hemiaminal (**b**). The first one was hydrolysis of hemiaminal (**b**) in *path B-1* to afford aniline **C** as one of by-product, observed during the reaction. From

Scheme 3.4, the *N*-formylation of aniline **C** could proceed under the same condition affording hemiaminal (**c**) followed by oxidation of this hemiaminal to amide **D**. The second pathway is the oxidation of hemiaminal (**b**) to generate the other amide product **B**.
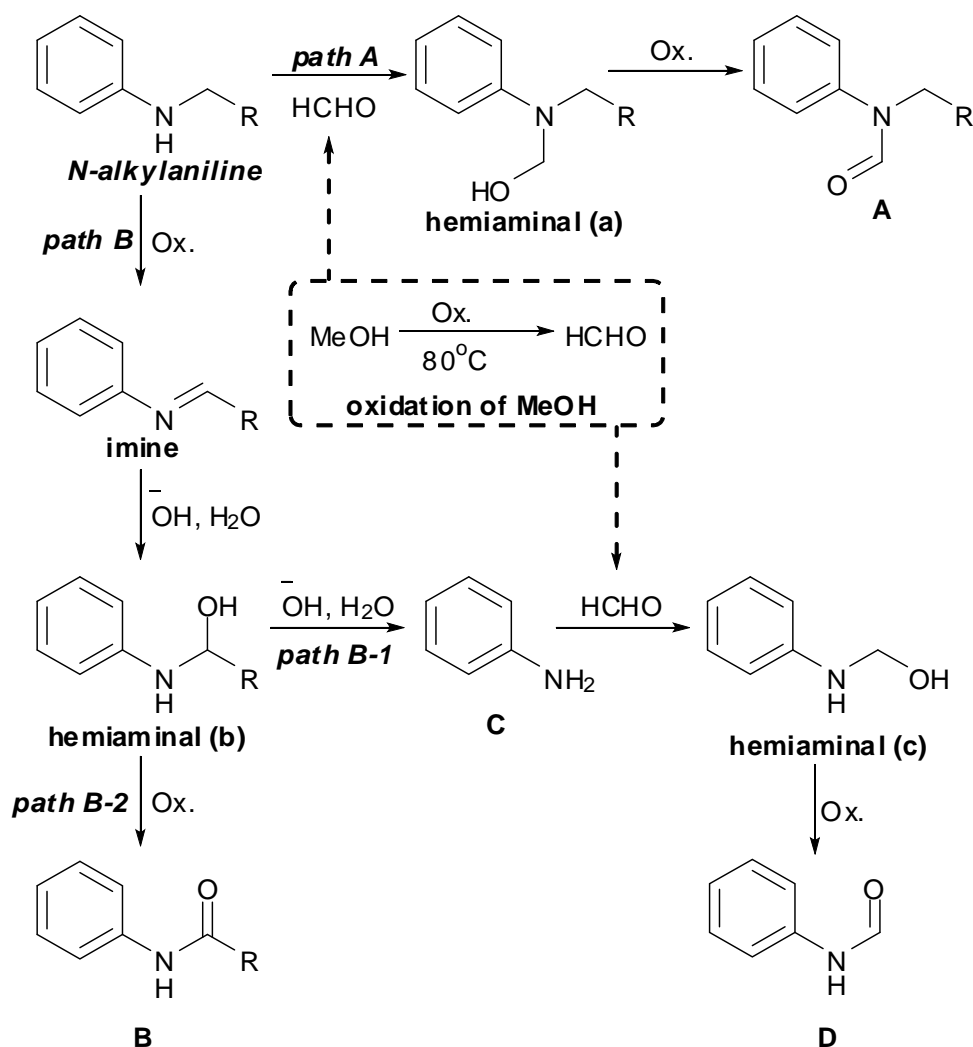
Figure 3.8 Proposed mechanism for *N*-formylation of amines.

In the case of *N*-methylaniline (**1a**), amide products **B** and **D** should be the same compounds. Thus, the *N*-formylation of *N*-ethylaniline (**1b**) was investigated to confirm the mechanism in *path B-2*.

3.3.2.4 *N*-formylation of *N*-ethylaniline (1b) and heterocyclic amine (1i) under aerobic MeOH oxidation condition

From the proposed mechanism in Figure 3.8, the *N*-formylation of **1b** was observed. The results are presented in Schemes 3.5 and 3.6.
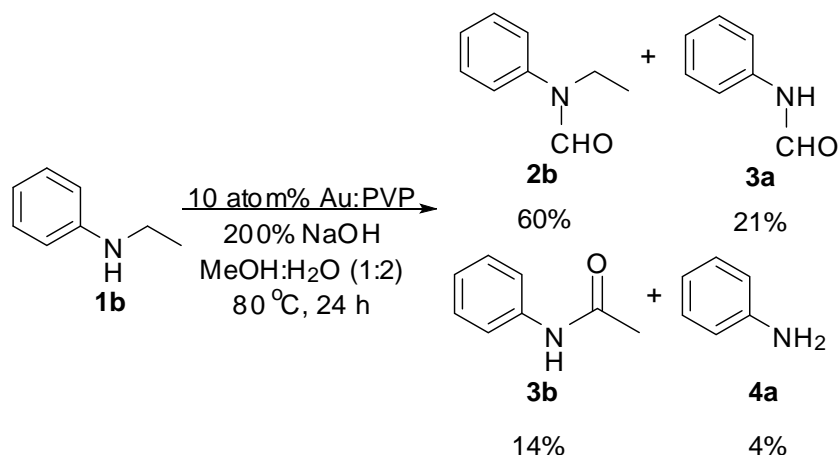
Scheme 3.5 *N*-formylation of *N*-ethylaniline (**1b**) under aerobic MeOH oxidation condition.

The oxidative dehydrogenation of amines in *path B* (Figure 3.8) could proceed faster when R group of amines was not hydrogen, such as *N*-ethylaniline (**1b**). The *N*-formylation of amine (**1b**) was carried out under the MeOH condition the same as under the optimization condition of **1a**. Four products were observed (Scheme 3.5). 60% of *N*-ethyl-*N*-phenylformamide (**2b**) was obtained as a major product from condensation of HCHO with **1b**. *N*-dealkylation of **1b** from oxidative dehydrogenation in *path B* was performed easier than that of *N*-methylaniline (**1a**). Thus, 21% of **3a** and 4% of **4a** were observed in higher yield relative to **1a**. In addition, 14% yield of **3b** was obtained from oxidative dehydrogenation of **1b** followed by hydration of imine and oxidation of hemiaminal to obtain an amide product. This is one of evidence for α-oxygenation of amines that proceed by Au:PVP catalysis (*path B-2*, Figure 3.8).
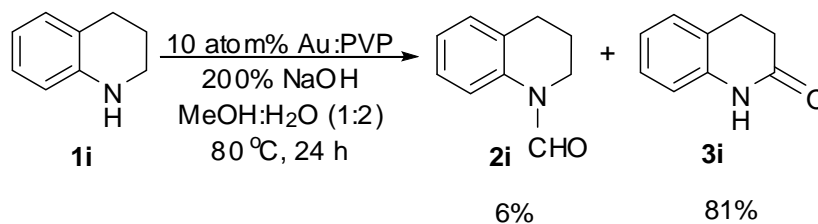
Scheme 3.6 *N*-formylation of 1,2,3,4-tetrahydroquinoline (**1i**) under aerobic MeOH oxidation condition.

The reaction of *N*-formylation of heterocyclic amines was next investigated. Interestingly, the reaction of 1,2,3,4-tetrahydroquinoline (**1i**) was proceeded to afford only 6% of *N*-formylated product and 81% of lactam **3i** was obtained as a major product. The imine formation of **1i** should derive easily in the case of *N*-ethylaniline, but the imine intermediate of **1i** is quite unstable. Thus, when the imine was formed, the hydration will proceed in a faster rate. The hydration reaction could proceed faster than oxidation, but in the case of heterocyclic amines the hydration might be easily reversible leading to the oxidation in the final step to form the lactam.

3.3.2.5 Isotope labeling experiment for *N*-formylation of 1a

The reaction of *N*-methylaniline (**1a**) with $^{13}CH_3OH$ took place with 10 atom% of Au:PVP in the presence of 200 mol% of LiOH under reflux temperature (80°C) in $^{13}CH_3OH$-H_2O (Scheme 3.7).
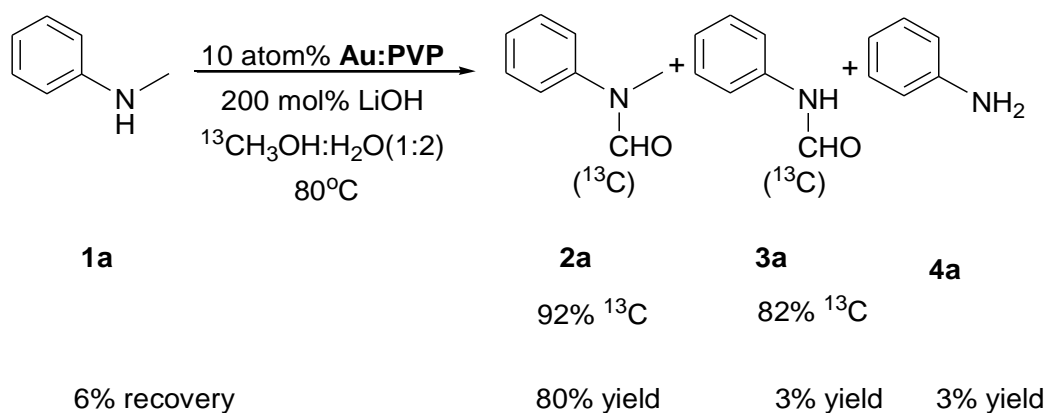
Scheme 3.7 Isotope labeling experiment for *N*-formylation of *N*-methylaniline (**1a**) under aerobic $^{13}CH_3OH$ oxidation.

The result showed that 92% of **2a-^{13}C** was observed from 80% yield of **2a**. Normally, the reaction of isotope labeling experiment could retard the reaction rate. However, the result indicated that the main source of formyl group was generated from aerobic ^{13}CH$_3$OH oxidation affording H^{13}CHO. Thus, 99% of ^{13}CH$_3$OH was used instead of CH$_3$OH in this experiment.

If **2a** was obtained by only condensation of amine **1a** and HCHO, the nearly 99% of **2a-^{13}C** should be observed from total yield of **2a**. However, only 92% of **2a-^{13}C** was observed from 80% yield of **2a**. Thus, 7% of **2a-^{12}C** should be formed by the condendation of amines with HCHO which generated from the other pathway. As shown in a proposed mechanism, HCHO should be generated from *N*-demethylation of **1a** through *path B* and *B-1* as a by-product (Figure 3.8). Thus, the reaction *path B* and *B-1* should carry out under this condition along with the *N*-formylation of **1a** and the formation of **2a-^{12}C** in 7% was attained.
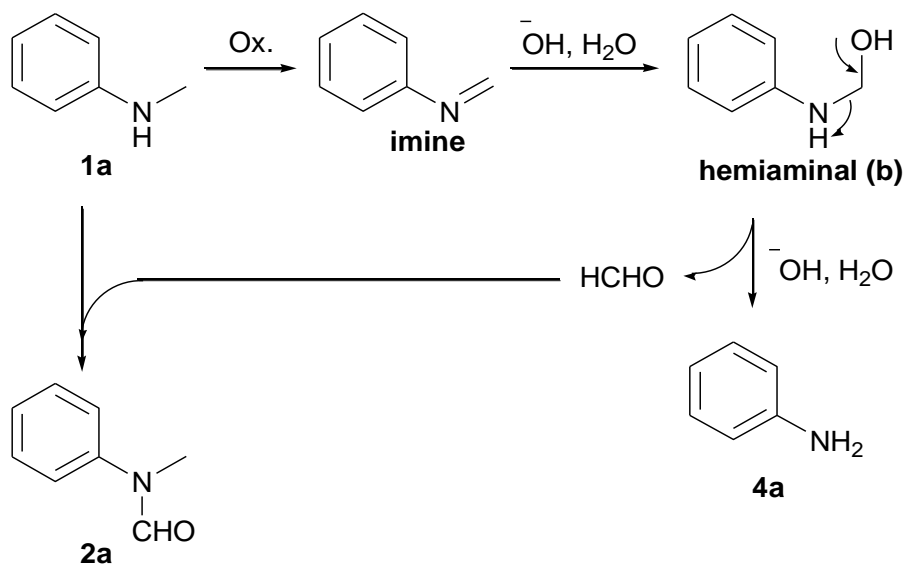
Figure 3.9 *N*-demethylation of **1a** under aerobic MeOH oxidation condition.

It must be noted that not only aniline should be formed by *N*-demethylation of amine **1a** but HCHO moiety could be formed as well (Figure 3.9). The amount of HCHO generated from *N*-demethylation should be roughly calculated from the amount of aniline. Thus, 94% conversion of this reaction was observed along with 80% of **2a** and 3% of **3a** the 8% of aniline should be obtained. Unfortunately, all

aniline in the solution mixture was difficult to extract, based on the recovery result of **1a** in only 6%. Possibly, about 5% of **4a** was still in the reaction mixture. However, it was explained that **2a-^{12}C** should generate from the condensation of amine **1a** with HCHO generated from *N*-demethylation of **1a**.

82% of **3a-^{13}C** was observed from 3% of **3a** indicating that the main source of formyl group was generated from aerobic ^{13}CH$_3$OH oxidation as well as in the case of the formation of **2a**, but the amount of **3a-^{12}C** (17% of 3 % of **3a**) was observed more than amide **2a**. The direct α-oxygenation of **1a** to **3a** in pathways B and B-2 should proceed in slower rate during reaction. The formation of **3a** by condensation with HCHO generated from *N*-demethylation of **1a** gave two possible pathways, which were caused more amount of ^{12}C-product **3a** than **2a**.

3.3.2.6 The pH of reaction mixture during the reaction and TOF of Au:PVP

As the reaction of *N*-formylation of **1a** in the presence of 200 mol% of LiOH and 10 atom% of Au:PVP under MeOH/H$_2$O (25/75) solution, TOF and pH were measured as shown in Figure 3.10.
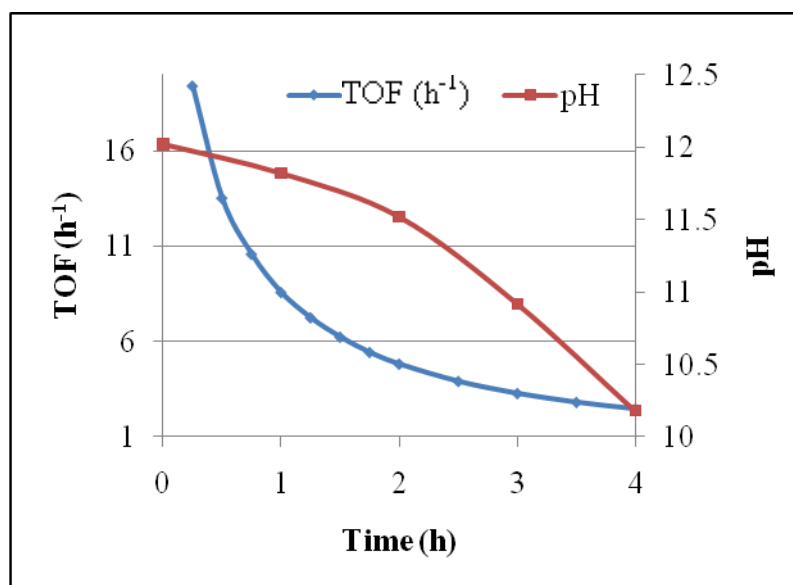
Figure 3.10 The turnover frequency (TOF) and pH of reaction mixture for *N*-formylation of **1a** under aerobic MeOH oxidation condition.

The pH for *N*-formylation of **1a** was gradually decreased from 12 to 10. Besides, hydroxide ion might be used to neutralize the formate ion which was generated from the over oxidation of MeOH. From previous report, the benzylic alcohol was oxidized to give benzoic acid as the major product. Therefore, more than 100 mol% of base was required. In addition, the formation of formate ion from the oxidation of MeOH by Au:PVP could diminish the reaction rate during the reaction which TOF of this reaction was decreased from 16 to 2 h^{-1} by aggregation of some Au nanoclusters in solution. It was simply investigated this aggregation by direct adding HCHO or HCOOH into the reaction mixture. The color was suddenly changed from dark brown to red brown. Although the aggregation occurred, the reaction could proceed under this condition.

3.3.3 Optimization study for *N*-formylation by HCHO condition

As known that the rate determining step would be the aerobic oxidation of MeOH to HCHO, and the oxidation of the hemiaminal to amide would occur smoothly, the reaction conditions were expected to be much milder in the presence of HCHO compared with MeOH. The screening condition using HCHO as a formyl reagent was investigated as shown in the following sections.

3.3.3.1 Effect of amount of Au:PVP

The amount of Au:PVP was investigated for *N*-formylation of **1a** by using 200 mol% of LiOH as an additive at 27 °C.

Table 3.7 The amount of Au:PVP for *N*-formylation of **1a** under HCHO condition
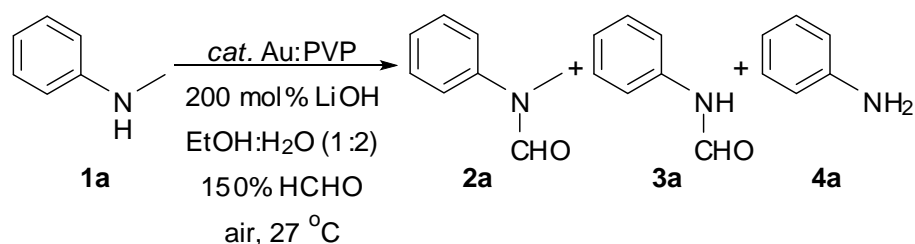
Entry	Au:PVP (atom%)	Time (h)	Recovery of 1a (%)	% Yield[a]		
				2a	3a	4a
1	1	2	6	79	-	-
2	1	4	6	80	-	-
3	1	24	3	97	-	-
4	3	2	2	80	-	-
5	5	2	2	82	-	-
6	10	0.5	-	> 99	-	-

[a] GC yields using hexadecane as an internal standard.

Quantitaive yield of **2a** was obtained in 0.5 hour when 10 atom% of Au:PVP was used and no by-products **3a** and **4a** were formed (entry 6). The increase of Au:PVP slightly increased the yield of **2a** from 79% to 82% when the amount of Au:PVP was increased from 1 to 5 atom% (entries 5, 4 and 1). %yield of **2a** using 1 atom% was up to 97%, but the reaction rate was dropped down very fast relative to the reaction at the beginning rate (entries 1, 2 and 3). The color of reaction mixture was investigated to check the aggregation of Au:PVP. It was found that the color of reaction solution suddenly changed from brown to red for all conditions after adding HCHO solution. It was possible that HCHO could cause the aggregation of Au:PVP in the reaction, so the reactions were nearly stop after 1-2 hours.

3.3.3.2 The variation of ratio of Au and HCHO

HCHO might cause the aggregation of Au:PVP and retarded *N*-formylation of amines by block surfaces of Au on PVP with HCHO, thus the oxidation by Au could

not proceed. The addition of HCHO to the reaction was investigated and the results are shown in Table 3.8.

Table 3.8 The variation of addition rate of HCHO for *N*-formylation of **1a**
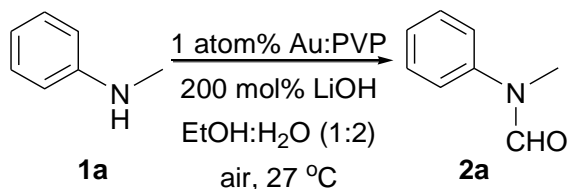
Entry	Amount of HCHO (total = 150 mol%)	Method for adding formalin	Time (h)	% Recovery of 1a	% Yield of 2a[a]
1	150	0 min	2	6	79
			4	6	80
			24	3	97
2	30×5	15 min-3 times and 30 min-2 times	2	1	87
			3	-	98
3	30×5	5 min-3 times and 10 min-2 times	0.75	11	79
			2	1	81
4	50×3	15 min-3 times	0.75	2	78
			1.5	1	81
			2	-	99

[a] GC yields using hexadecane as an internal standard.

After 2 hours, the amount of HCHO intermediate was retarded *N*-formylation. In entry 1, 79 and 80% of **2a** were obtained at 2 and 3 hours, respectively. If the reaction was prolonged until 24 hours, 97% of **2a** would be obtained. In entry 2, HCHO was added with 5 portions by adding at 0, 15, 30 minutes (3 portions was added in every 15 min), 1 and 1.5 hours (the other 2 portions were added in every 30 minutes). The reaction could complete within 3 hours yielding **2a** in 98%. To decrease the total time, the addition rate of HCHO was altered by adding 30 mol% in

5 portions at 0, 5, 10 minutes and then 20, 30 minutes (total addition time is 30 minutes) (entry 3). The reaction rate was dropped affording 79 and 81% of **2a** with 11 and 1% recovery of **1a** at 45 min and 2 hours, respectively. From entry 4, the addition of HCHO was finished in 45 minutes (50 mol% adding in 3 portions) giving 99% of **2a** within 2 hours. This optimization condition was used for further studies.

3.3.3.3 Variation of type and amount of bases

Various bases could be used as an additive for *N*-formylation of **1a**. The investigation on types of bases was carried out as shown in Table 3.9.

Table 3.9 The variation of type and amount of bases for *N*-formylation of **1a**
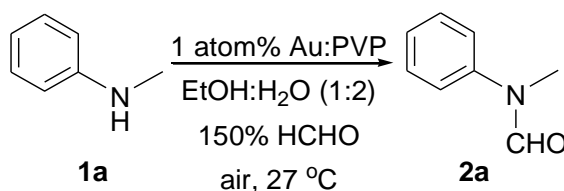
Entry	Base	Amount of base (mol%)	Time (h)	% Recovery of 1a	% Yield of 2a[a]
1	-	-	-	no reaction	
2	KHCO$_3$	200	5	-	100
3	NaHCO$_3$	200	5	-	99
4	NaHCO$_3$	100	5	-	94
5	NaHCO$_3$	50	9	-	100
6	LiOH	200	2	-	99
7	KOH	100	2	1	99
8	NaOH	100	2	-	99
9	NaOH	50	7	1	95
10	DBU	100	5	45	55
11	NaOAc	100	5	84	15
12	Et$_3$N	100	7	4	95

[a] GC yields using hexadecane as an internal standard.

N-formylation of **1a** could only proceed under basic conditions and no reaction was observed in the reaction without base (entry 1). GC yields of **2a** was obtained almost quantitative yield (95-100%) from each conditions except for entries 10 and 11. 55% of **2a** and 45% of **1a** were obtained when 100 mol% of DBU was used as an additive as well as 16% conversion of *N*-formylation of **1a** was observed under 100 mol% of NaOAc conditions giving only 15% of **2a**. Because of acetate anion in the reaction mixture generated from NaOAc could cause the aggregation of Au:PVP and deactivated gold nano-sized catalyst. The color of solution mixture was also changed from brown to red as a basic evidence for aggregation of Au nanoclusters. The weaker bases could complete the reaction within 5 hours with 94-100% yield of **2a** (entries 2-4). In entry 5, using 50 mol% of $NaHCO_3$ gave quantitative yield of **2a** at 9 hours. Similarly, the faster rate of *N*-formylation of **1a** was observed, the stronger base such as hydroxide was used. The reaction could complete within 2 hours even if 200 mol% or 100 mol% of base was used (entries 6-8) which almost no significance between 200 mol% base and 100 mol% base was observed. But in the case of using 50 mol% of NaOH, the reaction rate was slow down and 95% of **2a** was obtained after 7 hours (entry 9).

3.3.3.4 Effect of solvent

N-formylation of **1a** was then tried in mixed $EtOH-H_2O$ and H_2O. The results are shown in Table 3.10.

Table 3.10 The solvent effect for *N*-formylation
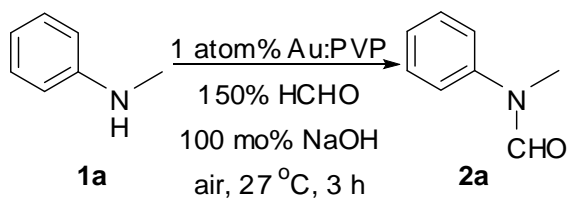
Entry	Solvent	% Recovery of 1a	% Yield of 2a
1	EtOH-H$_2$O	-	97
2	H$_2$O	11	78

a Isolated yields.

97% yield of **2a** was obtained in EtOH-H$_2$O (entry 1). On the other hand, only 78% yield with 89% conversion was observed under H$_2$O because of the poor solubility of amines in the reaction media. Thus, the activity of Au:PVP for *N*-formylation was retarded.

3.3.4 The variation of amines for practical method for *N*-formylation of amines with HCHO conditions

The above results motivated us to develop a practical method for *N*-formylation of amines with HCHO catalyzed by Au:PVP under aerobic conditions. Typical reaction conditions are as follows: 1 atom% of Au:PVP, 100 mol% of NaHCO$_3$, 150 mol% of HCHO (added as a 37% HCHO solution), EtOH:H$_2$O (1:2), 27°C, 9 h. The results of this reaction with various amines are summarized in Table 3.11.

Table 3.11 Scope and limitation of *N*-formylation catalyzed by Au:PVP

$$R^1\underset{H}{\overset{}{N}}R^2 \xrightarrow[\text{150 mol\% HCHO, EtOH:H}_2\text{O (1:2), 27 }^\circ\text{C}]{\text{1 atom\% Au:PVP, 100 mol\% NaOH}} R^1\underset{CHO}{\overset{}{N}}R^2$$

1a-n   **2a-n**
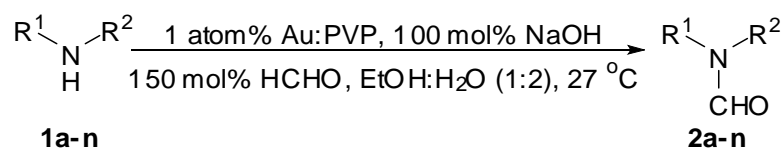
Entry	Amines	% Yield	Entry	Amines	% Yield
1		**1a** 97	8		**1h** 2
2		**1b** 91	9		**1i** 95
3		**1c (4a)** 53 (96[a])	10		**1j** 81
4		**1d** > 99[a]	11		**1k** 98[a]
5		**1e** 86	12[c]		**1l** 88 (100[b])
6		**1f** no reaction	13		**1m** 87
7		**1g** no reaction	14		**1n** 78[a]

[a] 10 atom% Au:PVP was used.
[b] 5 atom% Au:PVP was used.
[c] GC yields using hexadecane as an internal standard.

The slightly decrease of *N*-formyl product **2b** was observed in 91% yield when *N*-ethylaniline (**1b**) was used as a starting material (entry 2) comparing with **1a** (entry 1). The decrease of yield of **1b** may be because of the steric effect of ethyl group. In the case of secondary amine **1c**, the aggregation of Au clusters was observed during the reaction leading to 53% yield of desired product **2c** when the reaction underwent

with 1 atom% of Au:PVP. Then, the amount of catalyst was increased to 10 atom% and yield of **2c** was improved up to 96% (entry 3). A remarkable electronic effect was observed in the reactions of **1d**, **1e** and **1f**, *para*-substituted *N*-methylaniline derivatives. Electron-donating groups (**1d** and **1e**) in entries 4-5 gave high yield of *N*-formylated product in >99 and 86% of **2d** and **2e**, respectively. In contrary, no reaction was observed in the case of electron-withdrawing group (**1f**) (entry 6) due to the strong electron-withdrawing effect. The *ortho*-subsitituted *N*-methylaniline (**1g**) was carried out under the same condition, but no reaction was observed because of the steric effect at *ortho*-position (entry 7) [36]. In addition, it was also found in the case of *N,N*-diphenylamine (**1h**) that only 2% of **2h** was obtained because of the steric from diphenyl groups (entry 8).

In the case of cyclic arylamines **1i-1k** in entries 9-11, the reactions proceeded to give the desired products **2i-2k** in high yields (81-98%) which in the case of indoline (**1k**), 10 atom% of Au:PVP was required. In addition, piperidine (**1l**) was carried out with 1 atom% affording 88% and quantitative yield when 5 atom% of Au:PVP was used (entry 12). Alkyamine (**1m**) was also carried out yielding **2m** in high yield (87%, entry 13). A naphthlamine **1n** underwent *N*-formylation using 10 atom% of catalyst furnishing 78% of **2n**.

3.4   Conclusion

Au:PVP was found to be an excellent catalyst for direct *N*-formylation of amines with MeOH or HCHO as a formyl agent. 10 atom% of Au:PVP and 200 mol% LiOH under reflux MeOH-H_2O was the optimization condition. The reaction was carried out through the oxidation of MeOH as a rate determining step and then the condensation of amines and HCHO intermediate was proceeded, following the oxidation of hemiaminal to give *N*-formylated products. *N*-Demethylation of amines was the side reaction when *N*-formylation of amines was carried out under reflux temperature affording the side products. Therefore, the practical procedure of *N*-formylation of amines could undergo with milder condition using only 1 atom% of catalyst under basic condition at room temperature. The desired products were obtained in moderate to excellent yield with 100% selectivity.

CHAPTER IV

AEROBIC OXIDATION OF CYCLIC AMINES TO LACTAMS CATALYZED BY PVP-STABILIZED NANOGOLD

4.1 Introduction and literature reviews

4.1.1 Oxidation of amines

There are a variety of oxidizing agents for an oxidation of amines depending on types of amines (primary, secondary or tertiary amines) and desired products. In this research, direct oxidation of amines, especially heterocyclic amines, to corresponding lactam is focused.

4.1.1.1 Hypervalent iodines

Hypervalent iodines are firstly reported in 1988 for oxidation of amines. The oxidative decarboxylation of cyclic amino acids with iodosobenzene (ISB) yielded lactam under neutral conditions [80]. 2.2 Equiv of ISB was used for oxidation of *L*-proline affording pyrrolidinone in 70% isolated yield (Scheme 4.1). The first step for the oxidative decarboxylation was the formation of imine intermediate following the second oxidation of cyclic hemiaminal to give lactam.
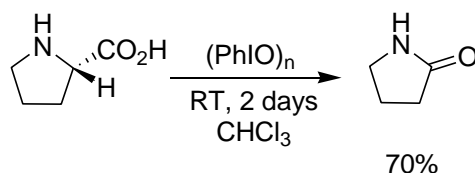
Scheme 4.1 Oxidative decarboxylation of *L*-proline.

In addition, dehydrogenation of cyclic amines by ISB could proceed at room temperature. Indole was obtained in 38% yield by the oxidation of indoline and 61% of 3,4-dihydroisoquinoline was formed from oxidative dehydrogenation of tetrahydro-

isoquinoline (Scheme 4.2) under the same condition with the oxidation in Scheme 4.1 except for 1.1 equivalent of ISB was used.
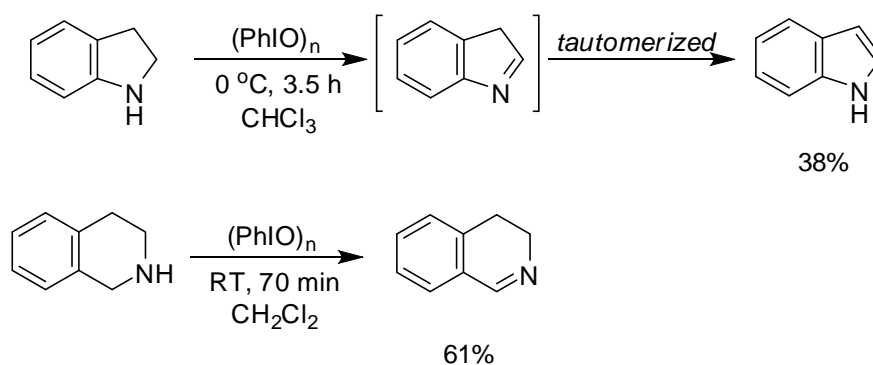
Scheme 4.2 Dehydrogenation of cyclic amines by ISB.

In the same year, the use of hypervalent iodine in amine oxidation was reported by Moriarty and Ochiai [81]. Secondary or tertiary heterocyclic amines were oxidized to give lactam around 70% yield. In the case of benzo-fused heterocyclic amines, tetrahydroisoquinoline was oxidized to afford the corresponding lactam in 45% using 3.2 equivalents of ISB (Scheme 4.3).
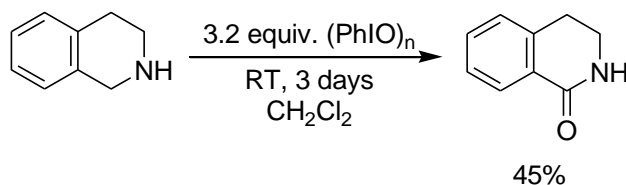
Scheme 4.3 Oxidation of 1,2,3,4-tetrahydroisoquinoline.

Using more ISB made the oxygenation at α-position of amines proceed faster than oxidative dehydrogenation. In fact this was a potent approach for the preparation of imine. To enhance an activity of ISB, metal complex or terminal oxidant and Lewis acid was used as a catalyst. For example, Mn(III) porphyrin, Mn(III) salen or Fe(III) porphyrin were selected to use in the oxidation of amines to imines by ISB [82]. Moderate to excellent yields were obtained. However, by products such as aldehyde or carboxylic acid were formed.

TBHP was also used as terminal oxidant in the oxidation of amines with iodinanes. Lewis acids such as $BF_3\text{-}Et_2O$, NO_2BF_4 or TMSOTf were required to activate ISB, but long reaction time was required [83-84].

In 2002, Huang reported the oxidation of amines with ISB using tetrabutylammonium iodide (TBAI) as a catalyst in a mixed solvent [85]. Quaternary ammonium salts such as TBAI could enhance the oxidation rate of ISB in the oxidation of benzo-fused heterocyclic tertiary amines to the corresponding amides in quantitative yield in MeCN or $MeCN/H_2O$ at room temperature. However, the oxidation of tetrahydroisoquinoline afforded a mixture of lactam and quinoline (Scheme 4.4).
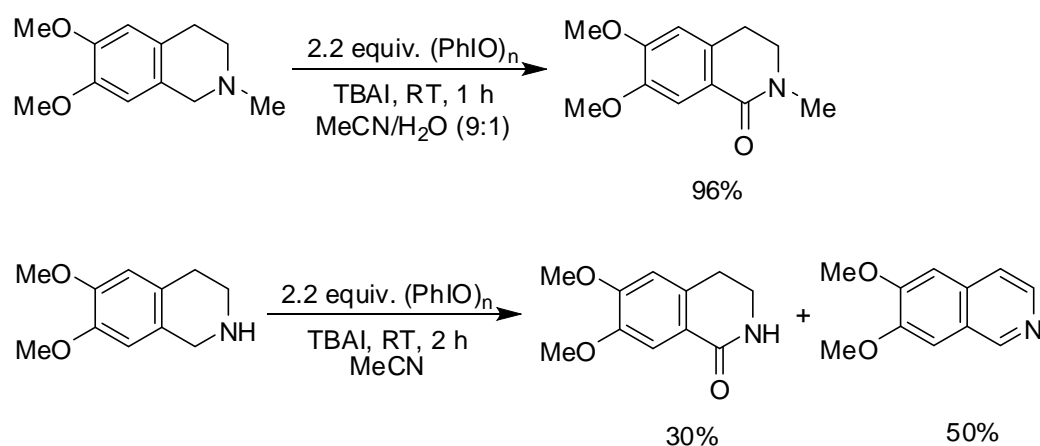
Scheme 4.4 Oxidation of 1,2,3,4-tetrahydroisoquinoline and substituted tetrahydroisoquinoline by ISB with TBAI as a catalyst.

Recently, Dohi published the benzylic C-H oxidation in water using activated polymeric iodosobenzene $(PhIO)_n$ with KBr in the presence of montmorillonite K-10 (M-K10) [86].

Aqueous solution of $(PhIO)_n$ 3 equivalents and KBr 0.2 equivalents could proceed the selective oxidation at benzyl positions adjacent to the heteroatom to afford 71% yield of the desired lactam (Scheme 4.5). However, there are no reports for the oxidation of tetrahydroquinoline.
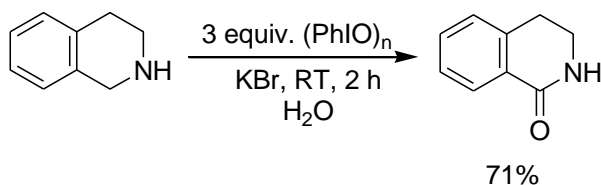
Scheme 4.5 Aqueous benzylic oxidation of aromatic compounds having activated benzyl groups.

4.1.1.2 Potassium permanganate (KMnO$_4$) [87]

KMnO$_4$ is a general oxidizing agent that could proceed many kinds of oxidation reactions. Among them, the oxidaition of isoquinoline and quinoline was reported in 1996 by Venkov. Tetrahydroquinoline, tetrahydro*iso*quinoline and *N*-substituted tetrahydro*iso*quinolines were tried in the oxidation condition using excess amount of KMnO$_4$ with catalytic amount of 18-crown-6 (Scheme 4.6).
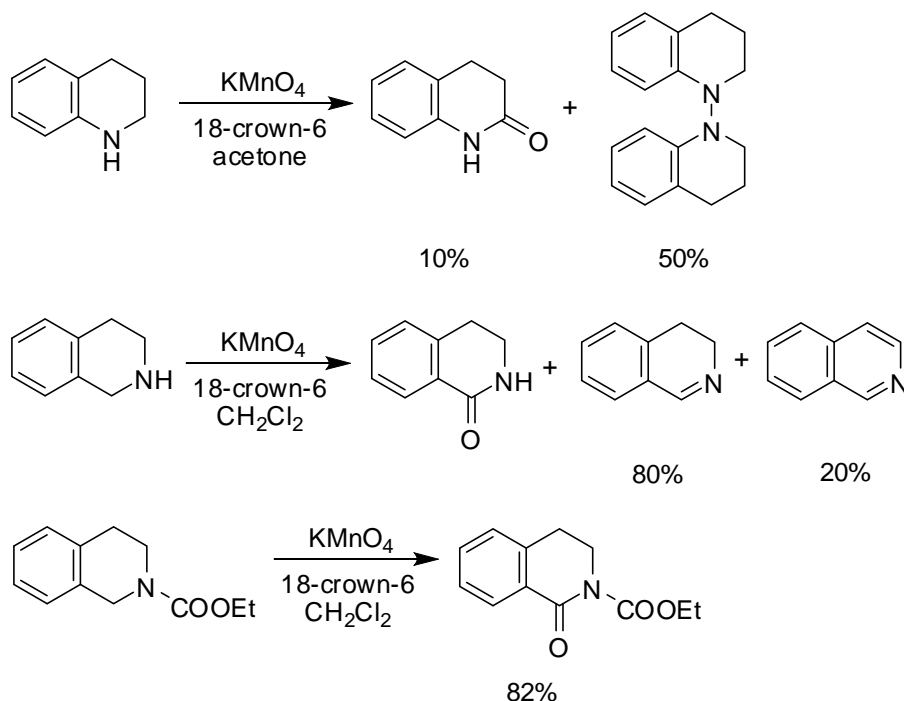
Scheme 4.6 Oxidation of amines with KMnO$_4$ in the presence of 18-crown-6.

The disadvantages were the mixture of products with low yield (Scheme 4.6). The stoichiometic excess of KMnO$_4$ was required to proceed the oxidation reaction.

4.1.1.3 Sodium chlorite [88]

Recently, the above mentioned oxidant was addressed for the oxidation of secondary amines or imines. The excellent yield of the corresponding lactam from the oxidation of 3,4-dihydro*iso*quinoline was obtained. However, the direct oxidation of tetrahydro*iso*quinoline was impossible. Only 4% of desired lactam in 34% conversion was observed. In addition, 98% of desired lactam was obtained after treated the reaction mixture for 5 min with 10% aqueous sodium thiosulfate (Scheme 4.7).

^{a}after work up with 10% aqueous of sodium thiosulfate
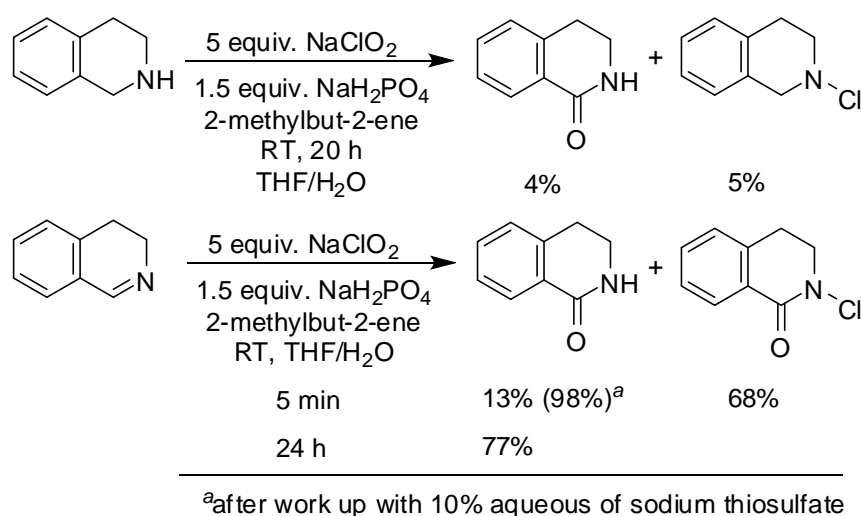
Scheme 4.7 Oxidation of amines and imines with sodium chloride under buffered condition.

However, the oxidation of imines to amides has been reported not only NaClO$_2$, but also various transition-metals such as nickel peroxide and other oxidizing agents: *m*CPBA, TBHP, and oxone.

4.1.1.4 Metal catalyst

Aerobic oxidation of amines is an interesting topic for green chemistry because the oxygen gas is inexpensive and clean oxidant. Many transition metal complexes have been reported for this purpose. For example, inexpensive Cu(I) or (II) chloride was used in aerobic oxidation of amines to imines or nitriles at 80 °C in toluene with dehydrating agent for 12 hours (Scheme 4.8) [89].
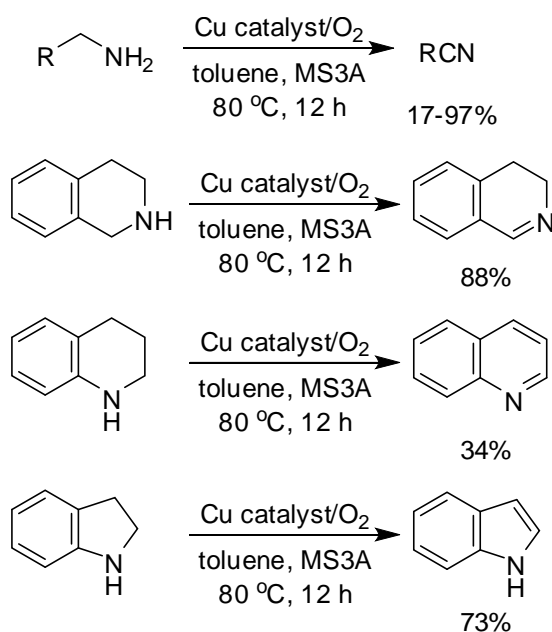
Scheme 4.8 Aerobic oxidation of amines by copper catalyst.

In 2006, palladium was firstly examined in the aerobic oxidation of amines [90]. The secondary amines were tried with Pd salt catalyst. 25-98% of imines were obtained from the oxidation of secondary amines under DMF condition at 80°C for 14 hours.

In the same year, dirhodium caprolactamate ($Rh_2(cap)_4$) was reported for the oxidation of amines in the presence of TBHP instead of molecular oxygen [91]. Under the conditions: at room temperature in MeCN of Rh catalyst and 2-4 equivalents of TBHP, the oxidative dehydrogenation of benzo-fused hetercyclic amines were proceeded affording the corresponding imines in high yield (> 80% yield) (Scheme 4.9).
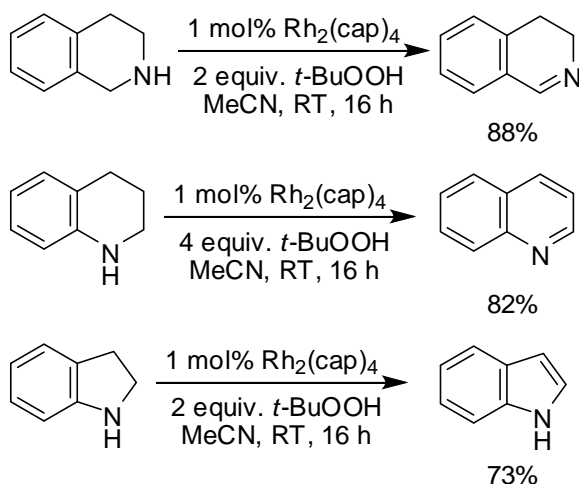
Scheme 4.9 Aerobic oxidation of amines by rhodium catalyst.

In addition, oxovanadium complex bearing 3-hydroxypicolinic acid ($VO(Hhpic)_2$) was reported in the oxidation of amines to imines under atmospheric molecular oxygen uisng imidazolium-type ionic liquids. This process made possible to attain recycling of the catalyst [92]. However, harsh conditions would be required (Scheme 4.10).
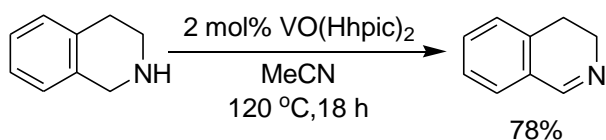
Scheme 4.10 Aerobic oxidation of amines by oxovanadium complex.

As shown above, the oxidation of amines by metal complexes with external oxidizing agents such as peroxide or molecular oxygen could proceed only oxidative dehydrogenation of amines. Nonetheless, there were no reports in the oxygenation of amines to amides.

4.1.2 Aerobic oxidation of amines catalyzed by gold

From 2007 until now, metallic gold, particularly nano-sized gold clusters, has attracted a great deal of interest as an aerobic amine oxidation catalyst.

4.1.2.1 Oxidative dehydrogenation

Zhu and Angelici firstly reported the catalysis for aerobic amine oxidation by bulk gold powder (~10^3 nm particle size) or micrometric size gold with molecular oxygen [93]. A novel and unexpected feature of this work was that bulk gold powder catalyzed this transformation, although at an extremely low rate (Scheme 4.11). This report initiated a great interest in developing efficient gold catalysts for the dehydrogenation of amines using molecular oxygen.

^{a}condition a, ^{b}condition b
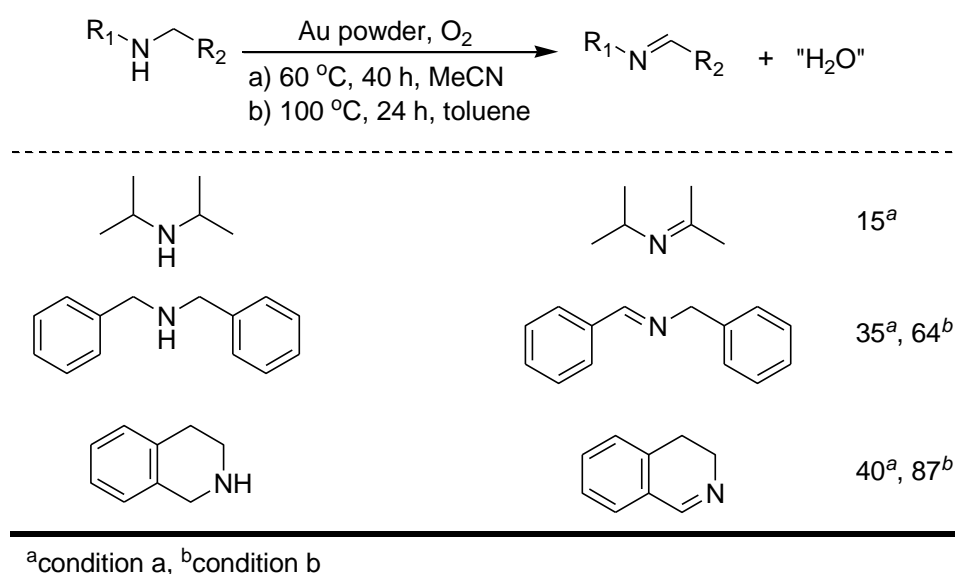
Scheme 4.11 Non-nanogold catalyzed aerobic oxidation of secondary amines to imines.

In 2008, the reports from Angelici using bulk gold metal of micrometric size and alumina-supported gold nanoparticles (size distribution 50-100 nm) as catalysts for the aerobic oxidative condensation of benzylamines indicated the low activity of bulk gold clusters [94-95]. Since these reports, the development of small size gold cluster for aerobic oxidative condensation of benzylamines to imines has been studied. In principle, it could be anticipated that by decreasing the gold crystallite size the activity of gold should increase. Corma and co-workers reported the heterogeneous gold nanocluster catalyst for aerobic oxidation of benzylamines (Table 4.1) [96].

Table 4.1 Average particle size (d), TOF, conversion and selectivity for benzylamine oxidation catalyzed by a series of gold catalysts with different particle sizes

	Catalyst				
	0.8 wt% Au/C	1.5 wt% Au/TiO$_2$	1.2 wt% Au/TiO$_2$	Au/TiO$_2$	Au/Al$_2$O$_3$
(d) (nm)	10	3.5	5.5	25	69
TOF (h^{-1})	280	70	20	0	0
Time (h)	1	30	30	30	30
Conversion (%)	99	98	76	58	48
Selectivity (%)	100	94	98	97	97

The activity of gold clusters increased when the smaller sizes of gold clusters were used (Table 4.1). 69 nm of Au/Al$_2$O$_3$ and 25 nm of Au/TiO$_2$ were used in benzylamine oxidation. Only 48 and 58% conversion were observed, respectively. The smaller size of Au/TiO$_2$ cluster was tried. 76% conversion was obtained in the reaction using 5.5 nm of Au/TiO$_2$ and 98% conversion was observed when using 3.5 nm of Au/TiO$_2$. Except for 10 nm of Au/C, this catalyst could proceed the oxidation up to 99% conversion in 1 hour with high TOF (280 h^{-1}). They explained that the catalyst may exhibit a large number of very small particles that were difficult to be seen and to be measured by TEM.

In 2009, Linda and co-workers published the oxidation of dibenzylamine to dibenzylimine with molecular oxygen using Au(OAc)$_3$/CeO$_2$. The reaction was furnished by using Au(OAc)$_3$/CeO$_2$ in toluene at 108°C. 99.7% yield with 91% selectivity of imine product was obtained (Scheme 4.12) [97].
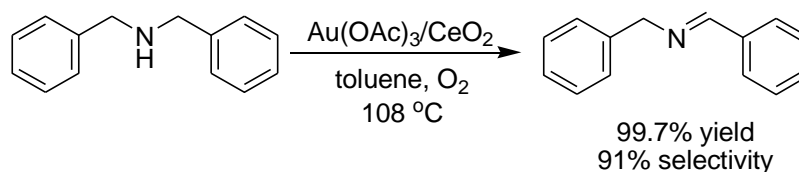
Scheme 4.12 Aerobic oxidation of dibenzylamine.

Au(OAc)$_3$ was dissolved and subsequently reduced by amine and the *in situ* formed gold nanoparticles was believed as the real active species of this reaction. In that year, they also reported the oxidation of indoline to indole using similar condition (Scheme 4.13) [98-99].
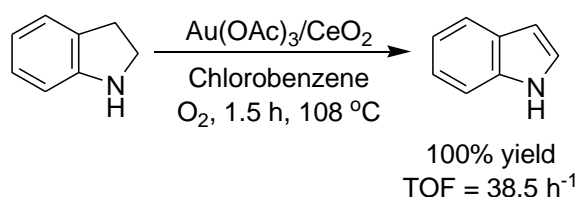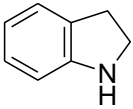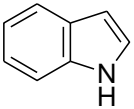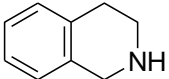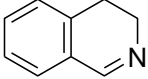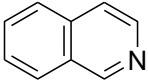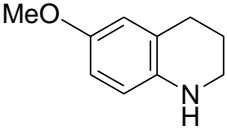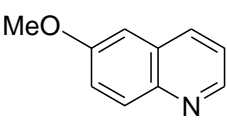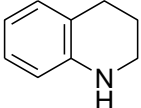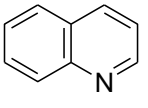
Scheme 4.13 Oxidation of indoline.

Furthermore, the magnetically separable gold nano-sized catalyst was developed. Au/CeO$_2$ showed high activity for oxidation of amines to imines. For instance, Linda and co-workers prepared Au/CeO$_2$/FeO$_x$ for simplicity and easily reused by magnetic separation from the reaction [100].

Che and co-workers studied the graphite-supported gold nanoparticles (AuNPs/C) to catalyze aerobic oxidation of cyclic amines to corresponding imines with 43-100% conversion (Table 4.2).[101] Comparing with the report of Angelici and co-coworkers, aerobic oxidation of 1,2,3,4-tetrahydroisoquinoline (entry 2, Table 4.2) was catalyzed by Au/Al$_2$O$_3$ at 100°C for 80 hours. This indicated that the small size of gold clusters catalyst was important for the activity in oxidation reaction.

Table 4.2 Aerobic oxidation of heterocyclic secondary amines using the AuNPs/C
and oxygen

Entry	Substrate	Product	Conversion (%)	Yield (%)[a]
1			68	66
2			100	95 (84:8)[b]
3			92	95
4			43	78

Condition: amines (0.4 mmol), AuNPs/C (Au: 5 mol%), toluene (8 mL), O_2
bubbling, 110 °C, 24 h. [a]yield was calculated based on substrate conversion.
[b]The ratio of products is shown in parentheses.

4.1.2.2 The synthesis of azo compounds [102]

Gold nanoparticles supported on TiO_2 and CeO_2 could catalyze the aerobic
oxidation of anilines to azo compounds with high yield (Scheme 4.14).
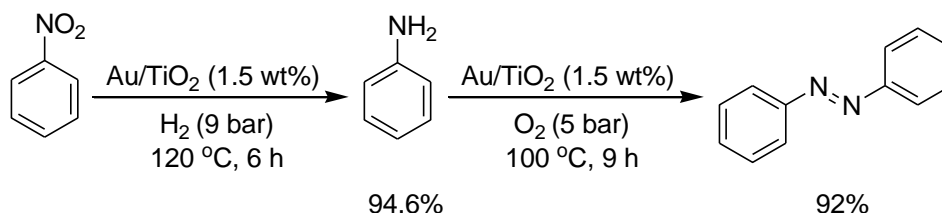
Scheme 4.14 Two steps synthesis for azo compound by reduction and oxidation of
Au/TiO_2 as a catalyst.

In addition, Au/TiO$_2$ could also act as a reductive catalyst to proceed the reduction of nitroaromatics to aniline in good yield by adding hydrogen molecule. Different metal oxide support could be accessed the reaction in different activity, such as Au/Fe$_2$O$_3$ or Au/C could not proceed the formation of azo compounds under this condition.

4.1.2.3 Enamine synthesis [103]

In 2010, the oxidative dehydrogenation of amines by Au nanoclusters catalyst could apply in the synthesis of enamines. The reaction of diazoalkanes with amines and O$_2$ giving enamines was reported by Zhou (Scheme 4.15).
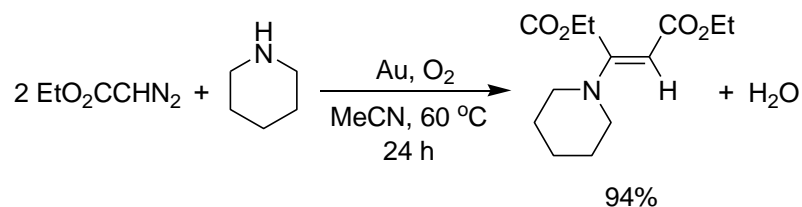
Scheme 4.15 Gold powder catalyzed reaction of ethyl diazoacetate (EDA) with piperidine and oxygen molecule.

4.1.2.4 Oxidation of tertiary amines

In 2009, Che reported the aerobic oxidation of tertiary amines catalyzed by AuNPs/C. *N*-alkyl or phenyl-1,2,3,4-tetrahydroisoquinoline were treated with AuNPs/C (Au 5 mol%) in reflux toluene (110°C) under O$_2$ bubbling in the precence of saturated NaHCO$_3$ (1 mL) (Scheme 4.16) [22].
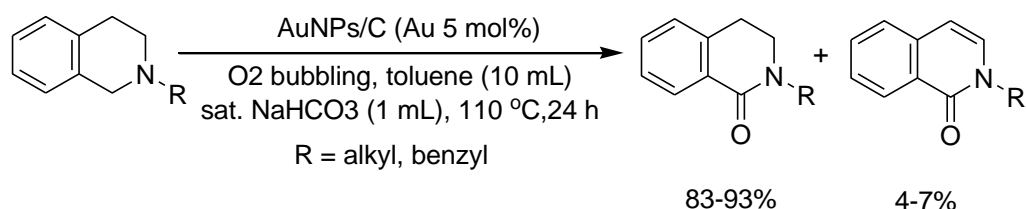
Scheme 4.16 Aerobic oxidation of tertiary amines using AuNPs/C and O$_2$ protocol.

The mixture of amide products was generated. Dehydrogenation yielding lactam was obtained as a minor product. As shown above, the aerobic oxidation of amines generally required high temperature. The size of gold nanoclusters is an important factor for catalytic activity of gold nano-sized catalyst.

Herein, Au:PVP was selected to explore the aerobic oxidation of heterocyclic amines. The higher catalytic activity was expected due to *quasi*-homogeneous system and smaller size of gold nanoclusters. As shown in Chapter III, Au:PVP demonstrated the excellent catalytic activity as *quasi*-homogeneous catalysts for aerobic oxidation of MeOH in aqueous solution. Both Au:PVP-catalyzed *N*-formylation of amines under MeOH oxidation and HCHO conditions could generate hemiaminal intermediate by the condensation of starting amines with HCHO. Then, the oxidation of that hemiaminal intermediate will proceed the amide formation to afford *N*-formyl products.

conditions	2a	3a
a. 1 atom% Au:PVP, 150 mol% HCHO 50 mol% NaHCO$_3$, EtOH-H$_2$O (1:2) 27 $^{\circ}$C, 9 h	97%	-
b. 10 atom% Au:PVP, 200 mol% LiOH MeOH-H$_2$O (1:2), 80 $^{\circ}$C, 4 h	94%	5%
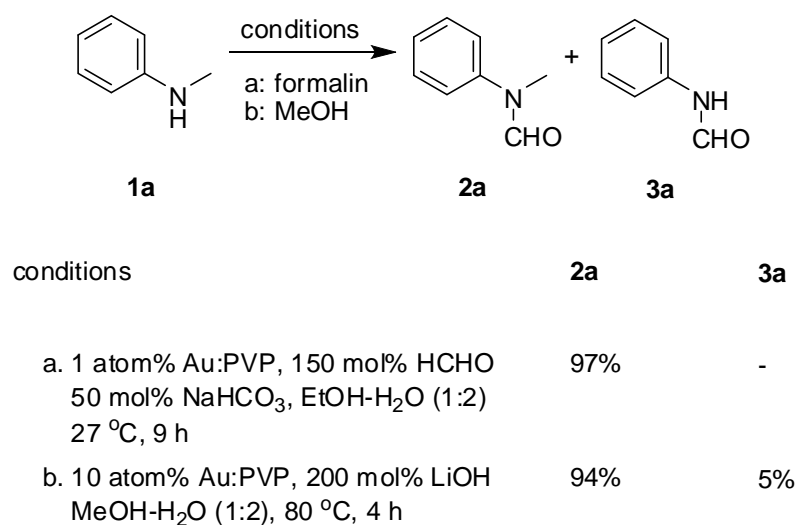
Scheme 4.17 *N*-formylation of **1a** under MeOH oxidation and HCHO condtion.

The model reaction, *N*-methylaniline (**1a**) was shown in Scheme 4.16. An excellent selectivity for *N*-formylation of **1a** was observed when 1 atom% of Au:PVP and HCHO solution was used in weak basic aqueous conditions at 27°C for 9 hours and 97% of **2a** was observed (condition a, Scheme 4.17). The selectivity of *N*-formylation of **1a** was slightly decreased when the reaction underwent with 10 atom% Au:PVP and 200 mol% LiOH under reflux MeOH and water for 4 hours. (condition b,

Scheme 4.17). 94% yield of **1a** was obtained along with 5% yield of *N*-formylaniline (**3a**) *via* oxidative demethylation of **1a**, followed by *N*-formylation.

conditions	2i	3i
a. 10 atom% Au:PVP, 150 mol% HCHO 200 mol% NaOH, EtOH-H$_2$O (1:2) 27 °C, 24 h	95%	-
b. 10 atom% Au:PVP, 200 mol% NaOH MeOH-H$_2$O (1:2), 80 °C, 24 h	6%	81%
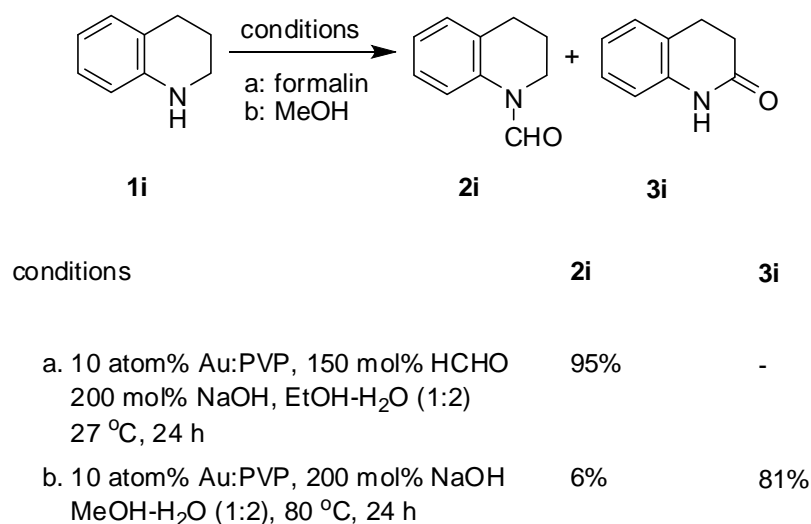
Scheme 4.18 *N*-formylation of **1i** under MeOH oxidation and HCHO conditions.

In the case of tetrahydroquinoline (**1i**), *N*-formylation product (**2i**) was obtained in 100% selectivity with 95% yield when the reaction was carried out in HCHO (condition a, Scheme 4.18). Interestingly, the selectivity was opposite under condition **b**. The lactam (**3i**) was afforded from MeOH oxidation condition (condition **b**, Scheme 4.18) as the main product in 81% yield along with only 6% desired *N*-formylation product (**2i**). The possible mechanism in Figure 4.1 could describe the different forms of two hemiaminal intermediates. One was generated from the condensation of **1i** with HCHO (hemiaminal **A**) and the other was formed from the oxidative dehydrogenation to imines followed by hydration of imine (hemiaminal **B**).
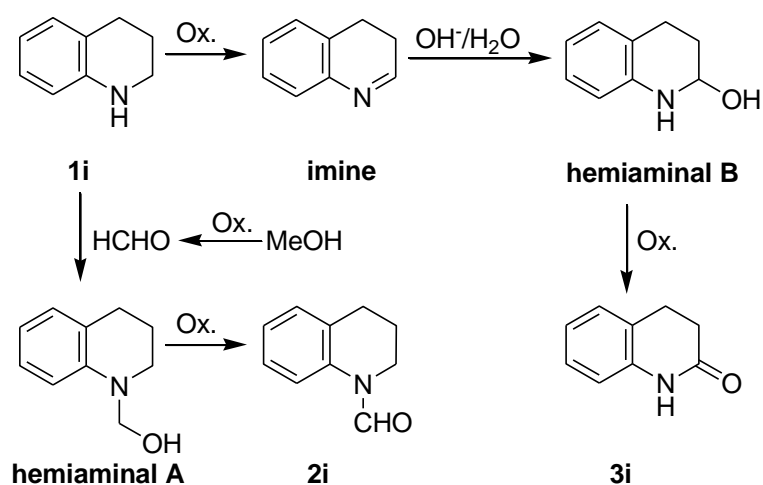
Figure 4.1 Possible pathways of *N*-formylation and oxidation of tetrahydroquinoline.

These results indicated that the oxidation of MeOH was slower than the imine formation *via* oxidative dehydrogenation of amine, especially cyclic secondary amines. In addition, this result was the first example of the α-oxygenation of a cyclic secondary amine by Au nano-sized catalyst. Because of benzo-fused lactam skeletons such as 3,4-dihydroquinolin-2-ones were important in pharmacologically and biologically active compounds, the aerobic oxygenation at the *α*-position of cyclic amines should be valuable for investigation.

4.2   Objective of this work

To study the highly selective α-oxygenation of a cyclic secondary amine catalyzed by Au nano-sized catalyst under basic aerobic conditions. The selectivity between oxidative dehydrogenation and oxygenation of amines would be investigated. Furthermore, the mechanism of *α*-oxygenation of amines was discussed.

4.3   Results and discussion

4.3.1   Optimization study

4.3.1.1 *α*-Oxygenation of 1,2,3,4-tetrahydroquinoline (1i)

As described above, *α*-oxygenation of 1,2,3,4-tetrahydroquinoline (**1i**) could proceed under reflux MeOH-H$_2$O catalyzed by 10 atom% of Au:PVP in the presence

of 200 mol% of LiOH. The optimization for selective α-oxygenation of **1i** was investigated and the results are listed in Table 4.3.

Table 4.3 The optimization for aerobic oxidation of **1i**
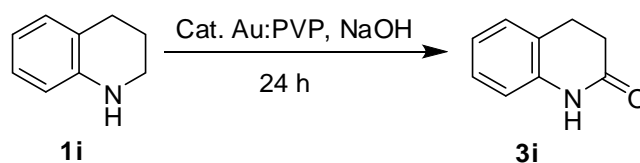
Entry	Au:PVP (atom%)	NaOH (mol%)	Solvent	Temperature (°C)	% Yield 3i
1	10	-	EtOH-H$_2$O (1:2)	27	-
2	-	200	EtOH-H$_2$O (1:2)	27	-
3[a]	10	200	EtOH-H$_2$O (1:2)	27	-
4	10[b]	200	EtOH-H$_2$O (1:2)	27	-
5	10	200	EtOH-H$_2$O (1:2)	27	91
6	10	100	EtOH-H$_2$O (1:2)	27	49[c]
7	10	200	H$_2$O	27	35[c]
8	10	200	H$_2$O	50	89
9[d]	1	200	EtOH-H$_2$O (1:2)	50	84

[a] Under argon atmosphere.
[b] Use of Au:PVP with 20 nm mean size.
[c] 51% of **1i** was recovered.
[d] 38 h.

No reaction was observed when the reaction underwent in the absence of base (entry 1) or Au:PVP (entry 2). As known in previous reports, the reaction catalyzed by Au:PVP could occur under oxygen atmosphere. When α-oxygenation of amine **1i** was carried out under argon atmosphere, no product was observed (entry 3). This result indicated that oxidation of amine to amide was promoted by adsorbed oxygen molecule on gold clusters surface. In addition, the clusters size of gold also played an important role in this reaction. When 20 nm of diameter size of Au:PVP clusters was used as catalyst, the oxidation of amine **1i** could not proceed (entry 4). Previously,

Au:PVP clusters having the mean size larger than 10 nm were almost inert for the aerobic oxidation [28]. When the reaction was performed in the presence of 10 atom% Au:PVP under basic condition at room temperature for 24 hours, the oxidation proceeded to give lactam **3i** in 91% yield without any other by-product (entry 5). All of these results were contrary to the previous example of bulky gold catalysts which could catalyze amine oxidation on gold surface [14-16].

The rate of oxidation was dropped when NaOH was reduced in a half from 200 mol% in entry 5 to 100 mol%. Only 49% of **3i** was obtained with 51% recovery of **1i** (entry 6). When the solvent was changed to only H_2O, the reaction rate was also decreased. The reaction was observed in 51% conversion along with 35% yield of **3i** (entry 7). The result could be explained that due to the poor solubility of amine **1i** in water, the reaction rate of the oxidation of amine was decreased. The conversion of this reaction in only water could be improved when the temperature was raised up to 50°C and 89% yield of **3i** was obtained (entry 8). The catalyst loading was attempted to reduce from 10 atom% to only 1 atom% under EtOH-H_2O solution at 50°C (entry 9). 84% yield of desired product **3i** was obtained for 38 hours. These optimized conditions were significantly milder compared to previous reactions catalyzed by gold.

4.3.1.2 *α*-Oxygenation of 1,2,3,4-tetrahydro*iso*quinoline (1j)

The *α*-oxygenation of amine **1j** was investigated and the results are shown in Table 4.4.

The optimization condition of **1i** was then applied to **1j**. No reaction was observed and the color of solution was not changed (entry 1). Thus, the reaction was then carried out at higher temperature. To increase the temperature, the solvent system was changed from EtOH-H_2O to *t*-BuOH-H_2O to avoid the oxidation of EtOH under reflux temperature affording the corresponding acetamide as a by-product. Under reflux conditions of *t*-BuOH-H_2O, 85% of desired product **3j** was obtained along with 7% of aromatization product **5j** *via* oxidative dehydrogenation (entry 2). Due to the observation of **5j**, the reaction mechanism should not involve the formation of

hemiaminal as shown in Figure 4.1 *via* the hydration of imine. Therefore, the blank reaction was performed under the same conditions without water at 90 °C. The result revealed that the formation of desired product lactam **3j** was not obtained and only oxidative dehydrogenation products **4j** and **5j** were observed in 48 and 9% yield, respectively (entry 3). On the other hand, when the solvent was changed to only water, the oxygenation of **3j** was observed in quantitative yield (99%) without oxidative dehydrogenation products **4j** and **5j** (entry 4). The temperature was tried to decrease to 80 °C, the reactivity of reaction was slightly dropped in the hydration

Table 4.4 The optimization for aerobic oxidation of **1j**
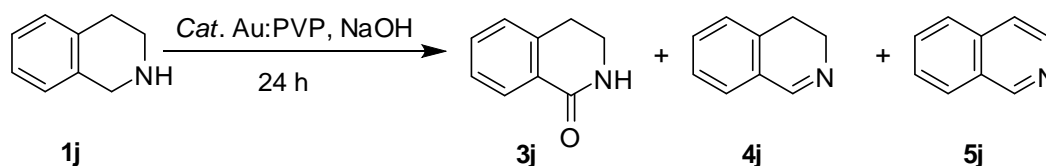
Entry	Au:PVP (atom%)	Solvent	Temperature (°C)	% Yield		
				3j	4j	5j
1	10	EtOH-H$_2$O (1:2)	27	no reaction		
2	10	*t*-BuOH-H$_2$O (1:2)	100	85	-	7
3	10	*t*-BuOH	90	-[a]	48	9
4	10	H$_2$O	90	99	-	-
5	10	H$_2$O	80	84	-	16
6	5	H$_2$O	90	97	-	1
7	5[b]	H$_2$O	90	no reaction		
8	-	H$_2$O	90	no reaction		
9	10	DMF- H$_2$O (1:2)	90	53	27	20
10[c]	10	DMF	90	-	93	1

[a] Recovery of **1j**: 42%.
[b] 20 nm of Au:PVP catalyst.
[c] 6 h.

process. The products **3j** and **5j** were obtained in 84 and 16%, respectively. Then, the decrease of Au:PVP loading was investigated. When 5 atom% Au:PVP was used as a

catalyst instead of 10 atom% under reflux at 90°C in water, 97% yield of **3j** was obtained with only 1% of **5j** (entry 6). In addition, the color of the reaction mixture at nearly reflux temperature either 90 or 80 °C was changed from dark brown to red. This observation indicated that the aggregation of Au nanoclusters occurred to destroy to activity of catalyst. Therefore, the bigger diameter size of Au:PVP (~ 20 nm) was tried, no reaction was taken place (entry 7). The blank reaction without catalyst was performed (entry 8). As expected, no reaction was observed.

The selectivity of oxidative dehydrogenation and α-oxygenation was investigated. As shown in entries 2 and 3, the selectivity of oxidation of amines was observed in the different media. The oxygenation took place in aqueous media, but the oxidative dehydrogenation could proceed in the reaction without water. To optimize the selective oxidation of amines **1j**, the reaction conditions in reflux DMF-H_2O and DMF were carried out. In a mixed solvent (entry 9), 100% conversion with 53% of oxygenation product was obtained with 27% yield of imine **4j** and 20% of aromatization product **5j**. To reduce the oxygenation product, the reaction was performed in DMF at 90°C. It was found that 100% conversion was observed within 6 hours and 93% of imine **4j** was attained with 1% yield of aromatized product **5j** (entry 10).

The aggregation of Au:PVP α-oxygenation of **1j** from optimization study (Table 4.4) was observed by changing of color reaction mixture from dark brown to red or purple. Au:PVP solution after reaction was detected by measuring with UV/vis absorption spectroscopy. The surface plasmon band at 520 nm was observed and gradually increased with longer reaction time (Figure 4.2). TEM of Au:PVP was measured after finish the reaction and diagram was shown in Figure 4.3. The aggregation of Au clusters was observed in some parts of TEM diagram. It indicated that the small size of Au clusters could activate the α-oxygenation of amines even if the aggregation was occurred.
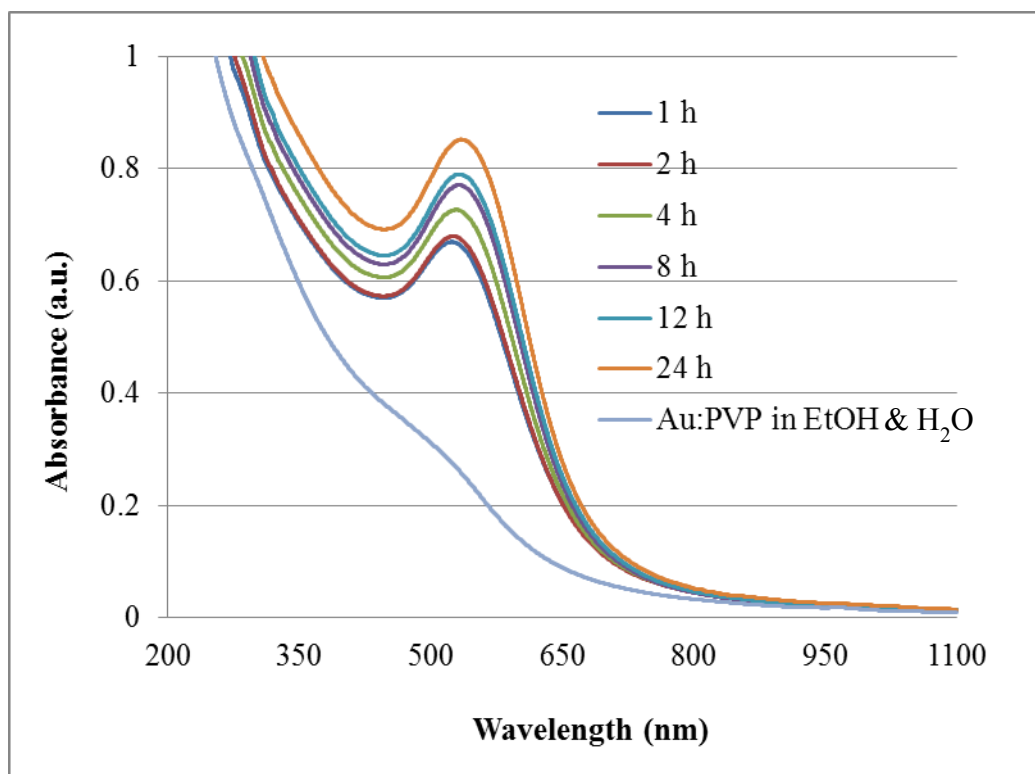
Figure 4.2 UV/Vis absorption spectra of Au:PVP during *α*-oxygenation of **1j**.
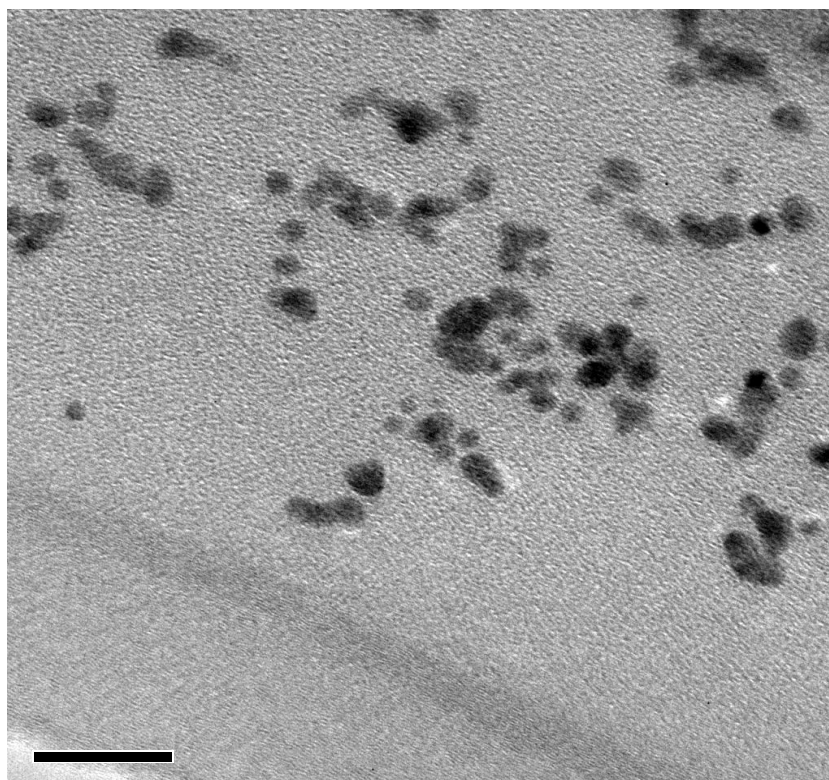
Figure 4.3 TEM image of Au:PVP after 24 h of *α*-oxygenation of **1j**.

According to this observation, Au:PVP was impossible to reuse for the next *α*-oxygenation of **1j**. Metallic character of Au nanoclusters was observed by UV/Vis absorption spectra (Figure 4.2) by sampling an equal amount of reaction mixture from 1 until 24 h to compare with the blank Au:PVP solution in EtOH-H_2O before adding into the reaction. The results indicated that Au:PVP was not good enough for being a catalyst in next run for oxidation of **1j**. On the other hand, the oxidation of **1i** did not reveal the aggregation of Au:PVP. This might be because of the lower temperature under the condition of the oxidation of **1i** and also the basicity of **1j** was higher than that of **1i** which could cause the aggregation of gold cluster by adsorption of **1j** on gold surface.

In addition, TEM image in Figure 4.3 could explain the aggregation clearer than the result of UV/Vis absorption spectra. The black dots in the picture were Au clusters which some of them were big and some were small. The smaller ones may have the activity to catalyze the oxidation, but the bigger ones (>2 nm) lost their activities during reaction. Thus, Au:PVP could proceed the *α*-oxygenation of **1j** even if the aggregation of Au:PVP was observed.

4.3.2 Mechanism

As shown in Figure 4.1, the oxygenation of **1i** was started from oxidative dehydrogenation of amines to form imine intermediate (path A), and then the hydration of this imine intermediate taken place under basic aqueous condition would give the hemiaminal intermediate. Finally, the oxidation of hemiaminal to corresponding lactam was occurred. The results strongly indicated that amine oxidation to imine (path A in Scheme 4.6) was slower than hemiaminal formation with HCHO followed by oxidation (path B), but sufficiently faster than the MeOH oxidation process.

The formation of imine in the first step could not be confirmed from the *α*-oxygenation of **1i**, because of the unstability of that imine. However, the investigation of imine formation as an intermediate could achieve in the oxygenation of **1j** and

imine (**4j**) which could be detected by GC during the reaction and isolated after the reaction (Table 4.4).
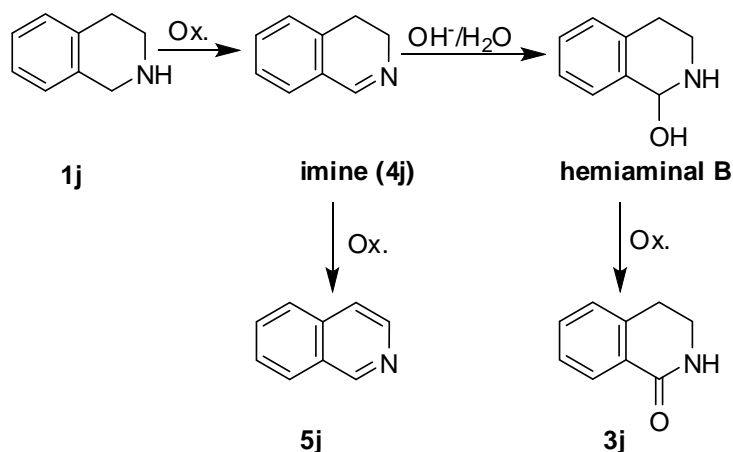
Figure 4.4 Proposed mechanism of α-oxygenation of 1,2,3,4-tetrahydroisoquinoline (**1j**) catalyzed by Au:PVP.

The selectivity for oxidative dehydrogenation and α-oxygenation to afford imine **4j** and **3j** could be clearly explained from Table 4.4. The conditions without water would proceed only the oxidative dehydrogenation to afford imine and aromatization product. A hydration step would occur faster than dehydrogenation to form **5o** under aqueous conditions, so hemiaminal **B** was then generated and oxidized to give lactam in faster rate than the formation of aromatization compound.

Other benzo-fused heterocyclic amines were investigated for α-oxygenation reaction using both optimization conditions of **1i** and **1j**.

4.3.3 Variation of amines

4.3.3.1 Effect of substituent group for α-oxygenation of benzo-fused heterocyclic amines

p-Methoxy-1,2,3,4-tetrahydroquinoline (**1p**) and *p*-bromo-1,2,3,4-tetrahydro-quinoline (**1q**) were firstly treated with the optimization condition for 1,2,3,4-tetra-hydroquinoline (**1i**) (Scheme 4.19). The selectivity of the formation of lactam decreased when *para*-substituted heterocyclic amines (**1p** and **1q**) were used. In the

presence of a donating group (methoxy group; **1p**), the reaction could not proceed at room temperature. 66% yield of lactam (**3p**) and 33% of aromatization product (**4p**) were obtained under reflux *t*-BuOH-H$_2$O. Imine intermediate of **1p** could not be observed the same as in the case of **1i**. α-Oxygenation of **1p** could not proceed at 100°C because of the very poor solubility in water. The reaction rate of **1p** was slower than that of **1i** because the electron donating group decreased the acidity of hydrogen at *N*-atom of amine **1p**. The process of oxidation of amines to imines would be slow and also the dehydrogenation of amines should be occurred as a side reaction at high temperature.
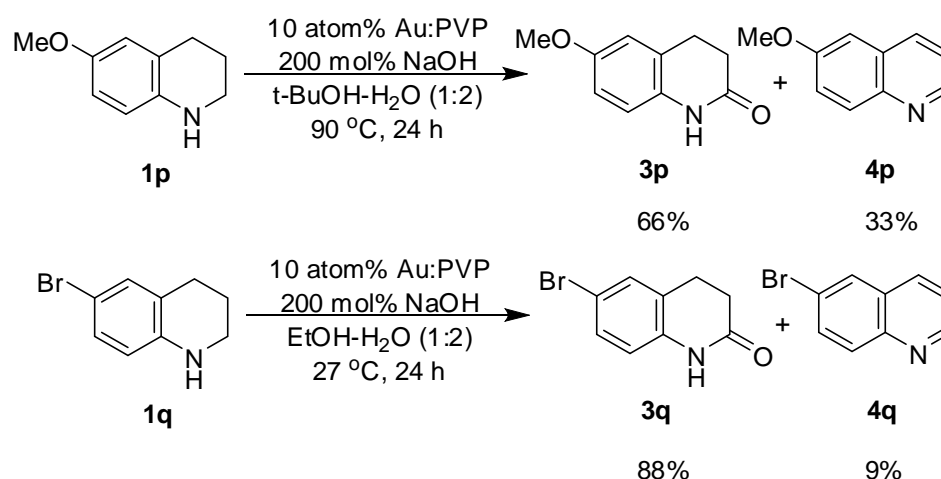
Scheme 4.19 α-Oxygenation of *para*-substituent heterocyclic amines.

In the case of **1q**, oxygenation was carried out under similar reaction condition with amine **1i** at room temperature. 88% yield of corresponding lactam **3q** was obtained with 9% yield of aromatization product **4q**. The α-oxygenation of **1q** could proceed even at room temperature, because the bromine group, electron withdrawing group, could increase the acidity of hydrogen of amines and increased the reaction rate of the formation of imine intermediate. In contrast with **1i**, 9% of aromatization product was formed, but the corresponding aromatization product of **1i** could not be observed, because high activity of starting amines **1q** could easily dehydrogenate to form **4q**.

These investigations indicated that the electronic effect from substituent group of heterocyclic amines could cause the selectivity of α-oxygenation of amines.

4.3.3.2 Ring size effect for α-oxygenation of benzo-fused heterocyclic amines

Benzo-fused hetercyclic amines **1r**, **1s** and **1t** were chosen for exploring the ring size effect in α-oxygenation catalyzed by Au:PVP. The results are shown in Scheme 4.19. Under the optimization conditions, no reaction was occurred for 2,3,4,5-tetrahydro-1H-benzo[b]azepine (**1r**) at room temperature either in water or mixed solvent between EtOH-H_2O. But 96% yield of the desired product **3r** could be accomplished when the reaction was conducted at 90°C (equation 1, Scheme 4.20). In the case of 1,2,3,4,5,6-hexahydrobenzo[b]azocine (**1s**) which the oxidation did not take place neither at room temperature nor 90°C (equation 2, Scheme 4.20). Interestingly, α-oxygenation of indoline (**1t**) could proceed affording lactam **3t** 5% yield along with 45% yield of indole **4t** *via* oxidative dehydrogenation and isomerisation of imine intermediate when the reaction was carried out at room temperature. On the other hand, the quantitative yield of **4t** was obtained when the reaction was conducted at 90°C for 6 hours and no lactam was generated (equation 2, Scheme 4.20).

(1)

1r   3r

temperature	
27 °C	no reaction
90 °C	96%

(2)

1s   3s

temperature	
27 °C	no reaction
90 °C	no reaction

(3)

1t   3t   4t

condition		
27 °C, 24 h	5%	45%(32%)[b]
90 °C, 6 h	-	99%

[a] no reaction under EtOH-H_2O (1:2)
[b] (-) is % yield of recovered starting material (1t)
[c] H_2O or *t*-BuOH-H_2O can used as solvent at 90 °C
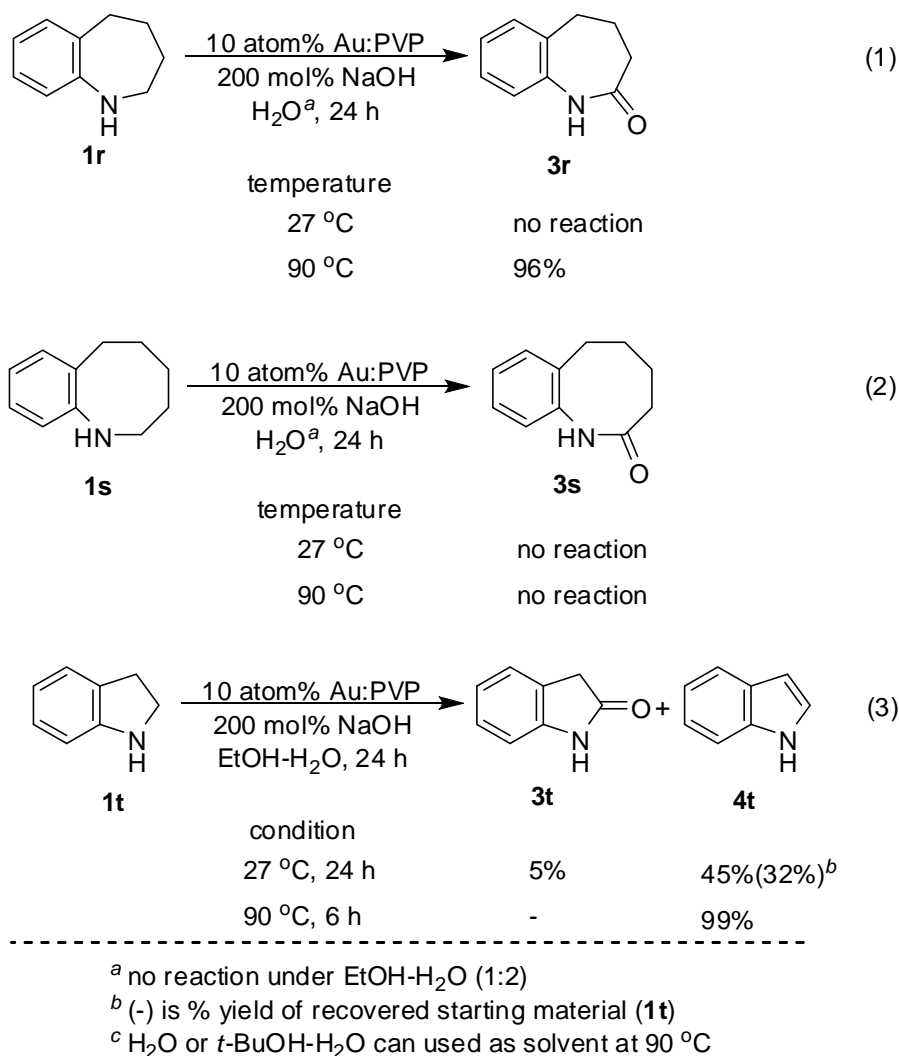
Scheme 4.20 *α*-Oxygenation of benzo-fused heterocyclic amines.

The formation of indole as a major product from oxidation of **1t** was described in Figure 4.5. Oxidative dehydrogenation of **1t** was carried out, the isomerization of imine intermediate would undergo to afford indole product (**4t**). According to the gathered results, an isomerization step was taken place faster than hydration of imine intermediate to form hemiaminal even if at room temperature, the *α*-oxygenation product (**3t**) was difficult to generate under this condition. When the reaction was carried out at high temperature, the rates of oxidative dehydrogenation of **1t** and isomerization of imine were increased. Thus, a hydration step was then hardly undergone at high temperature.
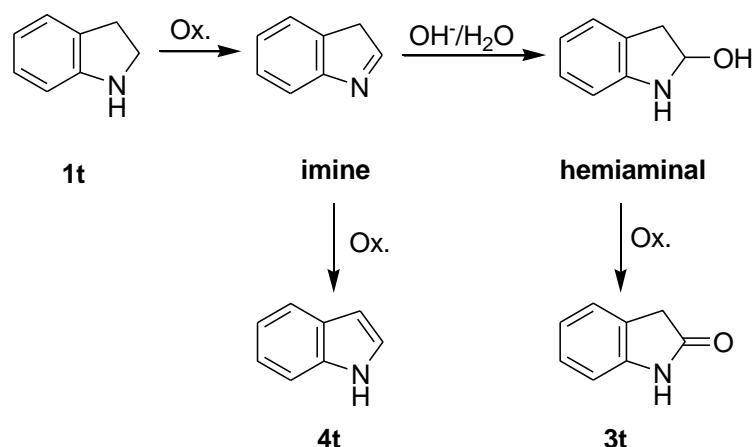
Figure 4.5 Possible mechanism of oxidation of indoline (**1t**) catalyzed by Au:PVP.

4.3.3.3 *α*-Oxygenation of tertiary amines

N-methyl-1,2,3,4-tetrahydro*iso*quinoline (**1u**) could be oxidized at *α*-position adjacent to *N*-atom of heterocyclic ring catalyzed by gold nanocluster supported on graphite (AuNPs/C) which was recently reported by Che. The reaction was carried out with 5 mol% of Au in AuNPs/C under reflux toluene affording lactam **3u** in 92% yield with enamide **4u** in 4% (Scheme 4.21, condition a). **4u** was obtained under Che's condition because high temperature would increase the rate of oxidative dehydrogenation step. In contrast, Au:PVP (5 atom%) in the presence of 100 mol% of NaHCO$_3$ in vigorous stirred of *t*-BuOH-water at 27°C was conducted in *α*-oxygenation of **1u** affording only the desired lactam (**3u**) in 94% without any of by-product (Scheme 4.21, condition b).
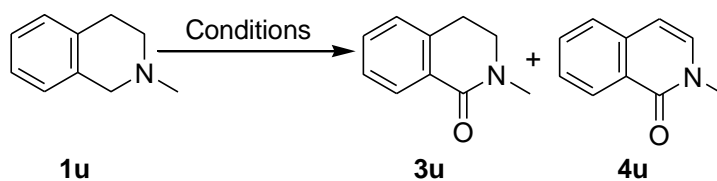
Scheme 4.21 α-Oxygenation of N-methyl-1,2,3,4-tetrahydroisoquinoline (**1u**).

The high temperature might permit the oxidative dehydrogenation of lactam **3u** to enamide **4u** by over oxidation. This indicated that a smaller size of gold nanocluster of Au:PVP promoted higher catalytic activity than AuNPs/C catalyst.
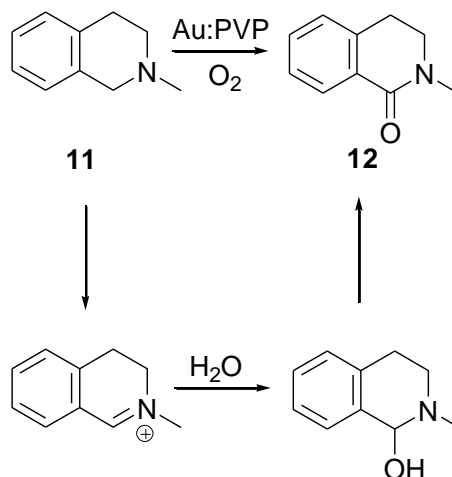
Figure 4.6 Possible mechanism of α-oxygenation of N-methyl-1,2,3,4-tetrahydroisoquinoline (**1u**).

The reaction conditions required for α-oxygenation of **1u** was milder than that of **1i** and **1j**. This could be explained by the iminium intermediate was undergone the hydration step much faster than imine intermediate and the nucleophilic attack to iminiun compound could undergo under weak base condition instead of strong base

condition (Figure 4.6). The reaction was then tried under neutral condition, but slower rate of reaction was observed. The reaction was not complete within 48 hours.

4.4   Conclusion

As described above, Au:PVP could be applied for aerobic oxidation of heterocyclic amines to lactam. The nearly quantitative yield was obtained by using Au:PVP as an excellent catalyst. This research demonstrated for the first time to use as a catalyst in selective aerobic oxidation of secondary heterocyclic amines to lactams. The milder reaction conditions, even at room temperature, in basic aqueous solvent was optimized for Au:PVP catalysis. According to a smaller size of Au clusters of Au:PVP (1.3 nm), the higher activity compared with previous reported heterogeneous catalysts such as AuNCs (mean size 12–15 nm) or bulk gold powder (ca. 50–1000 nm) was observed. Only Au:PVP could carry out the α-oxygenation of amines with excellent results.

In addition, the high selectivity between α-oxygenation and oxidative dehydrogenation process was viewed by changing solvent media. Oxidative dehydrogenation process could easily be selective in 100% by carrying out this reaction without water and α-oxygenation was also selective in water. Finally, quantitative yield in both processes were obtained.

CHAPTER V

CONCLUSION

This research is divided into two parts for the application of gold nanoclusters stabilized by poly(*N*-vinyl-2-pyrrolidone) (Au:PVP), hydrophilic polymer in direct *N*-formylation of amines and *α*-oxygenation of benzo-fused heterocyclic amines.

The excellent yield was observed for the *N*-formylation of *N*-methylaniline under optimization condition. 10 atom% Au:PVP in the presence of 200 mol% LiOH under reflux MeOH-H$_2$O. This reaction was studied under the hypothesis that formyl source will generate *in situ* from the oxidation of MeOH and reacted with amines leading to the corresponding amides. Formaldehyde is the formyl intermediate that generated *via* the oxidation of MeOH. Thus, the mechanism of *N*-formylation was then proposed that the condensation of amines with formaldedhyde intermediate to afford hemiaminal followed by the oxidation to give corresponding amides. Unfortunately, *N*-formylation under reflux condition was proceeded very well only in the case of *N*-methylaniline (**1a**), because of the *N*-demethylation of amines as a side reaction. Therefore, the direct *N*-formyltion of amines using formalin as a formyl source was investigated under milder condition. The excellent selectivity of *N*-formylation of amines was attained by using 1-10 atom% of Au:PVP under basic condition at room temperature. The desired products were obtained in moderate to excellent yield.

As described above, Au:PVP was then tried to use as a catalyst for aerobic oxidation of heterocyclic amines to lactam. The quantitative yield with excellent selectivity was obtained from *α*-oxygenation of 1,2,3,4-tetrahydroquinoline (**1i**) and 1,2,3,4-tetrahydroisoquinoline (**1j**) using 10 atom% Au:PVP as a catalyst in aqueous solution under basic condition at room temperature or 90 °C. The high selectivity between *α*-oxygenation and oxidative dehydrogenation process was investigated using

1j as a starting material. The oxidative dehydrogenation could proceed very well in organic solvent without water and α-oxygenation could be selective in aqueous solution. Not only **1i** and **1j** but the other heterocycyclic amines can transform to lactam under these optimization conditions. The excellent yields of lactam were obtained, except for indoline (**1t**) and 1,2,3,4,5,6-hexahydrobenzo[*b*]azocine (**1s**) because of the tautomerization of imine generated from **1t** and the configuration of amine **1s**. In contrast with the heterogeneous catalyst, the oxidation of tertiary amines using Au:PVP as a catalyst could undergo at room temperature under aqueous condition without any by-products generated from dehydrogenation process.

Overture for the future work

As described in this research, the mechanism of *N*-formylation of amines is still unclear regarding the role of base and water. The isotope labeling experiment should be done to confirm the *N*-demethylation pathway. The separation of Au:PVP comparing with the heterogeneous catalyst is still more difficult. Thus, the catalyst development will be required for easy separation, such as doping magnetic metal into Au:PVP to be magnetic catalyst. By the way, the development of aerobic oxidation of amines catalyzed by Au:PVP nanoclusters is interesting because the variety of the reaction can proceed under green and mild condition. From *N*-formylation of amines, the condensation of amines and aldehyde moiety will apply for the oxazoline derivatives *via* condensation of amino alcohols with aldehyde compounds. In addition, the C-C bond formation through aerobic oxidation process of cyclic amines with nucleophiles should be studied.

REFERENCES

[1]. Mohr, F. *Gold Chemistry.* Weinheim: Wiley-VCH GmbH, **2009**.

[2] Arcadi, A. Alternative Synthetic Methods through New Developments in Catalysis by Gold. *Chem. Rev.* 108(2008):3266-3325.

[3] Stephen, A.; Hashmi, K.; Hutchings G. J. Gold Catalysis. *Angew. Chem. Int. Ed.* 45(2006):7896-7936.

[4] Gorin, D. J.; Sherry B. D.; Toste, F. D. Ligand Effects in Homogeneous Au Catalysis. *Chem. Rev.* 108(2008):3351-3378.

[5] Haruta, M.; Kobayashi, T.; Sano, H.; Yamada, N. Novel Gold Catalysts for the Oxidation of Carbon Monoxide at a Temperature far Below 0 °C. *Chem. Lett.* 16(1987):405-408.

[6] Haruta, M. When Gold is not Noble: Catalysis by Nanoparticles. *Chem. Record* 3(2003):75-87.

[7] Comotti, M.; Pina, C. D.; Matarrese, R.; Rossi, M. The Catalytic Activity of "Naked" Gold Particles. *Angew. Chem. Int. Ed.* 43(2004):5812-5815.

[8] Socaciu, L. D.; Hagen, J.; Benhardt, T. M.; Wöste, L.; Heiz, U.; Häkkinen, H.; Landman, U. Catalytic CO Oxidation by Free Au_2^-: Experiment and Theory. *J. Am. Chem. Soc.* 125(2003):10437-10445.

[9] Landman, U.; Yoon, B.; Zhang, C.; Heiz, U.; Arenz, M. Factors in Gold Nanocatalysis: Oxidation of CO in the Non-Scalable Size Regime. *Topics Catal.* 44(2007):145-158.

[10] Kim, Y. D. Chemical Properties of Mass-Selected Coinage Metal Cluster Anions: Towards Obtaining Molecular-Level Understanding of Nanocatalysis. *Int. J. Mas. Spectrum.* 238(2004):17-31.

[11] Stolcic, D.; Fischer, M.; Ganteför, G.; Kim, Y. D.; Sun, Q.; Jena, P. Direct Observation of Key Reaction Intermediates on Gold Clusters. *J. Am. Chem. Soc.* 125(2003):2848-2849.

[12] Bongiorno, A.; Landman U. Water-Enhanced Catalysis of CO Oxidation on Free and Supported Gold Nanoclusters. *Phys. Rev. Lett.* 95(2005):1-4.

[13] Carrettin, S.; McMorn, P.; Johnston, P.; Griffin, K.; Kiely, C. J.; Attard, G. A.; Hutchings G. J. Oxidation of Glycerol Using Supported Gold Catalysts. *Topics Catal.* 27(2004):131-136.

[14] Westcott, S. L.; Oldnburg, S. J.; Lee T. R.; Halas, N. J. Formation and Adsorption of Clusters of Gold Nanoparticles onto Functionalzed Silica anoparticle Surfaces. *Langmuir.* 14(1998):5396-5401.

[15] Grisel, R.; Weststrate, K.- J.; Gluhoi, A.; Nieuwenhuys, B. E. Catalysis by Gold Nanoparticles. *Gold Bull.* 35(2002):39-45.

[16] Rodriguez, J. A.; Perez, M.; Jirsak, T.; Evans, J.; Hrbek, J.; Gonzalez, L. Activation of Au Nanoparticles on Oxide Surfaces: Reaction of SO_2 with Au/MgO(100). *Chem. Phys. Lett.* 378(2003):526-532.

[17] Corma, A.; Garcia, H. Supported Gold Nanoparticles as Catalysts for Organic Reactions. *Chem. Soc. Rev.* 37(2008):2096-2126.

[18] Pina, C. D.; Falletta, E.; Prati, L.; Rossi, M. Selective Oxidation Using Gold. *Chem. Soc. Rev.* 37(2008):2077-2095.

[19] Jin, R. Quantum Sized, Thiolate-Rotected Gold Nanoclusters. *Nanoscale* 2(2010):343-362. *and reference therein*.

[20] Tsukuda, T.; Tsunoyama, H.; Sakurai, H. Aerobic Oxidations Catalyzed by Colloidal Nanogold. *Chem. Asian. J.* 6(2011):736-748.

[21] Teranishi, T.; Miyake, M.; Hosoe, M. Formation of Monodispersed Ultrafine Platinum Particles and Their Electrophoretic Deposition on Electrodes. . *Adv. Mater.* 9(1997):65-67.

[22] a) Zhang, Y.; Grass, M. E.; Kuhn, J. N.; Tao, F. Habas, S. E.; Huang, W. Yang, P.; Somorjai, G. A. Highly Selective Synthesiss of Catalytically Active Monodisperse Rhodium Nanocubes. *J. Am. Chem. Soc.* 130(2008):5868-5869. b) Narayanan, R.; El-Sayed, M. A. Catalysis with Transition Metal Nanoparticles in Colloidal Solution: Nanoparticle Shape Dependence and Stability. *J. Phys. Chem. B* 109(2005):12663-12676.

[23] Biffis, A.; Cunial, S.;Spontoni, P.; Prati, L. Microgel-Stabilized Gold Nanoclusters: Powerful "Quasi-Homogeneous" Catalysts for the Aerobic Oxidation of Alcohols in Water. *J. Catal.* 251(207):1-6.

[24] Kanaoka, S.; Yagi, N.; Fukuyama, Y.; Aoshima, S.; Tsunoyama, H.; Tsukuda, T.; Sakurai, H. Thermosensitive Gold Nanoclusters Stabilized by Well-Defined Vinyl Ether Star Polymers: Reusable and Durable Catalysts for Aerobic Alcohol Oxidation. *J. Am. Chem. Soc*. 129(2007):12060-12061.

[25] Wang, Y.; Yan R.; Zhang, J.; Zhang, W. Synthesis of Efficient and Reusable Catalyst of Size-Controlled Au Nanoparticles within a Porous, Chelating and Intelligent Hydrogel for Aerobic Alcohol Oxidation. *J. Mol. Catal. A* 317(2010):81-88.

[26] Tsunoyama, H.; Sakurai, H.; Ichikuni, N.; Negishi, Y.; Tsukuda, T. Colloidal Gold Nanoparticles as Catalyst for Carbon-Carbon Bond Formation: Application to Aerobic Homocoupling of Phenylboronic Acid in Water. *Langmuir* 20(2004):11293-11296.

[27] Tsunoyama, H.; Ichikuni, N.; Tsukuda, T. Microfluidic Synthesis and Catalytic Application of PVP-Stabilized ~1 nm Gold Clusters. *Langmuir* 24(2008):11327-11330.

[28] Tsunoyama, H.; Sakurai, H.; Tsukuda, T. Size Effect on the Catalysis of Gold Clusters Dispersed in Water for Aerobic Oxidation of Alcohol. *Chem. Phys. Lett*. 429(2006):528-532.

[29] Tsunoyama, H.; Tsukuda, T. Magic Numbers of Gold Clusters Stabilized by PVP. *J. Am. Chem. Soc*. 131(2009):18216-18217.

[30] Tsunoyama, H.; Ichikuni, N.; Sakurai, H.; Tsukuda, T. Effect of Electronic Structures of Au Clusters Stabilize by Poly(*N*-vinyl-2-pyrrolidone) on Aerobic Oxidation Catalysis. *J. Am. Chem. Soc*. 131(2009):7086-7093.

[31] Tsunoyama, H.; Tsukuda, T.; Sakurai, H. Synthetic Application of PVP-stabilized Au Nanocluster Catalyst to Aerobic Oxidation of Alcohol in Aqueous Solution under Ambient Conditions. *Chem. Lett*. 259(2007):212-213.

[32] Uozumi, Y.; Nakao, R. Catalytic Oxidation of Alcohols in Water under Atmospheric Oxygen by Use of an Amphiphilic Resin-Dispersion of a Nanopalladium Catalyst. *Angew. Chem. Int. Ed*. 43(2004):5812-5815.

[33] Chaki, N. K.; Tsunoyama, H.;Negishi, Y.; Sakurai, H.; Tsukuda, T. Effect of Ag-Doping on the Catalytic Activity of Polymer-Stabilized Au Clusters in Aerobic Oxidation of Alcohol. *J. Phys. Chem. C* 111(2007):4885-4888.

[34] Conte, M.; Miyamura, H. Kobayashi, S.; Chechik, V. Spin Trapping of Au-H Intermediate in the Alcohol Oxidation by Supported and Unsupported Gold Catalysts. *J. Am. Chem. Soc*. 131(2009):7189-7196.

[35] Guzman, J.; Carrettin, S.; Corma, A. Spectroscopic Evidence for the Supply of Reactive Oxygen during CO Oxidation Catalyzed by Gold Supported on Nanocrystalline CeO_2. *J. Am. Chem. Soc*. 127(2005):3286-3287.

[36] Sakurai, H.; Tsunoyama, H.;Tsukuda, T. Oxidative Homo-Coupling of Potassium Aryltrifluoroborates Catalyzed by Gold Nanocluster under Aerobic Conditions. *J. Organomet. Chem.* 692(2007):368-374.

[37] Sakurai, H.; Tsunoyama, H.; Tsukuda, T. Aerobic Oxidation Catalyzed by Gold Nanoclusters as Quasi-Homogeneous Catalysts: Generation of Hydrogen Peroxide using Ammonium Formate. *Trans. Mater. Res. Soc. Jpn.* 31(2006):521-524.

[38] Kamiya, I.; Tsunoyama, H.; Tsukuda, T.; Sakurai, H. Lewis Acid Character of Zero-valent Gold Nanoclusters under Aerobic Conditions: Intramolecular Hydroalkoxylation of Alkenes. *Chem. Lett*. 36(2007):646-647.

[39] Kitahara, H.; Kamiya, I.; Sakurai H. Intramolecular Addition of Toluenesulfonamide to Unactivated Alkenes Catalyzed by Gold Nanoclusters under Aerobic Conditions. *Chem. Lett*. 38(2009):908-909.

[40] Kitahara, H.; Sakurai H. Gold Nanocluster as a Catalyst for Intramolecular Addition of Primary Amines to Unactivated Alkenes under Aerobic Conditions. *Chem. Lett*. 39(2010):46-48.

[41] Bencivenni, G.; Lanza, T.; Leardini, R.; Minozzi, M.; Nanni, D.; Spagnolo, P.; Zanardi, G. Iminyl Radicals from *α*-Azido *o*-Iodoanilides *via* 1,5-H Transfer Reactoins of Aryl Radicals: New Transformation of *α*-Azido Acids to Decarboxylated Nitriles. *J. Org. Chem*. 73(2008):4721-4724.

[42] Bao, K.; Zhang, W.; Bu, X.; Song, Z.; Zhang, L. cheng, M. A Novel Type of *N*-Formylation and Related Reactions of Amines *via* Cyanides and Esters as Formylating Agents. *Chem. Commun*. 44(2008):5429-5431.

[43] Yoshida, Y.; Asano, S. Inoue, S. Carbonylation of Amines Catalyzed by an Organozinc Compound. *Chem. Lett*. 7(1984):1073-1076.

[44] Ma'mani, L.; Sheykhan, M.; Heydari, A.; Faraji, M.; Yamini, Y. Sulfonic Acid Supported on Hydroxyapatite-Encapsulated-γ-Fe$_2$O$_3$ Nanocrystallites as a Magnetically Brønsted Acid for *N*-Formyaltion of Amines. *Appl. Catal., A*. 377(2010):64-69.

[45] Sarvari, M. H.-; Sharghi, H. ZnO as a New Catalyst for *N*-formylation of Amines under Solvent-Free Conditions. *J. Org. Chem*. 71(2006):6652-6654.

[46] Murahashi, S.; Oda, T.; Sugahara, T.; masui, Y. Tungstate-Catalyzed Oxidation of Tetrahydroquinolines with Hydrogen Peroxide: A Novel Method for the Synthesis of Cyclic Hydroxamic Acids. *J. Org. Chem*. 55(1990):1744-1749.

[47] Shunichi, M.; Yasushi, I.; Yoshiaki, H. Rhodium Catalyzed Hydrogenation of Quinolones and Isoquinolines under Water-Gas Shift Conditions. *Bull. Chem. Soc. Jpn.* 62(1989):2968-2976.

[48] Wang, Z.; Wan, W.; Jiang. H.; Hao, J. One-Pot Cyclization of 2-Aminophenethyl Alcohols: A Noel and Direct Approach to the Synthesis of *N*-Acyl Indolines. *J. Org. Chem*. 72(2007):9364-9367.

[49] Sharma, A. K.; Sharma, A.; Desai, D.; Madhunapantula, V.; Huh, S. J.; Robertson, G. P.; Amin, S. Synthesis and Anticancer Activity Comparison of Phenylalkyl Isoselenocyanates with Corresponding Naturally Occurring and Synthetic Isothiocyanates. *J. Med. Chem*. 51(2008):7820-7826.

[50] Aizpurua, J. M.; Palomo, C. Reagents and Synthetic Methods. 30. Pratical and Improved Method for Formylating Amino Compounds by Means of Formic Acid-Dimethylformaide System. *Synth. Commun*. 13(1983):745-752.

[51] Tsukamoto, H.; Suzuki, R.; Kondo, Y. Revisiting Benzenesulfonyl Linker for the Deoxygenation and Multifunctionalization of Phenols. *J. Comb. Chem*. 8(2006):289-292.

[52] Sahin, A.; Cakmak, O.; Demirtas, I.; Okten, S.; Tutar, A. Efficient and Selective Synthesis of Quinoline derivatives. *Tetrahedron*, 64(2008):10068-10074.

[53] Sams, A. G., Larsen, M.; Mikkelsen, G. *N*-Thiazol-2-yl-benzamide Derivatives. *PCT Int. Appl. WO 2005039572 A1* May 6, 2005.

[54] Ortiz-Marciales, M.; Rivera, L. D.; Jesús, M. D.; Espinosa, S.; Benjamin, J. A.; Casanoa, O. E.; Figueroa, I. G.; Rodríguez, S.; Correa, W. Facile Rearrangement of *O*-silylated Oximes on Reduction with Boron Trifluoride/Borane. *J. Org. Chem*. 70(2005):10132-10134.

[55] Cho, H.; Iwama, Y.; Sugimoto, K.; Mori, S.; Tokuyama, H. Regioselective Synthesis of Heterocycles Containing Nitrogen Neighboring an Aromatic Ring by Reductive Ring Expansion Using Diisobutylaluminum Hydride and Studies on the Reaction Mechanism. *J. Org. Chem*. 75(2010):627-636.

[56] Zhao, H.; Vandenbossche, C. P.; Koenig, S. G.; Singh, S. P.; Bakale, R. P. An Efficient Synthesis of Enamides from Ketones. *Org. Lett*. 10(2008):505-507.

[57] Bonvallet, P. A.; Todd, E. M.; Kim, Y. S.; McMahon, R. J. Access to the Naphthylcarbene Rearrangement Manifold *via* Isomeric Benzodiazocyclohepatrienes. *J. Org. Chem*. 67(2002):9031-9042.

[58] Ahlbrecht, H.; Düber, E. O.; Epsztajn, J.; Marcinkowski, R. M. K. Delocalisation, Conformation and Basicity of Anilines. *Tetrahedron* 40(1984):1157-1165.

[59] Almena, J.; Foubelo, F.; Yus, M. Nitrogent-Containing Remote Functionalised Organolithium Compounds by Reductive Opening of Five- and Six-Membered Heterocycles. *Tetrahedron* 52(1996):8545-8564.

[60] Felpin, F.- X.; Coste, J.; Zakri, C.; Fouquet, E. Preparation of 2-Quinolones by Sequential Heck Reduction-Cyclization (HRC) Reactions by Using a Multitask Palladium Catalyst. *Chem. Eur. J.* 15(2009):7238-7245.

[61] Winter, D. K.; Drouin, A.; Lessard, J.; Spino, C. Photochemical Rearrangement of *N*-Cholrolactams: A Route to *N*-Heterocycles through Concerted Ring Contraction. *J. Org. Chem.* 75(2010):2610-2618.

[62] Zhou, W.; Zhang, L.; Jiao, N. The Tandem Reaction Combining Radical and Ionic Processes: and Efficient Approach to Substituted 3,4-Dihydroquinolin-2-ones. *Tetrahedron* 65(2009):1982-1987.

[63] Monrad, R. N.; Madsen, R. Ruthenium-Catalysed Synthesis of 2- and 3-Substituted Quinolones from Anilines and 1,3-Diols. *Org. Biomol. Chem.* 9(2011):610-615.

[64] Occhiato, E. G.; Ferrali, A.; Menchi, G.; Guarna, A.; Danza, G.; Comerci, A.; Mancina, R.;Serio, M.; Garotta, G.; Cavalli, A.; Vivo, M. D.; Recanatini, M. Synthesis, Biological Activity, and Three-Dimensional Quantitative Structure-Activity Relationship Model for a Series of Benzo[*c*]quinolizin-3-ones, Nonsteroidal Inhibitors of Human Steroid 5α-Reductase 1. *J. Med. Chem.* 47(2004):3546-3560.

[65] Crosby, I. T.; Shin, J. K.; Capuano, B. The Application of the Schmidt Reaction and Beckmann Rearrangement to the Synthesis of Bicyclic Lactams: Some Mechanistic Considerations. *Aust. J. Chem.* 63(2010):211-226.

[66] Motoyama, Y.; Kamo, K.; Nagashima, H. Catalysis in Poysiloxane Gels: Platinum-Catalyzed Hydrosilylation of Polymethylhydrosiloxane Leading to Reusable Catalysts for Reduction of Nitroarenes. *Org. Lett.* 11(2009):1345-1348.

[67] Gramain, J. C.; Simonet, N.; Vermeersch, G.; Febvay-Garot, N.; Caplain, S.; Lablache-Combier, A. Photoreduction of Benzophenone by Phthlimidines and Dihydroisoquinolones. Chemical and CIDNP NMR Study. *Tetrahedron* 38(1982):539-550.

[68] Sasamoto, N.; Dubs, C.; Hamashima, Y.; Sodeoka, M. Pd(II)-Catalyzed Azymmetric Addition of Malonates to Dihydroisoquinolines. *J. Am. Chem. Soc*. 128(2006):14010-14011.

[69] Kumar, R. A.; Maheswari, C. U.; Ghantasala, S.; Jyothi, C.; Reddy, K. R. synthesis of 3*H*-Quinazolin-4-ones and 4*H*-3,1-Benzoxazin-4-ones *via* Benzylic Oxidation and Oxidative Dehydrogenation using Potassium Iodide-*tert*-Butyl Hydroperoxide. *Adv. Synth. Catal*. 353(2011):401-410.

[70] Dhakshinamoorthy, A.; Pitchumani, K. Facile Clay-Induced Fischer Indole Synthesis: A New Approach to Synthesis of 1,2,3,4-Tetrahydrocarbazole and Indoles. *Appl. Catal. A* 292(2005):305-311.

[71] Brahmachari G.; Laskar, S. A very Simple and Highly Efficient Procedure for *N*-Formylation of Primary and Secondary Amines at Room Temperature under Solvent-free Conditions. *Tetrahedron Lett*. 51(2010):2319-2322.

[72] Rahman, M.; Kundu, D.; Hajra, A.; Majee, A. Formylation without Catalyst and Solvent at 80 °C. *Tetrahedron Lett*. 51(2010):2896-2899.

[73] Dentsch, J.; Eckelt, R.; Köckritz, A.; Martin, A. Catalytic Reaction of Methyl Formate with Amines to Formamides. *Tetrahedron* 65(2009):10365-10369.

[74] Das, B.; Krishnaiah, M.; Balasubramanyam, P.; Veeranjaneyulu, B.; Kumar, N. D. A Remarkably Simple *N*-Formylation of Anilines using Polyethylene Glycol. *Tetrahedron Lett*. 49(2008):2225-2227.

[75] Shekhar, A. C.; Kumar, A. R.; Sathaiah, G.; Paul, V. L.; Sridhar, M.; Rao, P. S. Facile *N*-Formylation of Amines using Lewis Acids as Novel Catalysts. *Tetrahedron Lett*. 50(2009):7099-7101.

[76] Tumma, H.; Nagaraju, N.; Reddy, K. V. A Facile Method for the *N*-Formylation of Primary and Secondary Amines by Liquid Phase Oxidation of Methanol in the Presence of Hydrogen Peroxide over Basic Copper Hydroxyl Salts. *J. Mol. Catal. A* 310(2009):121-129.

[77] Ishida, T.; Haruta, M. *N*-Formylation of Amines *via* the Aerobic Oxidation of Methanol over Supported Gold Nanoparticles. *ChemSusChem* 2(2009):538-514.

[78] Zhou, L.; Freyschla, C. G.; Xu, B.; Friend, C. M.; Madix, R. J. Direct Selective Oxygen-Assisted Acylation of Amines Driven by Metallic Silver Surfaces: Dimethylamine with Formaldehyde. *Chem. Commun*. 46(2010):704-706.

[79] Xu, B.; Zhou, L.; Madix, R. J.; Friend, C. M. Highly Selective Acylation of Dimethylamine Mediated by Oxygen Atoms on Metallic Gold Surfaces. *Angew. Chem. Int. Ed*. 49(2010):394-398.

[80] Ochiai, M.; Inenaga, M.; Nagao, Y. Oxidative Decarboxylation of Cyclic Amino Acids and Dehydrogenation of Cyclic Secondary Amines with Iodosobenzene. *Tetrahedron Lett*. 29(1988):6917-6920.

[81] Moriarty, R. M.; Vaid, R. K.; Duncan, M. P.; Ochiai, M.; Inenaga, M.; Nagao, Y. Hypervalent Iodine Oxidation of Amines Using Iodosobenzene: Synthesis of Nitriles, Ketoes and Lactams. *Tetrahedron Lett*. 29(1988):6913-6916.

[82] Larsen, J.; Jørgensen, K. A. A Facile Oxidation of Secondary Amines to Imines by Iodosobenzene or by a Terminal Oxidant and Manganese or Iron Porphyrins ad Manganese Salen as the Catalysts. *J. Chem. Soc. Perkin Trans. 2* (1992):1213-1217.

[83] Ochiai, M.; Ito, T.; Masaki, Y. A Stable Crystalline (Alkylperoxy)iodinane: 1-(*tert*-Butylperoxy)-1,2-benziodoxol-3(1*H*)-one. *J. Am. Chem. Soc.* 114(1992):6269-6270.

[84] Sueda, T.; Kajishima, D.; Goto, S. Mechanistic Investigations on the Reaction between Amines or Amides and an Alkylperoxy-λ^3-iodane. *J. Org. Chem*. 68(2003):3307-3310.

[85] Huang, W.- J.; Singh, O. V.; Chen, C.- H.; Chiou, S.- Y.; Lee, S.- S. Activation of Iodosobenzene by Catalytic Tetrabutylammonium Iodide Application in the Oxidation of Some Isoquinoline Alkaloids. *Helv. Chim. Acta.* 85(2002):1069-1078.

[86] Dohi, T.; Takenaga, N.; Goto, A.; Fujioka, H.; Kita, Y. Clean and Efficient Benzylic C-H Oxidation in Water Using a Hyperalent Iodine Reagent: Activation of Polymeric Iodosobenzene with KBr in the Presence of Monotmoillonite-K10. *J. Org. Chem*. 73(2008):7365-7368.

[87] Venkov, A. P.; Statkova-Abeghe, S. M. Synthesis of 3,4-Dihydroisoquinolines, 2-Alkyl(Acyl)-1(2*H*)-3,4-Dihydroisoquinolinones by Oxidation with Potassium Permanganate. *Tetrahedron* 52(1996):1451-1460.

[88] Mohamed, M. A.; Yamada, K.; Tomioka, K. Accessing the Amide Functionality by the Mild and Low-Cost Oxidation of Imine. *Tetrahedron Lett.* 50(2009):3436-3438.

[89] Maeda, Y.; Nishimura, T.; Uemura, S. Copper-Catalyzed Oxidation of Amines with Molecular Oxygen. *Bull. Chem. Soc. Jpn*. 76(2003):2399-2403.

[90] Wang, J.-R.; Fu, Y.; Zhang, B.- B.; Cui, Z.; Liu, L.; Guo, Q.- X. Palladium-Catalyzed Aerobic Oxidation of Amines. *Tetrahedron Lett.* 47(2006):8293-8297.

[91] Choi, H.; Doyle, M. P. Oxidation of Secondary Amines Catalyzed by Dirhodium Caprolactamate. *Chem. Commun*. 43(2007):745-747.

[92] Kodama, S.; Yoshida, J.; Nomoto, A.; Ueta, Y.; Yano, S.; Ueshima, M.; Ogawa, A. Direct Conversion of Benzylamines to Imines *via* Atmospheric Oxidation in the Presence of VO(Hhpic)$_2$ Catalyst. *Tetrahedron Lett.* 51(2010):2450-2452.

[93] Zhu, B.; Angelici, R. J. Non-Nanogold Catalyzed Aerobic Oxidation of Secondary Amines to Imines. *Chem. Commun*. 43(2007):2157-2159.

[94] Zhu, B.; Lazar, M.; Trewyn, B. G.; Angelici, R. J. Aerobic Oxidation of Amines to Imines Catalyzed by Bulk Gold Powder and by Alumina-Supported Gold. *J. Catal*. 260(2008):1-6.

[95] Angelici, R. J. Organometallic Chemistry and Catalysis on Gold Metal Surfaces. *J. Organomet. Chem*. 693(2008):847-856.

[96] Grirrane, A.; Corma, A.; Garcia, H. Highly Active and Selective Gold Catalysts for the Aerobic Oxidative Condensation of Benzylamines to Imines and One-Pot, Two-Step Synthesis of Secondary Benzylamines. *J. Catal.* 264(2009):138-144.

[97] Aschwanden, L.; Mallat, T.; Grunwaldt, J.- D.; Krumeich, F.; Baiker, A. Gold-Catalyze Aerobic Oxidation of Dibenzylamine: Homogeneous or Heterogeneous Catalysis. *J. Mol. Catal. A: Chem*. 300(2009):111-115.

[98] Aschwanden, L.; Mallat, T.; Krumeich, F.; Baiker, A. A Simple Preparation of an Efficient Heterogeneous Gold Catalyst for Aerobic Amine Oxidation. *J. Mol. Catal. A: Chem*. 309(2009):57-62.

[99] Aschwanden, L.; Mallat, T.; Maciejewski, M.; Krumeich, F.; Baiker, A. Development of a New Generation of Gold Catalysts for Amine Oxidation. *ChemCatChem* 2(2010):666-673.

[100] Aschwanden, L.; Panella, B.; Rossbach, P.; Keller, B.; Baiker, A.Magnetically Separable Gold Catalyst for the Aerobic Oxidation of Amines. *ChemCatChem* 1(2009):111-115.

[101] So, M.- H.; Liu, Y.; Ho, C.- M.; Che, C.- M. Graphite-Supported Gold Nanoparticles as Efficient Catalyst for Aerobic Oxidation of Benzylic Amines to Imines and *N*-Substituted 1,2,3,4-Tetrahydroisoquinolines to Amines: Synthetic Applications and Mechanistic Study. *Chem. Asian J.* 4(2009): 1551-1561.

[102] Grirrane, A.; Corma, A.; Garcia, H. Gold –Catalyzed Synthesis of Aromatic Azo Compounds from Anilines and Nitroaromatics. *Science* 322(2008):1661-1663.

[103] Zhou, Y.; Angelici, R. J.; Woo, L. K. Bulk Gold-Catalyzed Reactions of Diazoalkanes with Amines and O_2 to Give Enamines. *Calal. Lett.* 137(2010):8-15.

APPENDIX

A.1 Calculation of percent GC yield

A.1.1 Sample preparation

A.1.1.1 Preparation of authentic sample for calibration curve

6 mM of hexadecane (C_{16}) diluted in ethyl acetate is used as internal standard solution in all reactions. Four concentration mixtures of each authentic sample have to prepare for each calibration curve. Ethyl acetate was used as solvent for dilution in all samples. The amount of authentic sample was prepared in 4 samples (180, 125, 75 and 50 ppm) and then C_{16} was added to that samples in 30, 60, 10 and 150 ppm, respectively. *N*-formyl-piperidine (**2l**) and internal standard (C_{16}) are shown in Table 1 as an example.

Table A.1 Example for preparation of authentic sample (**2l**) and C_{16} in 4 concentrations

	180 ppm	125 ppm	75 ppm	50 ppm
Authentic sample (**2l**)	16.3 mg	11.3 mg	6.75 mg	4.5 mg
	144.04 mmol	99.86 mmol	59.65 mmol	39.77 mmol
Internal standard (C_{16})	30 ppm	60 ppm	100 ppm	150 ppm
	3.5 µL	7.0 µL	11.7 µL	17.5 µL
	11.4 mmol	22.8 mmol	38 mmol	57 mmol
Mol ratio of C_{16}/authentic sample	0.0791	0.2283	0.6370	1.433

A.1.1.2 Calculation method for calibration curves

5 area values of internal standard (C_{16}) and authentic samples detected by gas chromatography (GC), A1-A5, were obtained in each concentration. The maximum and minimum values were discarded and area value of three data (A1, A2, A3) was calculated in Equation 1. The area ratio of C_{16}/authentic sample was calculated.

$$\bar{A} = \sqrt{\frac{(A1^2 + A2^2 + A3^2)}{2}} \qquad (1)$$

Calibration curves:

The mol ratio of C_{16}/authentic sample was set in X-axis and area ratio of C_{16}/authentic sample was Y-axis. Linear graphs of calibration curves between mol ratio and area ratio were done. Calibration curves of all authentic samples were shown here.
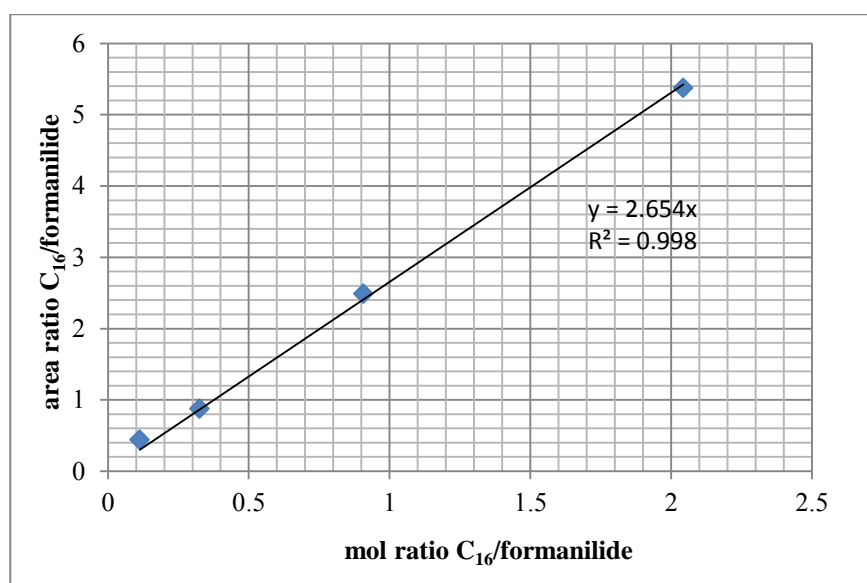

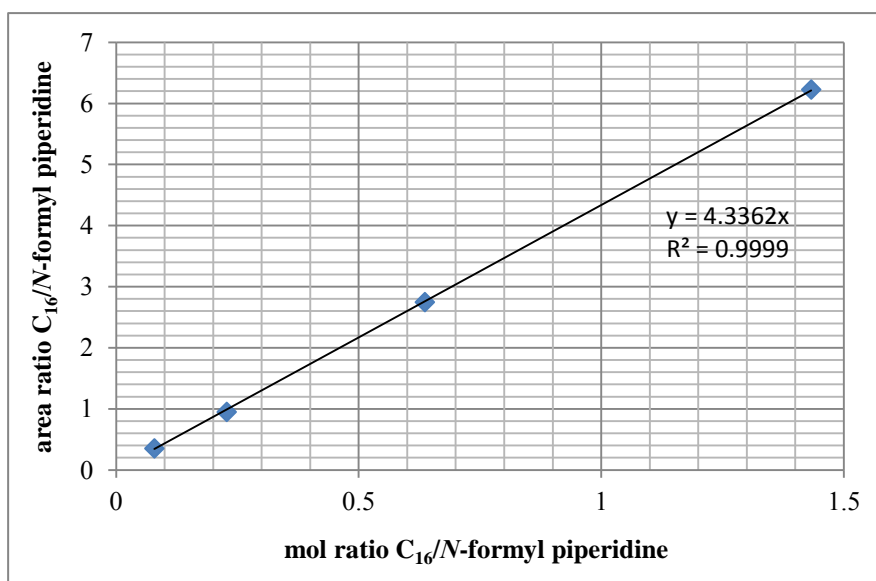**Figure A.1** Calibration curve of formanilide (**3a**)

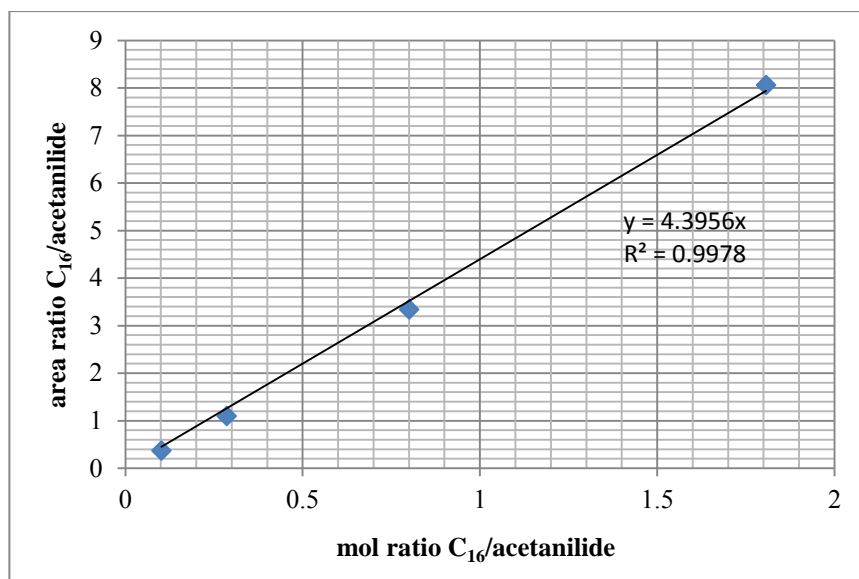**Figure A.2** Calibration curve of N-formyl piperidine (2)

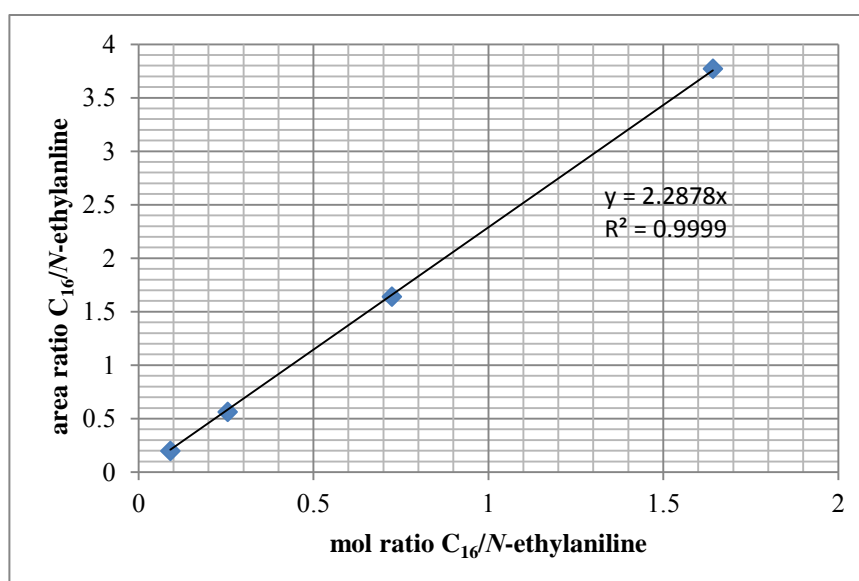**Figure A.3** Calibration curve of acetanilide (1)

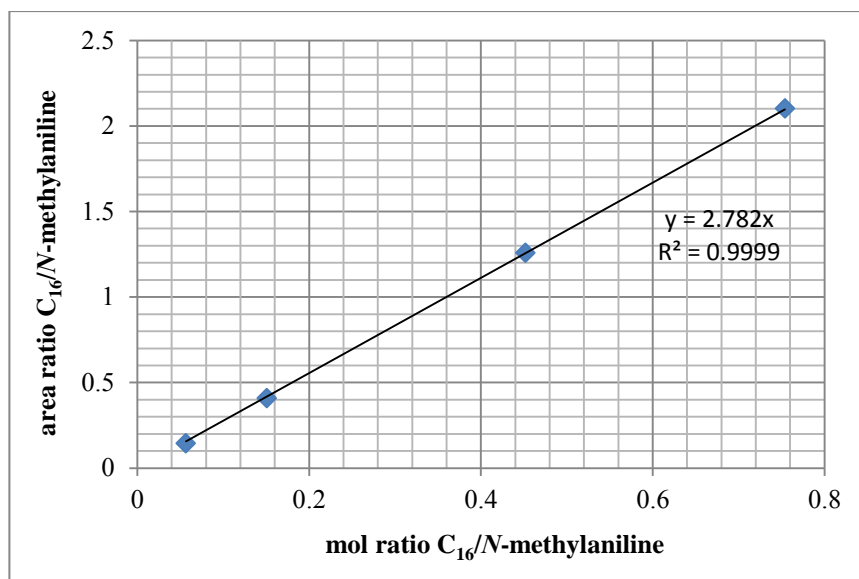**Figure A.4** Calibration curve of *N*-ethylaniline (1)

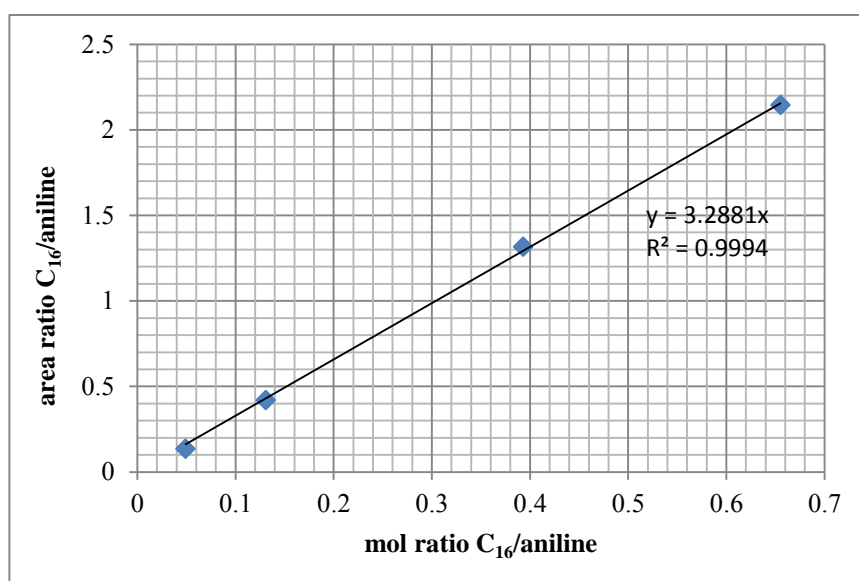**Figure A.5** Calibration curve of *N*-methylaniline (**1a**)

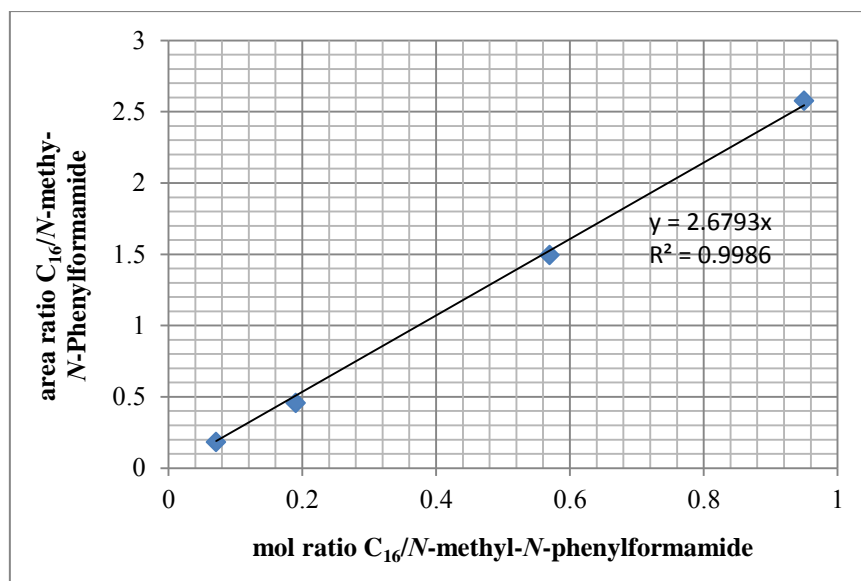**Figure A.6** Calibration curve of aniline (**4a**)

Figure A.7 Calibration curve of *N*-methylformanilide (2a)

The slope of all calibration curves were calculated and used for calculation of %GC yield by using Equation 2.

A.1.1.3 Preparation of sample from reaction mixture

0.2 mL of solution mixture from 15 mL of reaction solution was picked up. Sat. NaHCO$_3$ and sat. NaCl was added (0.5 mL) and the reaction mixture was extracted with ethyl acetate 3 times (0.5 mL×3). The organic layer was combined into GC vial and 50 µL of 6mM of internal standard (C$_{16}$) was added.

A.1.1.4 Calculation of percent yields of compound.

GC sample would be detected the amount of composition by gas chromatography 5 times per 1 sample and %GC yield of each component will calculate by Equation 2.

$$\%GC\ yield = \left(\frac{m \times \bar{A} \times mol\ of\ C_{16}}{\overline{C_{16}}}\right) \times \frac{V_{tol}}{V_{sam}} \times \frac{100}{mol\ of\ SM} \qquad (2)$$

$m = slope\ in\ calibration\ curve\ of\ authentic\ sample$

$\bar{A} = peak\ area\ of\ sample$

$$\overline{C_{16}} = peak\ area\ of\ internal\ standard$$

$$V_{tol} = total\ volume\ of\ reaction\ mixture\ (mL)$$

$$V_{sam} = sampling\ volume\ of\ reaction\ mixture\ (mL)$$

$$SM = starting\ material\ (mol)$$

A.2 Calculation of percent carbon-13 in Scheme 3.7

%Yield was detected and calculated as described above and %yield of ^{13}C in each compound was detected and calculated by GCMS.

1a

6% recovery

2a

92% ^{13}C

80% yield

3a

82% ^{13}C

3% yield

4a

3% yield
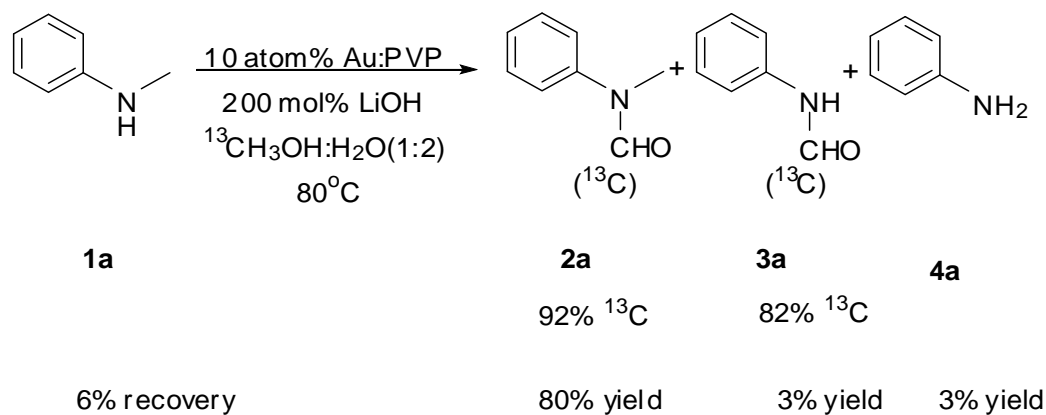
For example: *N*-methylformanilide (2a)

GCMS data:

MS	135	136	137	
^{12}C (GCMS intensity) (natural abundance)	99629	8667.7		108296.7 (A)
^{13}C (GCMS intensity)		1112085.3	94403	1206488.3 (B)

Calculation:

$$\%^{13}C = \frac{B}{A+B} \times 100 = \frac{1206488.3}{1314785} \times 100 = 91.8\%$$

VITA

Ms. Patcharee Preedasuriyachai was born on November 22, 1979, in Bangkok, Thailand. She graduated with Bachelor's Degree of Science in Chemistry from Faculty of Science, Chiang Mai University in 2000 and graduated with Master's Degree of Science in Organic Chemistry from Faculty of Science, Mahidol University in 2005. Since 2006, she has been a graduate student studying in the Program for Petrochemistry, Faculty of Science, Chulalongkorn University for Doctor of Philosophy's Degree and completed in 2011. During her studies, she was supported by The Development and Promotion of Science and Technology Talent Project (DPST), The Institute for the Promotion of Teaching Science and Technology (IPST) from Bacherlor's Degrees to Philosophy's Degree for 11 years.

Her present address is 696/133 S. siam condotown, Dindaeng Rd., Dindaeng District, Dindaeng, Bangkok, Thailand 10400.